Die approbierte Originalversion dieser Dissertation ist an der Hauptbibliothek der Technischen Universität Wien aufgestellt (http://www.ub.tuwien.ac.at).

The approved original version of this thesis is available at the main library of the Vienna University of Technology (http://www.ub.tuwien.ac.at/englweb/).

Doctoral Thesis

# ANALYTICAL SHEAR CAPACITY MODEL OF REINFORCED CONCRETE CIRCULAR CROSS-SECTION MEMBERS UNDER MONOTONIC LOAD

submitted in satisfaction of the requirements for the degree of
Doctor of Science in Civil Engineering
of the Vienna University of Technology, Faculty of Civil Engineering

---

Dissertation

# ANALYTISCHES MODEL DER QUERKRAFTTRAGFÄHIGKEIT KREISFÖRMIGER STAHLBETONBAUTEILE

ausgeführt zum Zwecke der Erlangung des akademischen Grades eines
Doktors der technischen Wissenschaften
eingereicht an der Technischen Universität Wien Fakultät für Bauingenieurwesen
von

Dipl.-Ing. Ildiko MERTA, M.Sc.
Matrikelnummer 0130717
Eduard Suessgasse 26/2, 1150 Wien, Österreich

Gutachter: Univ.Prof. Dipl.-Ing. Dr.techn. Andreas Kolbitsch
Institut für Hochbau und Technologie, Technische Universität Wien
Karlsplatz 13/206/4, 1040 Wien, Österreich

Gutachter: O.Univ.Prof. Dipl.-Ing. Dr.-Ing. M.Eng. Johann Kollegger
Institut für Tragkonstruktionen - Betonbau, Technische Universität Wien
Karlsplatz 13/212, 1040 Wien, Österreich

Wien, November 2006

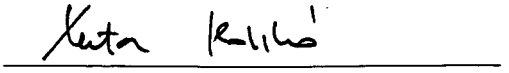

# Acknowledgements

This thesis was carried out during my employment as a research and teaching assistant at the Institute for Building Construction and Technology, Vienna University of Technology.

I would like to express my gratitude to my advisor Univ. Prof. Dipl.-Ing. Dr. techn. Andreas Kolbitsch, for support that made this thesis possible and for time consuming supervision of the work. I am greatly thankful for the granted academic freedom as well as for the necessary time and isolation to finish the thesis. For ensuring the financial support for my attendance on several international conferences during the last two years I own him a special thank!

For delivering the second opinion to the thesis I am greatly thankful to O.Univ.Prof. Dipl.-Ing. Dr.-Ing. Johann Kollegger, Institute for Structural Engineering, Vienna University of Technology. Many thanks also to Dipl.-Ing. Dr. techn. Rossitza Popov.

Thanks are also due to O.Univ.-Prof. Dipl.-Ing. Dr. techn. Lutz Sparowitz from the Concrete Institute, Graz University of Technology for awaking an interest to work on this topic as well as for his valuable support to perform the laboratory tests reported in this thesis.

Additionally, I want to express my gratitude to all the members of the Institute for Building Construction and Technology, Vienna University of Technology, for their kind support and for providing a pleasant working environment.

For the time consuming proof reading of the thesis special thanks to Prof. Igor Grbić.

Finally, I would like to thank my husband Fredi for his outstanding support and for making me laugh again and again. To my Family a special thanks for all the support!

Ildikó Merta

# ABSTRACT

In the thesis, an analytical model for the prediction of the shear capacity of reinforced concrete members with circular cross-section transversely reinforced with circular hoops has been developed. The proposed model is based on the truss analogy by adding an empirical concrete contribution term to the capacity of the shear reinforcement.

With the appearance of the first diagonal cracks the shear reinforcement is mobilized in resisting shear by tension in it. However, in the proposed model an additional shear carrying mechanism of hoops – present solely in members with curved transverse reinforcement – was identified and expressed analytically. This *deviatoric* shear resisting mechanism is explained by the fact that a curved reinforcing bar under tension induces compression in radial direction as well. The component of this compressive force in the direction of the external shear could thus be considered as an additional shear enhancing mechanism of the hoops. Its magnitude is expressed through the friction force that is present between the concrete and steel after the section is cracked and the bond partially destroyed.

The concrete shear capacity, taken as the capacity of the member without shear reinforcement, has been derived by a parameter study of the variables affecting shear concrete strength and by applying a curve fit on the database of circular members without shear reinforcement.

The validity and accuracy of the proposed model has been verified on a database of experimental results of 106 uniformly loaded members of circular sections with and without shear reinforcement and a good agreement has been obtained. The proposed shear model has been compared to other existing models as well, predicting the shear strength of circular sections in a more accurate and uniform way than the existing models.

Moreover, the applicability of the proposed model has been verified on a database of 29 elements tested under uniaxial cyclic shear. With the application of a strength degradation coefficient, proposed so far in literature, the members shear capacity under cyclic load with increasing ductility has been expressed. The proposed model has been compared to a recently proposed model and it has been found that it predicts reasonably well the shear capacity of circular sections under cyclic load as well. By applying the strength reduction factors a sufficiently conservative design equation could be obtained, suitable for design purposes and incorporation in design codes.

# Table of Contents

**Abstract** ..... **4**

**Notations** ..... **8**

**1 Introduction** ..... **11**

1.1 Background and Motivation of the Research ..... 11

1.2 Objectives ..... 13

1.3 Outline of the Thesis ..... 13

**2 State of the art and the Existing Shear Models** ..... **14**

2.1 Eurocode 2 (1992) ..... 16

2.2 Capon and de Cossio (1966) ..... 16

2.3 ACI 318M-02 (2002) ..... 17

2.4 Ang et al. (1989) ..... 17

2.5 Priestley et al. (1994) ..... 19

2.6 Kowalsky and Priestley (2000) ..... 20

2.7 Clarke and Birjandi (1993) ..... 21

2.8 Dancygier's (2001) Remark to Ang's et al. (1989) Model ..... 22

2.9 Kim and Mander's (2005) Remark to Ang's et al. (1989) Model ..... 22

**3 Circular Members Shear Database** ..... **23**

3.1 Introduction ..... 23

3.2 Database of Circular Members under Monotonic Shear Load ..... 24

**4 Proposed Shear Model for Circular Sections** ..... **29**

4.1 Introduction ..... 29

4.2 Shear Transfer Mechanism in Concrete ..... 30

4.3 Evaluation of Concrete Shear Capacity ..... 30

4.3.1 Effective Shear Area of Circular Sections ..... 31

4.3.2 Effect of Concrete Strength ..... 39

4.3.3 Effect of Longitudinal Reinforcement ..... 40

4.3.4 Effect of Shear Span-to-Depth Ratio ..... 43

4.3.5 Effect of Axial Load ..... 45

4.3.6 Size Effect ..... 46

4.3.7 Comparison of the Proposed Model to Other Models ..... 47

4.4 Evaluation of Shear Reinforcement Capacity ..... 56

4.4.1 Shear Resisting Mechanism of Hoops in Circular Sections ..... 56

4.4.2 Shear Resisting Mechanism by Tension in Hoops – Tension Component ..... 58

4.4.3 Relation between the Hoop's Tension and the Deviation Function ..... 62

4.4.4 Shear Resisting Mechanism of Hoops Resulting from Deviation Forces – Deviation Component ..... 68
Resultant Deviation Force of One Hoop ..... 69
Total Deviation Force of Hoops ..... 71
4.4.5 Total Shear Force Carried by Shear Reinforcement ..... 75

**5 Discussion of Results and Comparison to Other Models ..... 76**
5.1 Verification of the Proposed Model for Monotonic Load ..... 76
5.2 Verification of the Proposed Model for Cyclic Load ..... 86
5.3 Adequacy of the Proposed Model for Design ..... 90

**6 Conclusion and Future Work ..... 91**

**7 List of Figures and Tables ..... 93**

**8 References ..... 96**

# NOTATIONS

Latin upper case symbols

$A_g$ = area of the gross section;

$A_l$ = longitudinal reinforcement cross sectional area;

$A_{seff}$ = effective shear area;

$A_{sw}$ = shear reinforcement cross sectional area (area of hoops one leg);

$B$ = bond force;

$C$ = concrete compressive force;

$D$ = sections diameter;

$D_h$ = resultant deviation force;

$D(\varphi)$ = deviation function;

$N$ = normal force;

$P$ = axial load (compression is positive);

$T$ = tension force

$T(\varphi)$ = tension function;

$V$ = external shear force;

$V_a$ = shear force resisted by aggregate interlock;

$V_{ay}$ = vertical component of the shear force resisted by aggregate interlock;

$V_c$ = concrete shear capacity;

$V_{cz}$ = shear force resisted by uncracked concrete compression zone;

$V_d$ = shear force resisted by dowel action;

$V_s$ = shear reinforcement capacity;

$V_{sd}$ = hoops deviatoric shear resisting component;

$V_{exp}$ = experimental shear force;

$V_{theor}$ = theoretical shear force;

$V_{st}$ = hoops tension shear resisting component;

Latin lower case symbols

$a$ = shear-span;

$a/d$; $a/D$ = members aspect ratio (shear span-to-depth ratio);

$b$ = sections width;

$b_w$ = minimum width of the section (web);

$c$ = neutral axis depth;

$cov$ = concrete cover;

$d$ = sections effective depth;

$f_d$ = deviation stress;

$f_c'$ = cylinder compressive strength of concrete;

$f_{ck}$ = characteristic compressive strength of concrete;

$f_{yl}$ = longitudinal reinforcement yield strength;

$f_{yw}$ = transverse reinforcement yield strength;

$h$ = cross sections overall depth;

$k$ = aspect ratio enhancement constant;

$n$ = number of hoops crossing the diagonal crack;

$s$ = spacing of shear reinforcement along the member's longitudinal axis;

$v$ = average shear stress;

$z$ = internal lever arm;

Greek upper case symbols

$\tau_b$ = bond stress;

Greek lower case symbols

$\gamma_c$ = partial safety factor for concrete;

$\gamma_s$ = partial safety factor for steel;

$\theta$ = inclination angle of the concrete cracks with the longitudinal axis;

$\lambda$ = influence coefficient;

$\mu$ = coefficient of friction between concrete and steel;

$\rho_l$ = longitudinal reinforcement ratio, $\rho_l = A_l / A_g$ ;

$\rho_w$ = transverse reinforcement ratio, $\rho_w = 2A_{sw} / (D \cdot s)$ .

# 1 INTRODUCTION

## 1.1 Background and Motivation of the Research

Reinforced concrete structural elements of circular cross-section are widely used in different types of structures. They are preferred as columns in high rise buildings, placed either on the façade or in the buildings' interior, as structural elements favoured because of their decorative architectonical form. Moreover, they are preferred as bridge columns, secant pilings forming diaphragm walls or in the foundations of buildings. Generally, circular cross section columns are favoured because of their identical strength characteristics in all directions.

Columns are basically axial load carrying elements. However, as a result of lateral loads due to wind pressure, earthquake or vehicle impact, they are subjected to considerable shear load and should thus inevitably be designed to suppress a possible shear failure. Despite of rather frequent occurrence of shear in circular sections and its possible hazardous consequences, the majority of research in shear is conducted on members with rectangular cross-section. As a result, extensive shear capacity models for rectangular sections have been proposed in literature so far. On circular section members, however, a very limited number of experiments have been carried out. Consequently, neither has their basic structural

behaviour under shear been sufficiently understood, nor does the advantage (deficiency) of circular sections compared to rectangular ones happen to be apparent enough.

Generally, the majority of design codes do not distinguish between the design of a rectangular section and the one of a circular section under shear. It is simply assumed that the shear capacity of a circular section equals the capacity of an equivalent rectangular section, assuming that the shear transfer and the shear resisting mechanism of both sections are equivalent without any influence of the sections geometry.

The majority of earlier experiments on circular reinforced concrete members loaded monotonically in shear aimed for verification of the use of design equations developed for rectangular sections on circular sections (Capon and de Cossio, 1965; Khalifa and Collins, 1981; Clarke and Birjandi, 1993). No thorough design equation for circular sections has been proposed; solely a slight modification of existent equations was given when applying them to circular sections. Later, failures of circular columns in some recent earthquakes (Venezuela, 1967; San Fernando, 1971) triggered an extensive research in circular sections under seismic load in research centres such as the University of Canterbury, Christchurch, New Zealand (Paulay, Park, Priestley), the University of Toronto (Collins) and the University of California, San Diego (Priestley). Major concern was devoted to shear capacity under seismic load and as a result of these efforts a model for shear capacity of circular sections under seismic load was proposed by Ang et al. (1989), extended by Wong et al. (1993) for multi-directional seismic load, later generalized by Priestley et al. (1994) and finally by Kowalsky and Priestley (2000). This model is still the only one proposed so far in literature for circular sections under shear. Recently, however, its significant deficiency was reported by Dancygier (2001) and by Kim and Mander (2005). It was demonstrated that the applied integral averaging in the formula restricts its use only to members with diameter at least four times the spacing of the shear reinforcement. For all other ratios the formula could be even more than 50% nonconservative.

## 1.2 Objectives

Motivated by a lack of research in basic shear mechanism of circular sections as well as by the deficiencies of the single shear model so far proposed in literature, the main objective of this work was to develop a simple formula for shear capacity of reinforced concrete circular sections suitable for design purposes as well as for incorporation in the design codes. The particular intension was primarily to develop a shear capacity model for circular sections under monotonic load and then to express the capacity under seismic load. In order to take into account the strength degradation due to cyclic reversal, present in seismic load, the members shear capacity under monotonic load has been simply reduced by a degradation coefficient. This approach is consistent with the current state of the art.

Last but not least, it is of great interest to generally examine the basic shear transfer mechanism in circular sections since it sheds light on our knowledge of the influence of the cross-sections shape on the shear capacity, thus contributing to the development of a unified design method of reinforced concrete sections under shear regardless of the shape of the cross section. This work attempted to give a contribution to these efforts.

## 1.3 Outline of the Thesis

Chapter 2 presents a brief historical background of the shear design provisions and a summary of the current shear design models for circular sections. In chapter 3 a database of circular members without and with shear reinforcement tested under monotonic shear is collected, on the basis of what has been published so far in literature. In chapter 4 the proposed shear design model is presented. First the concrete shear capacity and then the shear reinforcement capacity is evaluated. In chapter 5 the results are discussed and compared to other existing models. Finally, in chapter 6 a summary of the work and suggestions for future work are presented.

# 2 STATE OF THE ART AND THE EXISTING SHEAR MODELS

Estimating the shear capacity of reinforced concrete members has received considerable attention in research since the turn of the century. During the time different approaches of the shear design have been proposed. In the early 1900s truss models were introduced as conceptual tools for the design of web reinforcement in concrete beams (Ritter 1899; Mörsch, 1902; Mörsch, 1912), implying an analogy between a diagonally cracked reinforced concrete beam with web reinforcement and a 45-degree-parallel-chord truss. Later it was observed that truss models give conservative results since they do not account for the effects of concrete shear capacity resulting from the shear carried by uncracked concrete, dowel action of the longitudinal reinforcements and shear transmitted by aggregate interlock along the cracks. In order to correct the conservative predictions of the 45-degree truss, several improvements have been proposed recently. A possible approach is to add a concrete shear capacity contribution term to the shear reinforcement capacity or to employ a truss with variable inclination angle. Additionally, several other approaches to the truss analogy have been proposed as well. One of them is the limit analysis, mainly introduced by Thürlimann and Nielsen (1999), as well as the compression field theory, first developed by Mitchell and Collins (1974) for torsion, and later adopted for shear (Collins, 1978). The theory was further modified to account for the influence of tensile stresses in cracked

concrete and published later as the modified compression field theory (Vecchio and Collins, 1986). A historical background of the shear provisions and a comprehensive overview of the existing shear approaches were published in the report of the ACI-ASCE Committee 445 on Shear and Torsion (1998, 2000), based on the landmark state of the art report by the ACI-ASCE Committee 426 (1973), as well as in Marti (1992), Regan (1993), Marti (1999) and Rebeiz (1999).

In most current building codes the shear capacity of a reinforced concrete member with transverse reinforcement is calculated on the basis of the truss analogy and thus added together from the concrete shear capacity and from the capacity of shear reinforcement (ACI 318M-02, 2002; Eurocode 2, 1992).

The concrete shear capacity is defined as the shear strength of the member without shear reinforcement at the onset of the diagonal cracks. The influence of the different variables on shear strength is still not so distinctive, resulting in literature offering us a wide range of different shear capacity models (Zsutty, 1968; Bažant and Sun, 1987; Watanabe and Ichinose, 1992; Kim and Park, 1996; Nielsen, 1999; Rebeiz, 1999; Sezen and Moehle, 2004; Russo et al., 2005). However, all these models are developed for rectangular sections. So far, there is no model originally derived to estimate the capacity of circular sections without shear reinforcement. Usually the design equations developed for rectangular sections are used also for circular sections with a slight adaptation, namely that instead of the actual circular cross section with diameter $D$ an equivalent rectangle of width $D$ and effective depth of $d$=0.8$D$ is employed.

The capacity of the shear reinforcement – in case of circular sections usually hoops or spirals – is calculated on the basis of the truss analogy. Usually the equations derived for rectangular sections have been used. There is in literature only one model originally derived for circular sections (Ang et al., 1989 later modified by Kowalsky et al., 2000). What follows is a brief review of the very limited number of the existing shear models and of recommendations for circular section members.

## 2.1 Eurocode 2 (2004)

Although Eurocode 2 for Design of Concrete Structures gives no instructions for shear design of circular sections, because of its practical relevance it will be briefly reviewed. The shear resistance of a section with shear reinforcement, $V_{Rd}$, is given as the sum of the shear resistance of the member without shear reinforcement (the so called concrete contribution), $V_{Rd,c}$, and the shear resistance of the shear reinforcement, $V_{Rd,s}$

$$V_{Rd} = V_{Rd,c} + V_{Rd,s} \tag{2.1}$$

The concrete contribution is calculated as

$$V_{Rd,c} = [C_{Rd,c} \cdot k(100 \cdot \rho_l \cdot f_{ck})^{1/3} + k_1 \cdot \sigma_{cp}] b_w d \tag{2.2}$$

where $C_{Rd,c}$ is a calibration factor and it is $0.18/\gamma_c$ for normal concrete and $0.15/\gamma_c$ for light concrete ($\gamma_c$ is the partial safety factor for concrete), $k$ is the size effect factor defined as $k = 1 + \sqrt{200/d} \le 2.0$, the longitudinal reinforcement ratio is $\rho_l = A_{sl}/(b_w d) \le 0.02$, $f_{ck}$ is the characteristic concrete compression strength, $k_1 = 0.15$, $\sigma_{cp} = N_{Ed}/A_c$ where $N_{Ed}$ is the axial load (compression positive), $A_c$ is the concrete cross-section and $b_w$ and $d$ are the section's width and effective depth respectively. The contribution of vertical shear reinforcement is calculated by truss analogy and is given by

$$V_{Rd,s} = \frac{A_{sw}}{s} z \cdot f_{ywd} \cdot ctg\theta \tag{2.3}$$

where $A_{sw}$ is the cross-sectional area (two times the area of the bar), $s$ the spacing and $f_{ywd}$ the yield strength of the shear reinforcement. The internal lever arm could be taken as $z = 0.9d$ and the inclination angle of the concrete struts $45° \le \theta \le 21.8°$.

## 2.2 Capon and de Cossio (1966)

One of the first researches in shear capacity of circular section members was carried out by Capon and de Cossio in 1966. Drawing on observations of test results of 21 members they proposed to use for circular sections the same equations as for rectangular sections, with

following adaptations: for the section's effective depth the external diameter should be used and for the section's effective shear area the gross area.

## 2.3 ACI 318M-02 (2002)

The shear strength of member is calculated as the sum of the concrete contribution, $V_c$, and the shear reinforcement contribution, $V_s$. The concrete contribution is given by

$$V_c = \left(1 + \frac{P}{14A_g}\right)\frac{\sqrt{f_c'}}{6}bd \tag{2.4}$$

where $P$ is the axial load (positive for compression), $A_g$ is the gross-sectional area, $f_c'$ is the concrete cylinder compressive strength and $b$ and $d$ are the section's width and the effective depth respectively. For circular sections, the shear area $bd$ shall be taken as the product of the diameter and effective depth of the concrete section. The effective depth is permitted to amount to 0.8 times the diameter of the concrete section.

The transverse reinforcement contribution is calculated as for rectangular sections

$$V_s = \frac{A_{sw}f_{yw}d}{s} \tag{2.5}$$

where $A_{sw}$ is the area of shear reinforcement (two times the area of the bar) within a distance $s$ and $f_{yw}$ is the yield strength of shear reinforcement. When circular ties, hoops or spirals are used for transverse reinforcement, the effective depth shall be taken as 0.8 times the diameter of the concrete section.

## 2.4 Ang et al. (1989)

Ang et al. (1989) proposed a model for calculating the shear strength of circular sections under cyclic load added together from concrete and transverse reinforcement capacity. The concrete contribution for low flexural ductilities ($\mu \leq 2$) was defined as the "initial concrete strength" and calculated as a strength at maximum lateral load as follows

$$V_c = 0.37\alpha(1 + 3\frac{P}{f_c' A_g})\sqrt{f_c'} \cdot A_e \tag{2.6}$$

For low aspect ratios ($a/D < 2$) a shear capacity enhancement factor was proposed as

$$\alpha = \frac{2}{a/D} \geq 1.0 \tag{2.7}$$

where $a$ is the shear span, $D$ the section's diameter, $P$ the axial load, $A_g$ the gross-sectional area, $f_c'$ the concrete compressive strength. The effective shear area, $A_e$, is proposed as 0.8 times the gross section area, which approximately corresponds to the area of the confined concrete core. The transverse reinforcement capacity was calculated from 45-degree truss mechanism as follows

$$V_s = \frac{\pi(2A_{sh}f_{yh})D'}{4s} \tag{2.8}$$

where $A_{sh}$ is the area of the shear reinforcement (one leg), $s$ the hoop's spacing, $f_{yh}$ their yield strength and $D'$ the distance between the centers of the peripheral hoop or the spiral. It was assumed that all transverse reinforcement exposed by a presumed 45° diagonal crack is at yield. An integral averaging has been imposed assuming that the spacing of the shear reinforcement $s$ is sufficiently small compared to the diameter $D'$. It was noted that for low $D'/s$ ratios the equation can be up to 10% nonconservative.

At higher flexural ductilities ($\mu > 2$) a degradation of the concrete term was assumed and the "final concrete strength" proposed. Since very limited test data were available, the influence of axial load was not clear and the concrete contribution term was defined without taking into account the axial load. A tentative formula was proposed, where a lower value of

$$V_c = 0.185\sqrt{f_c'} \cdot A_e \leq 18.5\rho_s\sqrt{f_c'} \cdot A_e \tag{2.9}$$

should be taken. The first formula represents a 50% of the initial concrete contribution (Equation 2.6) at zero axial load and the second reflects the fact that the transverse reinforcement provides an additional confining effect to the concrete core and, as a consequence, reduces the degradation of the concrete term ($\rho_s$ is the transverse reinforcement ratio). As a result of a decreased inclination of the diagonal cracks by cyclic

reversals ($\theta = 25°$), the contribution of the truss mechanism was assumed to increase and thus was defined as

$$V_s = \frac{\pi(2A_{sh}f_{yh})D'}{4s} ctg25° \tag{2.10}$$

## 2.5 Priestley et al. (1994)

Priestley et al. (1994) modified the model proposed by Ang et al. (1989) and separated the shear capacity term of the axial loads arch mechanism, $V_p$, from the concrete term, $V_c$. The member's shear capacity was thus added together from three components

$$V = V_c + V_s + V_p \tag{2.11}$$

where $V_s$ is the contribution of transverse reinforcement. The concrete contribution has been given by

$$V_c = k\sqrt{f_c'}A_e \tag{2.12}$$

where $k$ is a coefficient describing the degradation of concrete shear strength with an increasing displacement ductility (Figure 2.1). Note that for biaxial displacement ductility a stronger degradation was assumed. The effective shear area and the shear reinforcement contribution remained the same as defined by Ang et al. (1989)

$$V_s = \frac{\pi}{2}\frac{A_{sh}f_{yh}D'}{s} cot\theta \tag{2.13}$$

where $D'$ is the distance between the centers of the peripheral hoop or the spiral. The cracks' inclination angle was taken as $\theta = 30°$. The axial load enhancement is considered as the horizontal component of the diagonal compression strut (Figure 2.1)

$$V_p = P tan\alpha = \frac{D-c}{2a}P \tag{2.14}$$

where $D$ is the overall section diameter, $c$ the depth of the compression zone and $a$ the shear span. According to this model, the axial load component does not degrade with an increasing displacement ductility.

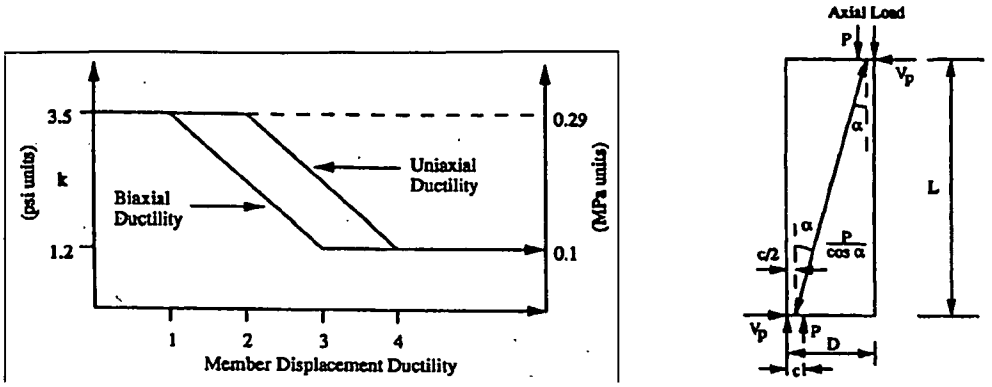


Figure 2.1 (Left) Degradation coefficient $k$ of concrete shear strength with displacement ductility and (Right) axial load contribution to the concrete shear capacity (Priestley et al. 1994)

## 2.6 Kowalsky and Priestley (2000)

The previous model of Priestley et al. (1994) was revised by Kowalsky and Priestley (2000) and the effect of aspect ratio and longitudinal reinforcement ratio has been incorporated. The concrete contribution was given by

$$V_c = \alpha\beta\gamma\sqrt{f_c'}\,0.8A_g \tag{2.15}$$

where $\alpha$ accounts for the aspect ratio and is given by $1 \le \alpha = 3 - a/D \le 1.5$ (Figure 2.2). It was noted that $\alpha$ probably continues to increase for $a/D < 1.5$, but no data are available to confirm this. The factor $\beta$ accounts for the effect of longitudinal reinforcement ratio and is given by $\beta = 0.5 + 20\rho_l \le 1$. $\gamma$ describes the degradation of concrete shear strength with displacement ductility (Figure 2.2) and $\rho_l$ is the longitudinal reinforcement ratio.

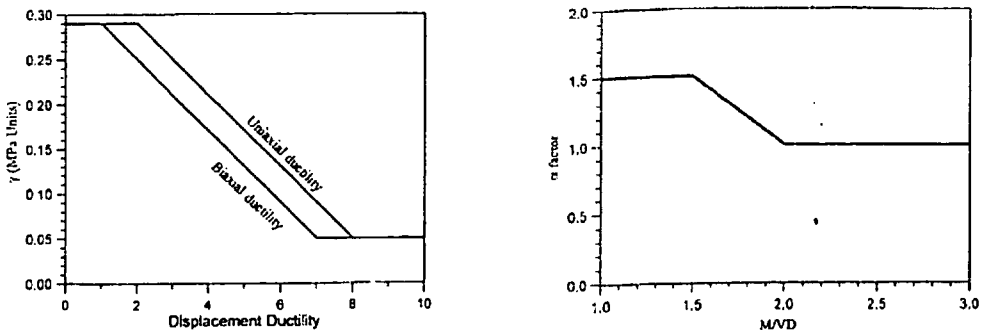


Figure 2.2 (Left) Degradation coefficient $\gamma$ of concrete shear strength with displacement ductility and (Right) Aspect ratio enhancement coefficient $\alpha$ (Kowalsky et al., 2000)

The truss mechanism component developed by Ang et al. (1989) has been slightly modified considering the fact that in the members compression zone the cracks are by definition closed. Therefore, shear cannot be transferred across it by tension in the transverse reinforcement. Thus only the spirals outside the compression zone are mobilized by tension along the crack plane

$$V_s = \frac{\pi}{2} A_{sh} f_{yh} \frac{D - c - cov}{s} cot\,\theta \tag{2.16}$$

Here $c$ is the compression zones depth and $cov$ the concrete cover. The axial component remained the same as by Priestley et al. (1994) model.

## 2.7 Clarke and Birjandi (1993)

On the basis of the results of tests undertaken by the British Cement Association, Clarke and Birjandi (1993) proposed to use for circular sections the same shear design approach as given by the British Codes of Practice, BS 5400 and BS 8110 for rectangular sections. However, a modification was suggested, i.e., that the section's effective depth should be considered as the distance from the extreme compression fibre to the centroid of the tension reinforcement. Following this, the effective shear area is then defined as the area corresponding to the effective depth. The design approach for rectangular sections in British Codes of Practice, BS 5400, is added together from the shear carried by concrete and transverse reinforcement. The concrete term is defined as

$$V_c = 0.27\alpha \left( \frac{100 A_s}{b_w d} \right)^{1/3} \left( \frac{500}{d} \right)^{1/4} (f_{cu})^{1/3} b_w d \tag{2.17}$$

where $A_s$ is the area of longitudinal steel, $b_w$ the section's width, $d$ the effective depth and $f_{cu}$ the concrete cube strength. For loads applied at a distance $a_v$ closer than $2d$ from the support, the concrete shear capacity is increased by

$$\alpha = \frac{2d}{a_v} \geq 1.0 \tag{2.18}$$

The shear force carried by transverse reinforcement is calculated as

$$V_s = \frac{A_{sv} f_{yv}\, d}{s} \tag{2.19}$$

In a member with axial compression load, $N$, the shear capacity should be multiplied by $(1+0.05N/A_c)$, where $A_c$ is the area of concrete, $A_{sv}$ the cross-sectional area of the links' both leg at the section's neutral axis and $f_{cu}$ is the links' yield strength.

## 2.8 Dancygier's (2001) Remark to Ang's et al. (1989) Model

Dancygier (2001) demonstrated that the capacity of the truss mechanism in the model proposed by Ang et al. (1989), where an integral averaging has been applied, could be used only in case the number of hoops intersected by diagonal crack $D'tan\theta/s$ is higher than 4. For lower values the proposed formula yields values that are 10% to more than 50% nonconservative. Thus Dancygier recommended a discrete computation especially for elements with relatively small diameters as micropiles.

## 2.9 Kim and Mander's (2005) Remark to Ang's et al. (1989) Model

Kim and Mander (2005) warned of calculation of the shear carried by transverse reinforcement by assuming a smeared distribution of shear reinforcement (Ang et al., 1989), which is well established in the majority of present design proposals and codes (ACI 318-02, 2002; Eurocode 2, 1992). In reality, a discrete distribution of transverse reinforcement should be considered for circular hoops and spirals as well as for rectangular hoops. For the case the number of spaces between reinforcement hoops crossing the shear crack, $n$, is lower than 5, they proposed reduction factors that should be applied to continuum truss solution to obtain the discrete solution. For $n \geq 5$ no capacity reduction is necessary.

# 3 CIRCULAR MEMBERS SHEAR DATABASE

## 3.1 Introduction

For the verification and calibration of shear capacity models it is inevitable to have representative data of test results on members where all the major parameters affecting shear are varied over a sufficiently wide range. An extensive amount of test results exists so far in literature regarding rectangular sections and by support of the Joint ACI-ASCE Committee 445 on Shear and Torsion, an Evaluation Shear Databank of members with/without transverse reinforcement was collected by Reineck et al. (2003) and Kuchma (2000). Furthermore, a comprehensive database of 917 rectangular members without shear reinforcement failed under shear was collected by Russo et al. (2005).

However, because of a very limited number of experiments carried out on circular sections under monotonic shear load, literature does not offer any database. Most of circular section specimens were tested under cyclic lateral load reversal and as a result an extensive database was published by the Pacific Earthquake Engineering Research Center (PEER) at the University of California, Berkeley. A total of 165 spiral- or hoop-reinforced concrete columns was collected in the Structural Performance Database and published on the web site of PEER (2006) and of the University of Washington (2006).

The usual way to derive the shear strength of a member under cyclic load is to first define the capacity of the member under monotonic load and then to apply the so called "degradation coefficient" to take into account the shear capacity degradation of the member under cyclic reversal. In order to follow this procedure for circular sections it is necessary to have sufficient experimental results of circular members tested under monotonic load. Therefore, one of the objectives of this work was to collect test data of circular cross-section members loaded under monotonic shear.

## 3.2 Database of Circular Members under Monotonic Shear Load

A literature survey was performed resulting in a total of 106 tests of reinforced concrete circular cross section members under monotonic shear load. 44 specimens have no shear reinforcement and 62 have spirals or hoops as shear reinforcement. Only specimens reported to fail under shear were included in the database. The test data specimens have been collected from the following researches: Capon and de Cossio (1965); Khalifa and Collins (1981), Clarke and Birjandi (1993), Merta et al. (2003), as well as the tests carried out by Kim in 2000, published by Collins et al. (2002). Four tests by Aregawi from 1974, published by Collins et al. (2002), were not included in the database according to Kowalsky and Priestley's (2000) suggestion, namely that "because of the non-standard boundary conditions, the results should be omitted". The specimen of Clarke and Birjandi (1993) with an aspect ratio of $a/D$ = 1.1 was not included in the database, since it was the only specimen with such a low aspect ratio and it would not have been possible to make any conclusion about the shear strength trend in this range.

The details and test results of specimens without shear reinforcement and with shear reinforcement are listed in Tables 3.1 and 3.2 respectively. The specimens' aspect ratio ranges between $2.04 \le a/D \le 4.39$, the concrete strength $13 \le f_c' \le 50$ MPa, longitudinal reinforcement yield strength $400 \le f_{yl} \le 700$ MPa, longitudinal reinforcement ratio $0.89 \le \rho_l \le 5.6\%$, transverse reinforcement yield strength $250 \le f_{yw} \le 1728$ MPa, transverse reinforcement ratio $0.05 \le \rho_w \le 0.45\%$ and the axial load ratio $0 \le P/(f_c' A_g) \le 0.38$.

Since no specimens with an aspect ratio lower than 2 have been tested so far, it is not possible to make a firm conclusion about the shear capacity behaviour within this range. Likewise, no specimens over a broad range of a variable depth have been tested by maintaining all other variables influencing shear strength constant. Consequently the size effect of circular section specimens could not be investigated. In order to overcome these deficiencies a comprehensive experimental research is necessary in the future.

Table 3.1 Details and test results of specimens with circular cross-section without shear reinforcement

| Reference | Specimen | $D$ [mm] | a/$D$ [-] | $f'_c$ [MPa] | $cov$ [mm] | $f_{yl}$ [MPa] | $\rho_l$ [%] | $P$ [kN] | $P/(f'_c A_g)$ [-] | $V_{test}$ [kN] |
|---|---|---|---|---|---|---|---|---|---|---|
| Clarke, Birjandi (1993) | 01-1 | 300 | 2.20 | 22.7 | 20 | 500 | 0.89 | 0 | 0 | 65.0 |
| | 03-1 | 300 | 2.20 | 22.8 | 20 | 500 | 2.28 | 0 | 0 | 91.0 |
| | 03-2 | 300 | 2.20 | 22.8 | 20 | 500 | 2.28 | 0 | 0 | 97.0 |
| | 04-1 | 300 | 2.20 | 44 | 20 | 500 | 2.28 | 0 | 0 | 129.0 |
| | 04-2 | 300 | 2.20 | 44 | 20 | 500 | 2.28 | 0 | 0 | 109.0 |
| | 05-1 | 300 | 2.20 | 26.7 | 20 | 500 | 5.56 | 0 | 0 | 148.0 |
| | 05-2 | 300 | 2.20 | 26.7 | 20 | 500 | 5.56 | 0 | 0 | 130.0 |
| | 06-1 | 300 | 2.20 | 43.6 | 20 | 500 | 5.56 | 0 | 0 | 152.0 |
| | 06-2 | 300 | 2.20 | 43.6 | 20 | 500 | 5.56 | 0 | 0 | 148.0 |
| | 29-1 | 300 | 2.20 | 31.2 | 20 | 500 | 3.56 | 270.6 | 0.12 | 146.0 |
| | 29-2 | 300 | 2.20 | 31.2 | 20 | 500 | 3.56 | 0 | 0 | 86.0 |
| | 30-1 | 300 | 2.20 | 29.7 | 20 | 500 | 3.56 | 273.3 | 0.13 | 132.0 |
| | 30-2 | 300 | 2.20 | 29.7 | 20 | 500 | 3.56 | 0 | 0 | 90.0 |
| | 31-1 | 300 | 2.20 | 20.9 | 20 | 500 | 3.56 | 535.4 | 0.36 | 146.0 |
| | 31-2 | 300 | 2.20 | 20.9 | 20 | 500 | 3.56 | 0 | 0 | 98.0 |
| | 32-1 | 300 | 2.20 | 20.1 | 20 | 500 | 3.56 | 532.9 | 0.38 | 134.0 |
| | 33-1 | 300 | 2.20 | 21.6 | 20 | 500 | 5.56 | 271.2 | 0.18 | 151.0 |
| | 33-2 | 300 | 2.20 | 21.6 | 20 | 500 | 5.56 | 0 | 0 | 116.0 |
| | 34-1 | 300 | 2.20 | 34.8 | 20 | 500 | 5.56 | 270.8 | 0.11 | 174.0 |
| | 34-2 | 300 | 2.20 | 34.8 | 20 | 500 | 5.56 | 0 | 0 | 125.0 |
| | 35-1 | 300 | 2.20 | 37.7 | 20 | 500 | 5.56 | 536.8 | 0.20 | 159.0 |
| | 35-2 | 300 | 2.20 | 37.7 | 20 | 500 | 5.56 | 0 | 0 | 125.0 |
| | 36-1 | 300 | 2.20 | 34.9 | 20 | 500 | 5.56 | 539.1 | 0.22 | 164.0 |
| | 36-2 | 300 | 2.20 | 34.9 | 20 | 500 | 5.56 | 0 | 0 | 136.0 |
| | 41-1 | 500 | 2.40 | 34 | 20 | 500 | 2.56 | 0 | 0 | 236.0 |
| | 42-1 | 500 | 2.40 | 33.5 | 20 | 500 | 2.56 | 0 | 0 | 234.0 |
| | 42-2 | 500 | 2.40 | 33.5 | 20 | 500 | 2.56 | 0 | 0 | 222.0 |
| | 45-1 | 500 | 2.40 | 29.4 | 20 | 500 | 3.84 | 0 | 0 | 234.0 |
| | 46-2 | 500 | 2.40 | 30.6 | 20 | 500 | 3.84 | 0 | 0 | 281.0 |
| Capon, de Cossio (1965) | 24.6-2-A | 247 | 4.25 | 25.6 | 15 | 400 | 2.12 | 0 | 0 | 46.5 |
| | 24.6-2-B | 246 | 4.27 | 29.2 | 15 | 400 | 2.14 | 0 | 0 | 49.0 |
| | 25-3-A | 252 | 4.17 | 46.1 | 15 | 400 | 3.06 | 0 | 0 | 71.6 |
| | 25-3-B | 251 | 4.18 | 44.4 | 15 | 400 | 3.08 | 0 | 0 | 67.7 |
| | F-25-3-A | 251 | 2.39 | 29.6 | 15 | 400 | 3.08 | 0 | 0 | 70.0 |
| | F-25-3-B | 252 | 2.38 | 30.6 | 15 | 400 | 3.06 | 0 | 0 | 77.0 |
| | F-00 | 251 | 2.39 | 13.4 | 15 | 400 | 3.08 | 0 | 0 | 47.5 |
| | P-25-3-A | 252 | 4.17 | 23.7 | 15 | 400 | 3.06 | 0 | 0 | 45.8 |
| | P-25-3-B | 251 | 4.18 | 24.8 | 15 | 400 | 3.08 | 0 | 0 | 47.0 |
| | P-25-3-C | 252 | 4.17 | 24.9 | 15 | 400 | 3.06 | 0 | 0 | 56.8 |
| | P-25-3-D | 251 | 4.18 | 28.7 | 15 | 400 | 3.08 | 0 | 0 | 53.0 |
| | FU-00 | 251 | 2.39 | 13.7 | 15 | 400 | 3.08 | 0 | 0 | 59.0 |
| | F-A | 252 | 2.38 | 20.7 | 15 | 400 | 1.18 | 0 | 0 | 50.5 |
| Kim (2000) | YJC CONT | 445 | 3.75 | 30.8 | 25 | 460 | 3.86 | 0 | 0 | 212.0 |
| Khalifa, Collins (1981) | SC0 | 445 | 2.85 | 23.4 | 0 | 516 | 3.86 | 1022 | 0.28 | 326.0 |

Table 3.2 Details and test results of specimens with circular cross-section with shear reinforcement

| Reference | Specimen | $D$ [mm] | a/$D$ [-] | $f_c$ [MPa] | $cov$ [mm] | $f_{yl}$ [MPa] | $\rho_l$ [%] | $f_{yw}$ [MPa] | $\rho_w$ [%] | $s$ [mm] | S/H | $P$ [kN] | $P/(f_c A_g)$ [-] | $V_{test}$ [kN] |
|---|---|---|---|---|---|---|---|---|---|---|---|---|---|---|
| Clarke, | M1/2 | 152 | 2.04 | 28 | 10 | 500 | 2.2 | 300 | 0.37 | 100 | H | 0 | 0 | 45.0 |
| Birjandi | M1/3 | 152 | 2.17 | 28 | 10 | 500 | 2.2 | 300 | 0.37 | 100 | H | 0 | 0 | 46.0 |
| (1993) | M1/4 | 152 | 2.24 | 28 | 10 | 500 | 2.2 | 300 | 0.37 | 100 | H | 0 | 0 | 38.0 |
| | 11-1 | 300 | 2.20 | 24.1 | 20 | 500 | 5.6 | 300 | 0.22 | 150 | H | 0 | 0 | 186.0 |
| | 11-2 | 300 | 2.20 | 24.1 | 20 | 500 | 5.6 | 300 | 0.22 | 150 | H | 0 | 0 | 188.0 |
| | 12-1 | 300 | 2.20 | 23.8 | 20 | 500 | 5.6 | 300 | 0.45 | 75 | H | 0 | 0 | 211.0 |
| | 12-2 | 300 | 2.20 | 23.8 | 20 | 500 | 5.6 | 300 | 0.45 | 75 | H | 0 | 0 | 239.0 |
| | 13-1 | 300 | 2.20 | 48.4 | 20 | 500 | 5.6 | 300 | 0.22 | 150 | H | 0 | 0 | 227.0 |
| | 13-2 | 300 | 2.20 | 48.4 | 20 | 500 | 5.6 | 300 | 0.22 | 150 | H | 0 | 0 | 228.0 |
| | 14-1 | 300 | 2.20 | 50.5 | 20 | 500 | 5.6 | 300 | 0.45 | 75 | H | 0 | 0 | 279.0 |
| | 14-2 | 300 | 2.20 | 50.5 | 20 | 500 | 5.6 | 300 | 0.45 | 75 | H | 0 | 0 | 288.0 |
| | 15-1 | 300 | 2.20 | 24.3 | 20 | 500 | 3.6 | 300 | 0.22 | 150 | H | 0 | 0 | 145.0 |
| | 15-2 | 300 | 2.20 | 24.3 | 20 | 500 | 3.6 | 300 | 0.22 | 150 | H | 0 | 0 | 148.0 |
| | 16-1 | 300 | 2.20 | 46.7 | 20 | 500 | 3.6 | 300 | 0.22 | 150 | H | 0 | 0 | 185.0 |
| | 16-2 | 300 | 2.20 | 46.7 | 20 | 500 | 3.6 | 300 | 0.22 | 150 | H | 0 | 0 | 186.0 |
| | 17-1 | 300 | 2.20 | 23.7 | 20 | 500 | 2.3 | 300 | 0.13 | 150 | H | 0 | 0 | 117.0 |
| | 17-2 | 300 | 2.20 | 23.7 | 20 | 500 | 2.3 | 300 | 0.13 | 150 | H | 0 | 0 | 115.0 |
| | 19-1 | 300 | 2.20 | 26.6 | 20 | 500 | 3.6 | 300 | 0.13 | 150 | H | 0 | 0 | 113.0 |
| | 19-2 | 300 | 2.20 | 26.6 | 20 | 500 | 3.6 | 300 | 0.13 | 150 | H | 0 | 0 | 129.0 |
| | 20-1 | 300 | 2.20 | 49.3 | 20 | 500 | 3.6 | 300 | 0.13 | 150 | H | 0 | 0 | 149.0 |
| | 20-2 | 300 | 2.20 | 49.3 | 20 | 500 | 3.6 | 300 | 0.13 | 150 | H | 0 | 0 | 137.0 |
| | 21-1 | 300 | 2.20 | 22.2 | 20 | 500 | 5.6 | 300 | 0.13 | 150 | H | 0 | 0 | 131.0 |
| | 21-2 | 300 | 2.20 | 22.2 | 20 | 500 | 5.6 | 300 | 0.13 | 150 | H | 0 | 0 | 151.0 |
| | 22-1 | 300 | 2.20 | 45.5 | 20 | 500 | 5.6 | 300 | 0.13 | 150 | H | 0 | 0 | 163.0 |
| | 22-2 | 300 | 2.20 | 45.5 | 20 | 500 | 5.6 | 300 | 0.13 | 150 | H | 0 | 0 | 164.0 |
| | 23-1 | 300 | 2.20 | 25.1 | 20 | 500 | 2.3 | 300 | 0.13 | 150 | S | 0 | 0 | 101.0 |
| | 23-2 | 300 | 2.20 | 25.1 | 20 | 500 | 2.3 | 300 | 0.13 | 150 | S | 0 | 0 | 113.0 |
| | 24-1 | 300 | 2.20 | 48.9 | 20 | 500 | 2.3 | 300 | 0.13 | 150 | S | 0 | 0 | 114.0 |
| | 24-2 | 300 | 2.20 | 48.9 | 20 | 500 | 2.3 | 300 | 0.13 | 150 | S | 0 | 0 | 128.0 |
| | 25-1 | 300 | 2.20 | 24.3 | 20 | 500 | 3.6 | 300 | 0.13 | 150 | S | 0 | 0 | 98.0 |
| | 25-2 | 300 | 2.20 | 24.3 | 20 | 500 | 3.6 | 300 | 0.13 | 150 | S | 0 | 0 | 122.0 |
| | 26-1 | 300 | 2.20 | 47.1 | 20 | 500 | 3.6 | 300 | 0.13 | 150 | S | 0 | 0 | 114.0 |
| | 26-2 | 300 | 2.20 | 47.1 | 20 | 500 | 3.6 | 300 | 0.13 | 150 | S | 0 | 0 | 150.0 |
| | 27-1 | 300 | 2.20 | 22.8 | 20 | 500 | 5.6 | 300 | 0.13 | 150 | S | 0 | 0 | 125.0 |
| | 27-2 | 300 | 2.20 | 22.8 | 20 | 500 | 5.6 | 300 | 0.13 | 150 | S | 0 | 0 | 134.0 |
| | 28-1 | 300 | 2.20 | 45.3 | 20 | 500 | 5.6 | 300 | 0.13 | 150 | S | 0 | 0 | 158.0 |
| | 28-2 | 300 | 2.20 | 45.3 | 20 | 500 | 5.6 | 300 | 0.13 | 150 | S | 0 | 0 | 175.0 |
| | 37-1 | 300 | 2.20 | 43.9 | 20 | 500 | 5.6 | 300 | 0.22 | 150 | H | 270.9 | 0.09 | 232.0 |
| | 37-2 | 300 | 2.20 | 43.9 | 20 | 500 | 5.6 | 300 | 0.22 | 150 | H | 0 | 0 | 218.0 |
| | 38-1 | 300 | 2.20 | 36.1 | 20 | 500 | 5.6 | 300 | 0.22 | 150 | H | 270.9 | 0.11 | 209.0 |
| | 38-2 | 300 | 2.20 | 36.1 | 20 | 500 | 5.6 | 300 | 0.22 | 150 | H | 0 | 0 | 206.0 |
| | 39-1 | 300 | 2.20 | 36.3 | 20 | 500 | 5.6 | 300 | 0.22 | 150 | H | 270.6 | 0.11 | 217.2 |
| | 39-2 | 300 | 2.20 | 36.3 | 20 | 500 | 5.6 | 300 | 0.22 | 150 | H | 0 | 0 | 197.0 |
| | 40-1 | 300 | 2.20 | 34.1 | 20 | 500 | 5.6 | 300 | 0.22 | 150 | H | 274.1 | 0.11 | 225.0 |
| | 40-2 | 300 | 2.20 | 34.1 | 20 | 500 | 5.6 | 300 | 0.22 | 150 | H | 0 | 0 | 183.0 |
| | 43-1 | 500 | 2.40 | 37.8 | 20 | 500 | 2.6 | 300 | 0.14 | 140 | H | 0 | 0 | 313.0 |
| | 43-2 | 500 | 2.40 | 37.8 | 20 | 500 | 2.6 | 300 | 0.14 | 140 | H | 0 | 0 | 366.0 |
| | 44-1 | 500 | 2.40 | 32.9 | 20 | 500 | 2.6 | 300 | 0.14 | 140 | H | 0 | 0 | 301.0 |
| | 44-2 | 500 | 2.40 | 32.9 | 20 | 500 | 2.6 | 300 | 0.14 | 140 | H | 0 | 0 | 329.0 |

Table 3.2 (Continued)

| Reference | Specimen | $D$ [mm] | a/$D$ [-] | $f'_c$ [MPa] | $cov$ [mm] | $f_{yl}$ [MPa] | $\rho_l$ [%] | $f_{yw}$ [MPa] | $\rho_w$ [%] | $s$ [mm] | S/H | $P$ [kN] | $P/(f_cA_g)$ [-] | $V_{test}$ [kN] |
|---|---|---|---|---|---|---|---|---|---|---|---|---|---|---|
| Khalifa, Collins (1981) | SC1 | 445 | 2.85 | 19.3 | 23 | 516 | 3.79 | 410 | 0.10 | 150 | H | 1017 | 0.34 | 324.0 |
| | SC2 | 445 | 2.85 | 23 | 23 | 516 | 3. 79 | 510 | 0.30 | 150 | H | 1083 | 0.30 | 478.0 |
| | SC3 | 445 | 2.85 | 24.5 | 23 | 516 | 3. 79 | 510 | 0.45 | 100 | H | 1085 | 0.28 | 578.0 |
| | SC4 | 445 | 2.85 | 26.5 | 23 | 516 | 3. 79 | 430 | 0.30 | 150 | H | 1050 | 0.25 | 456.0 |
| Merta et al. (2003) | 1 | 400 | 2.50 | 42.20 | 0 | 700 | 3.75 | 700 | 0.24 | 60 | S | 0 | 0 | 430.0 |
| | 2 | 400 | 2.50 | 42.20 | 0 | 700 | 3.75 | 700 | 0.24 | 60 | S | 0 | 0 | 432.0 |
| Capon, de Cossio (1965) | F-25 | 251 | 2.39 | 13.2 | 15 | 400 | 3.08 | 250 | 0.10 | 250 | H | 0 | 0 | 59.5 |
| | F-12.5 | 251 | 2.39 | 13.1 | 15 | 400 | 3.08 | 250 | 0.20 | 125 | H | 0 | 0 | 82.0 |
| Kim (2000) | YJC200R | 445 | 3.75 | 40.4 | 25 | 460 | 3.86 | 445 | 0.16 | 200 | S | 0 | 0 | 323.0 |
| | YJC150R | 445 | 3.75 | 36 | 25 | 460 | 3.86 | 445 | 0.21 | 150 | S | 0 | 0 | 411.0 |
| | YJC100R | 445 | 3.75 | 36 | 25 | 460 | 3.86 | 445 | 0.32 | 100 | S | 0 | 0 | 479.0 |
| | YJC200W | 445 | 3.75 | 33.2 | 25 | 460 | 3.86 | 1728 | 0.05 | 200 | S | 0 | 0 | 315.0 |
| | YJC100W | 445 | 3.75 | 36 | 25 | 460 | 3.86 | 1728 | 0.10 | 100 | S | 0 | 0 | 434.0 |

The meaning of the symbols used in the tables:

$D$ = gross column diameter;

$a/D$ = members aspect ratio (shear span-to-depth ratio);

$f'_c$ = cylinder compressive strength of concrete;

$A_g$ = gross section area;

$cov$ = concrete cover;

$f_{yl}$ = longitudinal reinforcement yield strength;

$\rho_l$ = longitudinal reinforcement ratio;

$f_{yw}$ = transverse reinforcement yield strength;

$\rho_w$ = transverse reinforcement ratio;

$s$ = spacing of shear reinforcement along the member's longitudinal axis;

S/H = spiral/hoop transverse reinforcement;

$P$ = axial load (compression is positive);

$V_{test}$ = experimental (observed) shear force.

# 4 PROPOSED SHEAR MODEL FOR CIRCULAR SECTIONS

## 4.1 Introduction

In this chapter a shear strength model for circular section members has been developed resulting from the continuous improvements of the recently proposed model (Merta, 2004; Merta, 2004a). The proposed shear capacity model is a semi-empirical equation based on the truss analogy by adding an empirical concrete contribution term to the capacity of the shear reinforcement.

The concrete shear capacity, taken as the capacity of the member without shear reinforcement, has been derived by a parameter study of the variables affecting shear strength and by applying a curve fit on the database of the members without shear reinforcement (Table 3.1). The shear reinforcement capacity is derived analytically, based on the truss analogy, by taking into account the identified additional deviatoric shear resisting mechanism of hoops present only by members with curved transverse reinforcement. Based on the shear database of transversely reinforced circular members (Table 3.2), the validity and accuracy of the proposed model have been compared to other recently proposed models.

## 4.2 Shear Transfer Mechanism in Concrete

The principal shear transfer mechanisms in reinforced concrete members identified by ACI-ASCE Committee 426 (1973) are the following: shear transfer by uncracked compression concrete above the top of the diagonal crack $V_{cz}$, interface shear transfer along the diagonal crack or aggregate interlock $V_a$, shear carried by the longitudinal reinforcement (dowel action) $V_d$, tension in shear reinforcement $V_s$ and the arch action, see Figure 4.1. The contributions of individual shear mechanism $V_{cz}$, $V_d$ and $V_{ay}$ are interdependent and not easy to separate and model. Therefore the most modern design procedures collect these three components into one term, namely into the shear "carried by the concrete", denoted by $V_c$. The whole shear transfer mechanism is then added together from the shear carried by concrete and from the shear carried by shear reinforcement $V_s$ (McGregor, 2005).

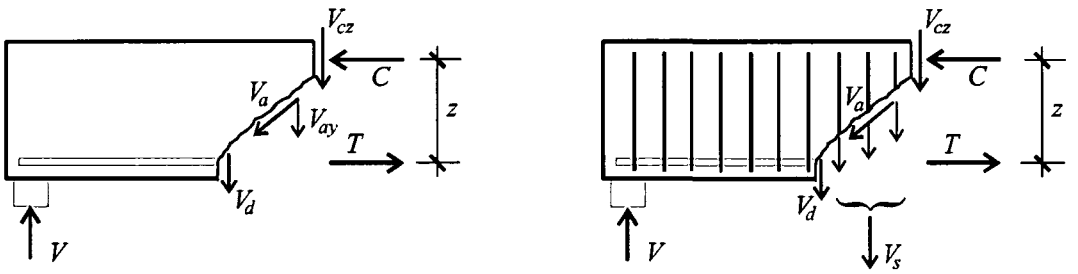


Figure 4.1 Components of shear strength in a beam without and with shear reinforcement

## 4.3 Evaluation of Concrete Shear Capacity

Shear failure in concrete members is a diagonal tension phenomenon. As the value of the diagonal tension stress is difficult to determine, the shear strength prediction of reinforced concrete members without shear reinforcement is based on the assumption that shear failure at the critical section occurs on a vertical plane when the fictitious shear stress at the section

$$v = \frac{V_c}{A_{seff}} \tag{4.1}$$

exceeds the concrete nominal shear strength. Here $A_{seff}$ is the so called "effective shear area" and for rectangular sections it represents the area corresponding to the effective depth.

However, for circular sections the term "effective shear area" is not defined as unambiguously. Different empirical proposals have been suggested recently, based either on experimental observations or intuitive estimations, but no analytical solution exists so far in literature. As a part of this research in the following chapter the effective shear area for circular sections has been derived on the base of a detailed analytical calculation.

The shear capacity of a member without shear reinforcement is influenced by various parameters such as: cross section shape, concrete strength, longitudinal reinforcement ratio, members shear span-to-depth ratio or aspect ratio, axial load level, type of loading (monotonic, cyclic...), axial load level, cross section size and shape, maximum aggregate size and spacing of the flexural cracks. Nevertheless, it is widely accepted that the main variables affecting the section's shear capacity without shear reinforcement are the concrete compressive strength, $f_c'$, longitudinal reinforcement ratio, $\rho_l$, aspect ratio, $a/D$, and axial load level, $P$. In the proposed model these four main variables will be considered and the concrete shear strength has been proposed by an equation of form

$$v = \frac{V_c}{A_{seff}} = \left[f(\rho_l) + f(P)\right] \cdot f(a/D) \cdot f(f_c') \tag{4.2}$$

The functions $f(\rho_l)$, $f(P)$, $f(a/D)$ and $f(f_c')$ describe the influence of the main variables. They will be determined empirically, based on test data of members without shear reinforcement (Table 3.1). By segregation of the data with respect to a particular variable, and maintaining all other variables constant, a curve fit has been applied and the influence of the individual parameter derived.

### 4.3.1 Effective Shear Area of Circular Sections

This chapter is based on the paper: Merta, I., Kolbitsch, A. (2006), "Analytical Evaluation of the Effective Area of Reinforced Concrete Circular Sections under Shear", published in the proceedings of the *Tenth East Asia-Pacific Conference on Structural Engineering and Construction, EASEC-10,* Bangkok, Thailand, 3-5 August 2006.

**Tenth East Asia-Pacific Conference on Structural Engineering and Construction**
**EASEC-10**
Bangkok, Thailand, 3-5 August 2006

# ANALYTICAL EVALUATION OF THE EFFECTIVE AREA OF REINFORCED CONCRETE CIRCULAR SECTIONS UNDER SHEAR

**Ildiko MERTA[1], Andreas KOLBITSCH[2]**

## SUMMARY

The shear strength of reinforced concrete members without shear reinforcement is related to the shear stress carried by the concrete effective shear area. For rectangular sections the effective shear area represents the area corresponding to the effective depth. However, for circular sections this area is not as readily defined. Different empirical proposals have been suggested recently but no analytical solution exists so far in literature. In this work the effective shear area of circular sections has been derived purely analytically. The ratio of the effective shear area to gross section area was expressed as a function of the neutral axis depth for different values of the concrete cover. For a typical value of neutral axis depth, it was shown that the effective shear area ranges between 0.6 and 0.8 times the sections gross area depending on the depth of the concrete cover. Thus, an average value of 0.7 seems to be a reasonably accurate value for design purposes and, moreover, it is in good agreement with other recent proposals.

## 1. INTRODUCTION

Reinforced concrete (RC) structural elements of circular cross-section are widely used in different types of structures. Because of their identical strength characteristics in all directions they are preferred as building or bridge columns, secant pilings forming diaphragm walls or as foundations of buildings. Columns are predominantly axial load carrying elements. However, as a result of lateral loads due to wind pressure, earthquake or vehicle impact, they are subjected to considerable shear loads. Thus, columns should be inevitable designed to suppress a possible shear failure. The sections geometry (rectangular, T- or circular cross-section) strongly influences the members shear capacity. It determines the area that effectively resists the external shear load.

According to most design codes [1, 2] the shear capacity of RC sections is added together from the so called concrete capacity term and from the capacity of the shear reinforcement. The concrete shear capacity, $V_c$, is usually defined as the shear capacity of the section without transverse reinforcement and is calculated as

$$V_c = v \cdot A_{seff} \tag{1}$$

where $v$ is the sections nominal shear strength and $A_{seff}$ its effective shear area. Whereas for rectangular sections the effective shear area is clearly defined as the area corresponding to the effective depth, i.e. the product of the sections width and the effective depth, for circular sections this definition is not so distinctive.

The European code for design of RC structures [Eurocode 2, 1992], does not give any guidelines about the area that should be considered in case of circular sections. The American code [ACI 318M-02, 2002] recommends to

[1] Vienna University of Technology, Institute for Building Construction and Technology, Karlsplatz 13/206/4, A-1040 Vienna, Austria
Email: imerta@hochbau.tuwien.ac.at
[2] Vienna University of Technology, Institute for Building Construction and Technology, Karlsplatz 13/206/4, A-1040 Vienna, Austria
Email: kolbitsch@hochbau.tuwien.ac.at

calculate the effective shear area by circular sections as the product of the diameter and the effective depth, where the effective depth is permitted to be taken as at least 0.8 times the diameter of the concrete section. Ang et al. [Ang et al., 1989] as well as Priestley et al. [Priestley et al., 1994] noted that in such a way there is an apparent discrepancy between rectangular and circular section design. Namely, the effective shear area of circular sections is $0.8 \cdot D^2 = 1.02 \cdot A_g$, where $A_g$ is the sections gross area and $D$ the sections diameter, and consequently the effective shear area exceeds the sections gross area. Ang et al. [Ang et al., 1989] and Priestley et al. [Priestley et al., 1994] suggested taking $0.8A_g$ for the effective shear area, which approximately corresponds to the area of the confined concrete core. Clarke and Birjandi [Clarke and Birjandi, 1993] and Feltham [Feltham, 2004] proposed to take the area of concrete from the extreme compression fibre down to the depth, where the depth was estimated with $0.81D$. Capon and de Cossio [Capon and de Cossio, 1965] employed the sections gross area, which they based on test results of circular members under shear. All existent proposals are empirical, based either on experimental observations or intuitive estimations, but no analytical solution of the effective shear area of circular sections has been derived until yet. The objective of this paper was, thus, to derive the effective shear area of circular sections analytically.

## 2. EFFECTIVE SHEAR AREA OF CIRCULAR SECTIONS

Consider a RC member of circular cross-section with longitudinal reinforcement bars uniformly distributed along the sections perimeter (see Figure 1(a)). Under a positive bending moment the part of the section below the neutral axis is under tension and the part above under compression. Consistent with the design of rectangular sections and with recent proposals [Clarke and Birjandi, 1993 and Feltham, 2004] the effective shear area, $A_{seff}$, has been defined as the area corresponding to the effective depth, $d$. For the effective depth, the distance from the sections extreme compression fiber to the centroid of the longitudinal bars under tension ($C_T$) was taken. However, the position of the centroid of tension bars depends on the position of the neutral axis within the section. Consequently, for the determination of the centroid, the moment of each single tension bar about a selected reference axis (e.g. neutral axis) should be summed up. To overcome the deficiency of the current time-consuming calculation a different approach is proposed.

The discretely distributed longitudinal bars in the section have been rearranged in continuous distribution in form of a reinforcement ring (or tube in longitudinal direction) with the same cross-sectional area (or volume) as the sum (volume) of all bars in the section (see Figure 1). In that way, the centroid of the tension bars could be simply determined by calculating the center of gravity of the part of the reinforcement ring under tension. From the condition that the cross-sectional area of discretely distributed longitudinal reinforcement

$$A_l = \rho_l \, D^2 \pi / 4 \tag{2}$$

and the cross-sectional area of continuously distributed reinforcement

$$A_d = (D/2 - cov)^2 \, \pi - (D/2 - cov - a)^2 \, \pi \tag{3}$$

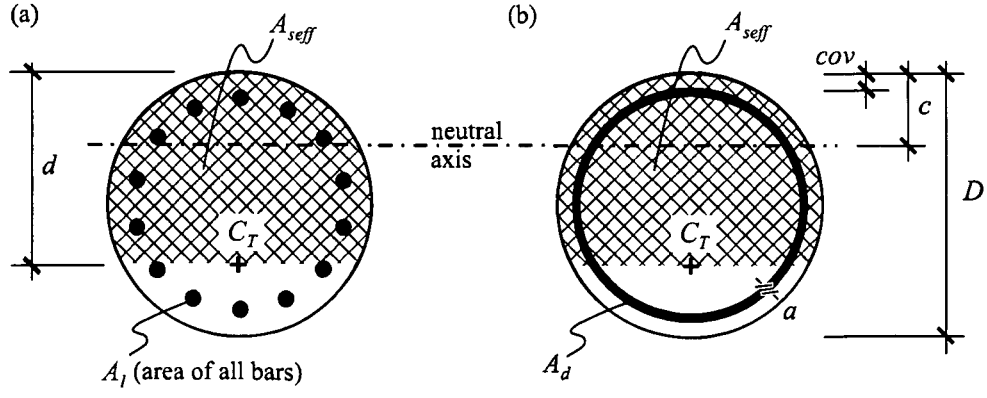


**Figure 1: (a) Discretely distributed longitudinal reinforcement, and (b) continuously distributed reinforcement**

within the section remains unchanged, $A_l = A_d$, the thickness of the reinforcement ring is calculated

$$a = -\frac{D}{2} + cov + \frac{1}{2}\sqrt{(D - 2 \cdot cov)^2 + \rho_l \cdot D^2} \tag{4}$$

where $D$ is the diameter of the section, $cov$ the depth of the concrete cover, and $\rho_l$ the longitudinal reinforcement ratio.

The next step is to calculate the center of gravity of the part of the reinforcement ring that is under tension. It represents a ring segment. However, for easier calculation a ring sector will be considered (see Figure 2(a)), inducing a negligible error in calculation, resulting from the difference between the locations of the centroids of two geometric figures. The distance of the centre of gravity of the ring sector from the sections bottom fibre, $y_T$, will be derived by means of the static moment of an infinitesimal ring sector area, $dA$, about the sections bottom fiber. The area of the infinitesimal ring sector element, $dA$, is calculated by subtracting the area of the circular sector element, $dA_1$, with radius $r_1$ from the area of the circular sector element, $dA_2$, with radius $r_2$ (see Figure 2(b)). Thus the center of gravity is located at

$$y_T = \frac{\int_{\alpha}^{2\pi-\alpha} y_2 \, dA_2 - \int_{\alpha}^{2\pi-\alpha} y_1 \, dA_1}{\int_{\alpha}^{2\pi-\alpha} dA_2 - \int_{\alpha}^{2\pi-\alpha} dA_1} \tag{5}$$

where the angle $\alpha$ is defined as

$$\alpha = \arccos\left(\frac{D/2 - c}{D/2 - cov}\right) \tag{6}$$

For an infinitesimal angle $d\varphi$, it is allowed to replace the circular sector element with a rectangular triangle of basis $r_i \, d\varphi$ and height $r_i$. The area of the triangle is

$$dA_i = \frac{1}{2} r_i^2 d\varphi \qquad (i = 1,2) \tag{7}$$

and its center of gravity is at 2/3 of its height. Thus, the distance of the center of gravity of the element $dA_i$ from the sections bottom fibre is

$$y_i = \frac{D}{2} + \frac{2}{3} r_i \cos\varphi \qquad (i = 1,2) \tag{8}$$

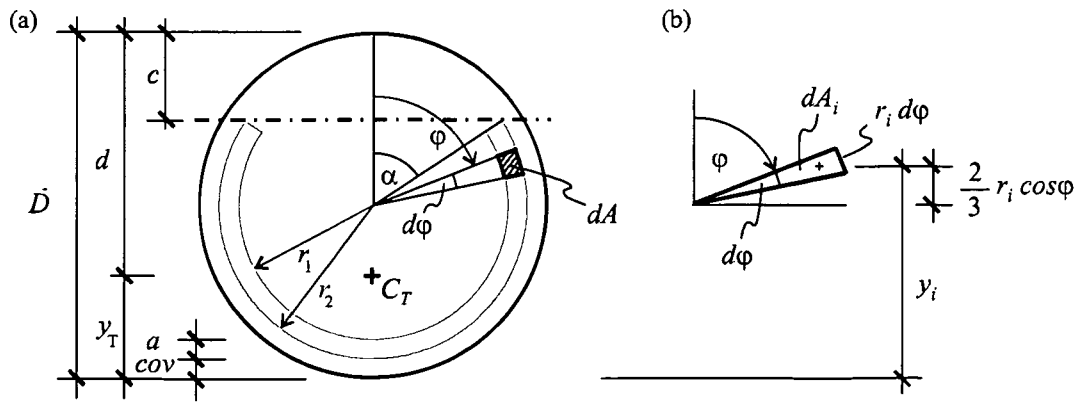


**Figure 2: (a) Reinforcement ring sector under tension, and (b) Infinitesimal circular sector element, $dA_i$**

The index $i$ corresponds to the circular sector of radius $r_1$ and $r_2$, respectively. Substituting Equations (7) and (8) into Equation (5) and solving it, the distance of the center of gravity of the ring sector from the sections bottom fibre is obtained as

$$y_T = \frac{D}{2} + \frac{2}{3}\frac{\left(r_2^3 - r_1^3\right)}{\left(r_2^2 - r_1^2\right)}\frac{\int_{\alpha}^{2\pi-\alpha} \cos\varphi \cdot d\varphi}{\int_{\alpha}^{2\pi-\alpha} d\varphi} \tag{9}$$

$$y_T = \frac{D}{2} - \frac{2}{3}\frac{\sin\alpha\left(r_2^3 - r_1^3\right)}{(\pi-\alpha)\left(r_2^2 - r_1^2\right)} \tag{10}$$

where

$$r_1 = \frac{D}{2} - cov - a \tag{11}$$

and

$$r_2 = \frac{D}{2} - cov \tag{12}$$

The last term in Equation (10) is negative and, hence, subtracted from the sections radius $D/2$. It follows that the center of gravity, $C_T$, lies always under the horizontal symmetry axis of the section. Finally, the sections effective depth is equal to $d = D - y_T$ or

$$d = \frac{D}{2} + \frac{2}{3}\frac{\sin\alpha\left(r_2^3 - r_1^3\right)}{(\pi-\alpha)\left(r_2^2 - r_1^2\right)} \tag{13}$$

Equation (13) in combination with Equations (4), (6), (11) and (12), enables the calculation of the effective depth of circular sections with known geometries – diameter of the section, $D$, depth of the concrete cover, $cov$, longitudinal reinforcement ratio, $\rho_l$, and neutral axis depth, $c$.

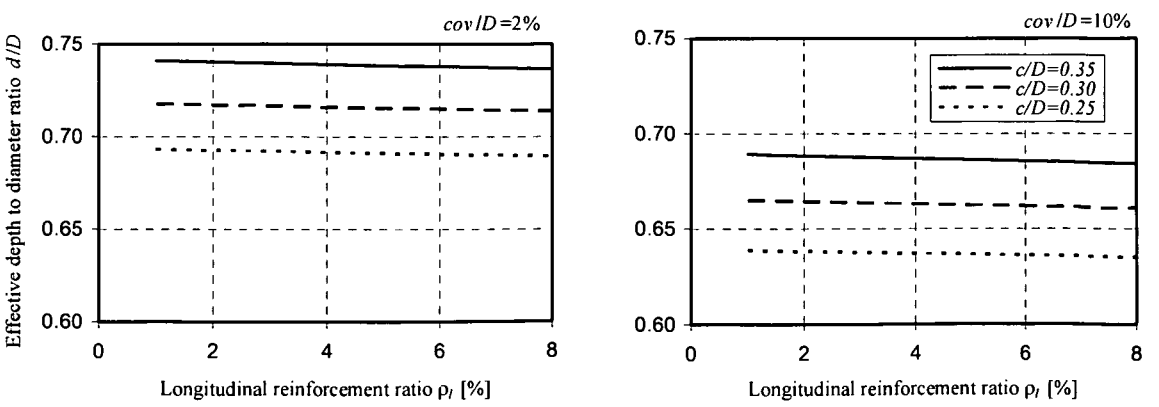


**Figure 3: Sections effective depth to diameter ratio, $d/D$, versus longitudinal reinforcement ratio, $\rho_l$, for various ratios of concrete cover to diameter, $cov/D$ (left: $cov/D$ = 2% and right: $cov/D$ = 10%)**

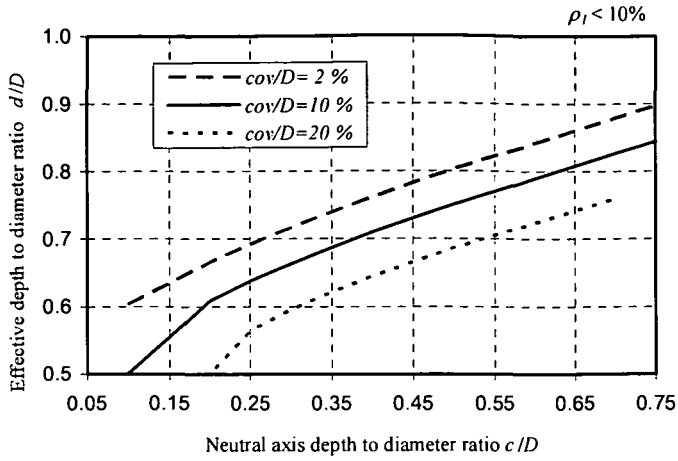


**Figure 4: Sections effective depth to diameter ratio *d/D* versus neutral axis depth to diameter ratio *c/D* for various *cov/D* ratios ($\rho_l < 10\%$)**

To reduce the number of variables, the ratio of concrete cover to diameter, *cov/D*, has been introduced. Further, the sections effective depth to diameter ratio, *d/D*, is plotted versus longitudinal reinforcement ratio, $\rho_l$, for various neutral axis depths, *c/D*, and concrete cover to diameter ratios, *cov/D* (see Figure 3). Note, that within a definite *cov/D* ratio and for normally RC sections ($\rho_l < 10\%$), the longitudinal reinforcement ratio does not have a significant influence on the sections effective depth to diameter ratio, *d/D*. Hence, its influence could be neglected without greater influence on the accuracy of the final result. Omitting the reinforcement ratio variable, the sections effective depth to diameter ratio, *d/D*, is expressed as a function of two variables, i.e., neutral axis depth to diameter ratio, *c/D*, and concrete cover to diameter ratio, *cov/D* (see Figure 4).

Further, if the sections effective depth is known, the area corresponding to it, i.e., the effective shear area, $A_{seff}$, could be determined as

$$A_{seff} = \frac{D^2\pi}{4} - \frac{D^2[2\beta - \sin(2\beta)]}{8} \tag{14}$$

where $\beta$ is (see Figure 5) defined as

$$\cos\beta = \frac{2d}{D} - 1 \tag{15}$$

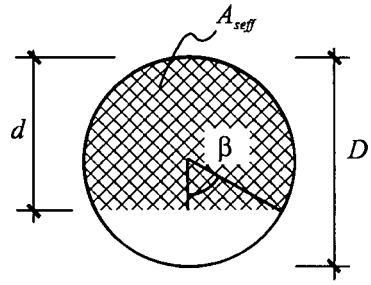


**Figure 5: Effective shear area of a circular section**

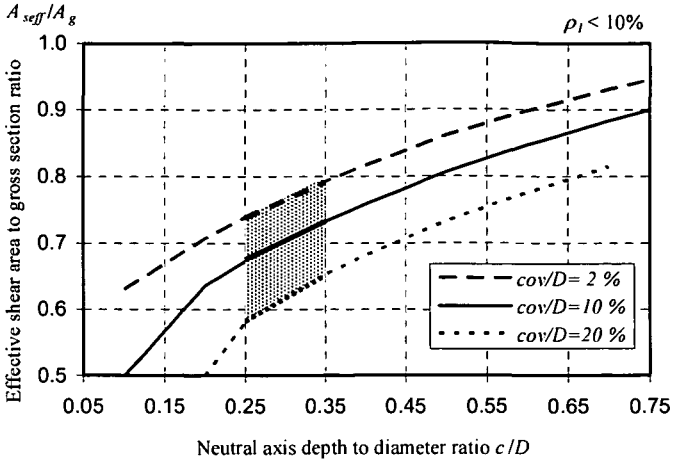


**Figure 6: Sections effective shear area to gross section ratio $A_{seff}/A_g$ versus neutral axis depth to diameter ratio *c/D* for various *cov/D* ratios ($\rho_l < 10\%$)**

The effective shear area has been expressed as a ratio to the sections gross area, $A_g$, and plotted for various neutral axis depths, *c/D*, and concrete covers, *cov/D* (see Figure 6).

Generally, the sections neutral axis depth, *c*, is known from the flexural analysis. Kowalsky and Priestley [Kowalsky and Priestley, 2000] observed that for circular sections the typical value of the ratio of the neutral axis depth and the diameter, *c/D*, is about 0.25 to 0.35. Within these limits of neutral axis depth, the ratio of the effective shear area to gross sections area ranges between 0.6 and 0.8, depending on the depth of the concrete cover, *cov/D*.

Concerning further the most frequent value of concrete cover to diameter ratio in practice of about *cov/D*=10%, the ratio of $A_{seff}$ to $A_g$ is further limited between 0.67 and 0.73. Taking the mean value of 0.7, the effective shear area of circular sections is proposed as

$$A_{seff} = 0.7 \cdot A_g = 0.7 \cdot \frac{D^2 \pi}{4} \tag{16}$$

The proposed expression (Equation (16)) is valid for circular sections, where the longitudinal reinforcement is uniformly distributed along the sections perimeter and consequently its influence could be replaced with a reinforcement ring. The obtained effective shear area of $0.7A_g$ is somewhat lower than the recent proposals of $0.8A_g$ [Ang et al., 1989 and Priestley et al., 1994]. However, the advantage of the proposed approach is that it is analytical and, thus, gives an exact solution of the effective shear area of circular sections. Moreover, it enables to determine the shear area of circular sections for various geometries (sections diameter and concrete cover depth) as well as for various neutral axis depths resulting from different loading situations of the member.

## 3. CONCLUSION

In the present work the effective shear area of RC circular sections has been proposed based on an analytical derivation. The effective shear area was defined as the area corresponding to the effective depth, which in turn is taken as the distance from the sections extreme compression fiber to the centroid of the longitudinal reinforcement bars under tension.

The ratio of the effective shear area to the sections gross area has been expressed as a function of the neutral axis- and concrete cover depth. Only the variables most typical ranges, appearing in practice, have been considered and it was found that the shear area ranges between 0.6 and 0.8 times the sections gross area. For design purposes a value of 0.7 is proposed, which is in good agreement with other existing works.

## 4. REFERENCES


ACI 318M-02 and Commentary ACI 318RM-02 (2002), Building Code Requirements for Structural Concrete, American Concrete Institute, Farmington Hills, Michigan.

Ang, B.G.,Priestley, M.J.N., Paulay, T. (1989), Seismic Shear Strength of Circular Reinforced Concrete Columns, *ACI Structural Journal*, American Concrete Institute, V. 86, No. 1, pp. 45-59.

Capon, M.J.F., de Cossio, R.D. (1965), Diagonal Tension in Concrete Members of Circular Section, *Ingenieria, Mexico*, pp. 257-280, (Translation by Portland Cement Association, Foreign Literature Study No. 466, 1966).

Clarke, J.L., Birjandi, F.K. (1993), The Behaviour of Reinforced Concrete Circular Sections in Shear, *The Structural Engineer*, Institution of Structural Engineers, V. 71, No. 5, pp. 73-81.

Eurocode 2 - Design of Concrete Structures (1992): ENV1992-1-1: Part 1.1: General rules and rules for buildings, CEN.

Feltham, I. (2004), Shear in Reinforced Concrete Piles and Circular Columns, *The Structural Engineer*, V. 82, No. 11, pp. 27-31.

Kowalsky, M.J., Priestley, M.J.N. (2000), Improved Analytical Model for Shear Strength of Circular Reinforced Concrete Columns in Seismic Regions, *Structural Journal*, American Concrete Institute, V. 97, No. 3, pp. 388-396.

Priestley, M.J.N., Verma, R., Xiao,Y. (1994), Seismic Shear Strength of Circular Reinforced Concrete Columns, *Journal of Structural Engineering*, ASCE, V. 120, No. 8, pp. 2310-2329.

### 4.3.2 Effect of Concrete Strength

One of the main parameters that influence the members' shear strength is concrete strength. In the early stage of knowledge (in the years 1900-1950) the shear capacity was exclusively addressed to concrete compressive strength. The intensive research on shear in the years 1950-1970 showed that, since shear failure is a diagonal shear failure, the concrete shear strength is in better correlation with the concrete tensile strength than with its compressive strength. Paw's (1960) observation that the concrete tensile strength is approximately proportional to the square root of the compressive strength is today widely accepted and introduced in most Codes (Park and Paulay, 1975; ACI-318M-02, 2002). Based on a statistically derived equation, Zsutty (1968) proposed to relate the shear strength to $(f_c')^{1/3}$. In Eurocode 2 (1992) it is defined as $(f_c')^{2/3}$. Desai (2004) proposed that the concrete nominal shear strength should be defined by splitting tensile strength. In high strength concrete the cracks intersect the aggregate particles and the crack surface thus is relatively smooth. Consequently the shear resistance due to aggregate interlock will be relatively lower in high strength concrete than in normal strength concrete (Vecchio et al., 1994; Elzanaty et al., 1986).

In the proposed model the effect of concrete strength has been accounted for with the square root of concrete compressive strength, $\sqrt{f_c'}$. Substituting further the influence of the concrete compressive strength into the Equation 4.2 as well as the effective shear area (Equation 16) derived in chapter 4.3.1, the shear force carried by concrete could be expressed as

$$V_c = \left[f(\rho_l) + f(P)\right] \cdot f(a/D) \cdot \sqrt{f_c'} \cdot 0.7 \cdot A_g \tag{4.17}$$

### 4.3.3 Effect of Longitudinal Reinforcement

Previous studies on rectangular sections have reported that the percentage of longitudinal reinforcement has considerable influence on the concrete shear strength (Kani, 1966; Krefeld et al., 1966; Elzanaty et al., 1986). For all concrete strengths with an increasing longitudinal reinforcement ratio the specimens' shear strength increased. The same is valid for circular sections. Nevertheless, there have been opposite observations for circular sections reported by Priestley and Benzoni (1996), according to which the shear strength of circular columns does not appear to be influenced with the longitudinal reinforcement ratio. This was corrected later by Kowalsky and Preistley (2000).

Segregating the test data of circular sections without shear reinforcement (Table 3.1) by concrete compressive strength and aspect ratio, there is an obvious increasing trend in shear capacity with an increasing longitudinal reinforcement ratio, see Figure 4.8. It is based on the fact that by increasing longitudinal reinforcement ratio, $\rho_l$, the dowel area and consequently the dowel capacity of the member increase as well. Since the cracks' width and height are also governed by $\rho_l$, the aggregate interlock capacity is enhanced by increase of $\rho_l$. The higher $\rho_l$, the shorter and narrower the cracks. In Figure 4.9 the data are further separated by axial load and aspect ratio and the normalized shear strength versus longitudinal reinforcement ratio is plotted. An enhancement of shear capacity is obvious as $\rho_l$ increases.

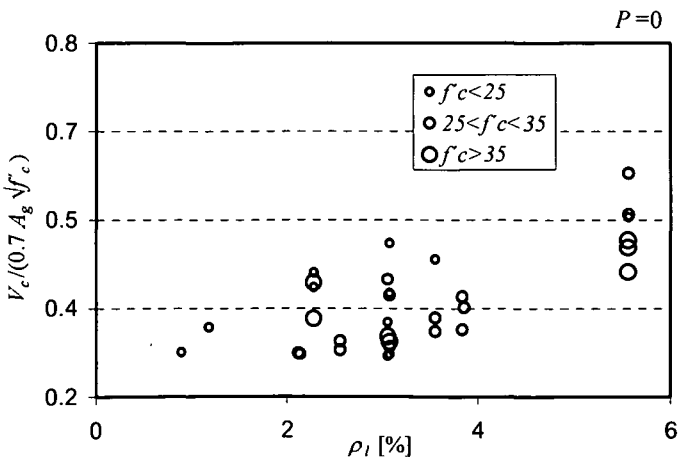


Figure 4.8 Effect of longitudinal reinforcement ratio, $\rho_l$, on normalized shear strength

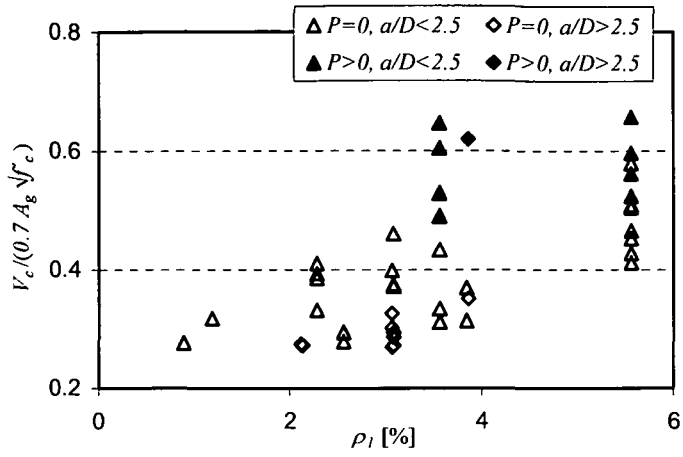


Figure 4.9 Effect of longitudinal reinforcement ratio, $\rho_l$, on normalized shear strength for specimens with different aspect ratio, $a/D$, and axial load, $P$

The actual influence of the longitudinal reinforcement ratio on shear strength could be expressed only when all other variables affecting shear strength are maintained constant. In order to eliminate the beneficial effect of both the compressive axial load and the low shear span-to-depth ratio on the shear strength, specimens without axial load and shear span-to--depth ratio higher than 2.5 have been selected. In such a way the influence function of the axial load is $f(P)=0$, and the one of the shear span-to-depth ratio is $f(a/D)=1$. Further, the members' experimental shear capacity is normalized with respect to concrete compression strength and the results are plotted in Figure 4.10.

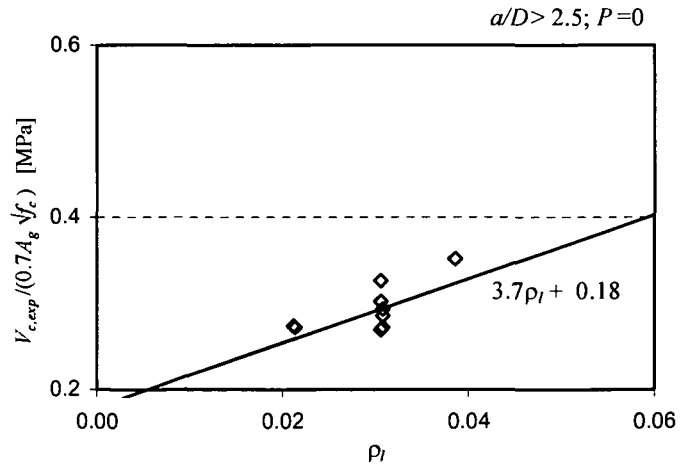


Figure 4.10 Normalized shear strength versus longitudinal reinforcement ratio

Through the points the best fit function is expressed

$$f(\rho_l) = 3.7\rho_l + 0.18 \tag{4.18}$$

Concerning the influence of the longitudinal reinforcement yield strength on shear capacity of the member, researchers (Mathey and Watstein, 1963) reported that the shear strength at the diagonal cracking load was not influenced by the yield strength of longitudinal reinforcement. This conclusion is adopted also in the report of the ACI-ASCE Committee 426, (1973). Kani (1966) also pointed out that the longitudinal reinforcement yield strength should not have any influence on concrete shear capacity since the diagonal failure occurs regularly before the reinforcement yield strength has been reached.

To investigate the influence of the longitudinal reinforcement yield strength on concrete shear capacity, the data are segregated first by axial load ratio and additionally by shear span-to-depth ratio, see Figure 4.11. However, the range of data was insufficient to determine whether the influence of the reinforcement yield strength is significant and thus no firm conclusion could be made about the trend. Further experiments should be carried out with systematically varying the reinforcement strength over a wide range, by keeping other variables constant. In the proposed model the longitudinal reinforcement yield strength was not introduced as a variable.

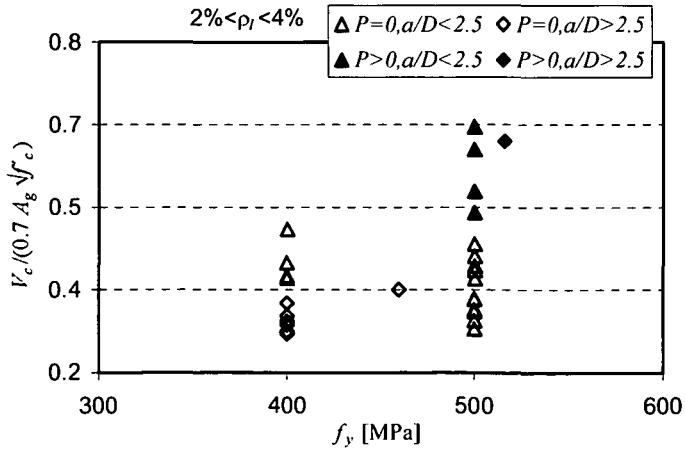


Figure 4.11 Effect of longitudinal reinforcement yield strength on normalized shear strength

### 4.3.4 Effect of Shear Span-to-Depth Ratio

It has been known for a long time that the shear span-to-depth ratio, *a/d*, or aspect ratio, has a considerable influence on the members' shear strength. In 1907 Talbot showed the influence of span length on ultimate shear stress. But only in 1951 did Clark introduce and incorporate the important parameter *a/d* into an empirical formula. The conclusion of all tests was that with an increasing aspect ratio the shear strength of the element decreases. A very important observation was reported by Kani (1966), namely that members are sensitive of shear failure if the aspect ratio ranges within $a/d = 1$ and $a/d = 6.5$. He called this region "valley of diagonal shear failure". Outside this region, failure occurs after the members' flexural capacity has been reached. He also observed that at $a/d = 2.5$ a turning point occurs and the laws governing the shear strength of members with $a/d < 2.5$ and $a/d > 2.5$ are completely different. For $a/d < 2.5$ or squat members, the shear strength of the member is governed by arch action, which means that the applied load is directly transferred to the support by a concrete strut. Short members can sustain a very significant additional load beyond the formation of the first diagonal crack before total failure. These members fail in shear-compression. Conversely, long members where $a/d > 2.5$ fail suddenly almost immediately after the formation of the first major diagonal crack.

In circular sections, the diameter, *D*, is usually employed instead of members' effective depth, *d*. Selecting from the database only members without axial load, i.e. $f(P) = 0$, and with a similar longitudinal reinforcement ratio, it could be noted that with an increasing aspect ratio the member shear capacity considerably decreases (Figure 4.12). In order to determine solely the influence of the aspect ratio on shear strength, the experimental shear capacity should be further normalized with respect to longitudinal reinforcement ratio as follows

$$f(a/D) = \frac{V_c}{(\sqrt{f_c'} \cdot 0.7 A_g)(3.7\rho_l + 0.18)} \tag{4.19}$$

The obtained normalized shear strength versus aspect ratio is plotted in Figure 4.13. There is an obvious shear capacity enhancement as the aspect ratio reaches 2.5, but no data are available for aspect ratios lower than 2.0.

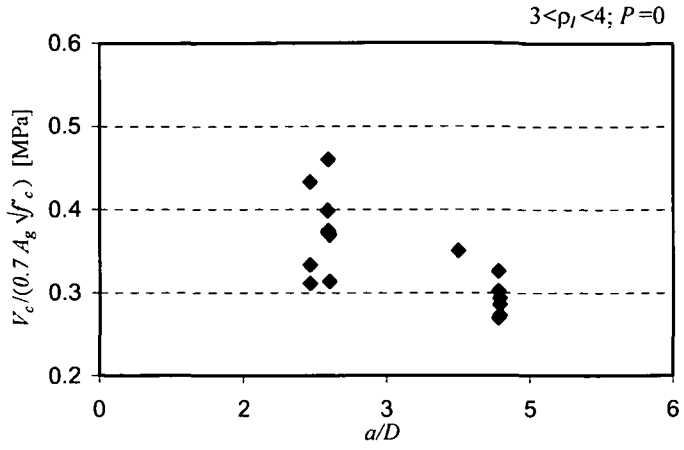


Figure 4.12 Effect of the members' aspect ratio on normalized shear strength

Kowalsky and Priestley (2000) presumed that as $a/D$ further decreases the shear capacity probably continues to increase. Because of insufficient information in the proposed model a 25% enhancement for specimens with $a/D \leq 2.5$ has been conservatively assumed, although Kowalsky and Priestley (2000) proposed a 50% enhancement. Thus, a shear enhancement coefficient, $k$, due to the aspect ratio is proposed as follows

$$k = \begin{cases} 1.00 & \text{for} \quad a/D > 2.5 \\ 1.25 & \text{for} \quad a/D \leq 2.5 \end{cases}$$

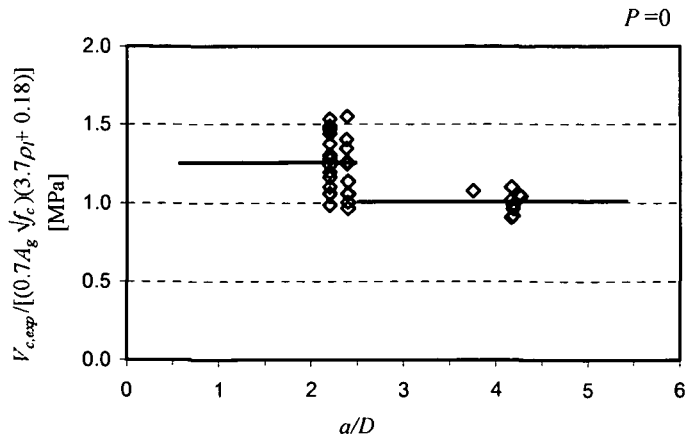


Figure 4.13 Influence of the members' aspect ratio on normalized shear strength

### 4.3.5 Effect of Axial Load

Axial compression tends to increase the member's shear capacity because of the fact that the onset of flexural cracking is delayed and as a consequence cracks do not penetrate as far into the beam. Axial tension, in turn, causes an increase in inclined crack width, decreasing the shear stress that could be transmitted across the crack by aggregate interlock, resulting in a reduced shear capacity of the member (Bhide and Collins, 1989). This trend is obvious for members under compression load from Figure 4.14.

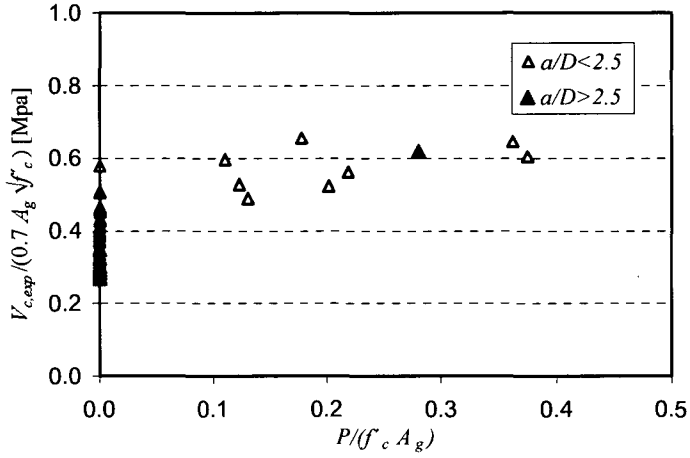


Figure 4.14 Effect of compressive axial load ratio on normalized shear strength

Normalizing the members' shear capacity with respect to concrete compression strength, shear span-to-depth ratio and longitudinal reinforcement ratio, the influence of the axial load level on the shear strength could be express as

$$f(P) = \frac{V_c}{k \cdot \sqrt{f'_c} \cdot 0.7 A_g} - (3.7\rho_l + 0.18) \tag{4.20}$$

The best exponential fit through the data (Figure 4.15) is as follows

$$f(P) = 0.08\left(\frac{P}{A_g}\right)^{0.3} \tag{4.21}$$

Because of the lack of data on members tested under axial tension the proposed formula is in this form valid only for axial compression.

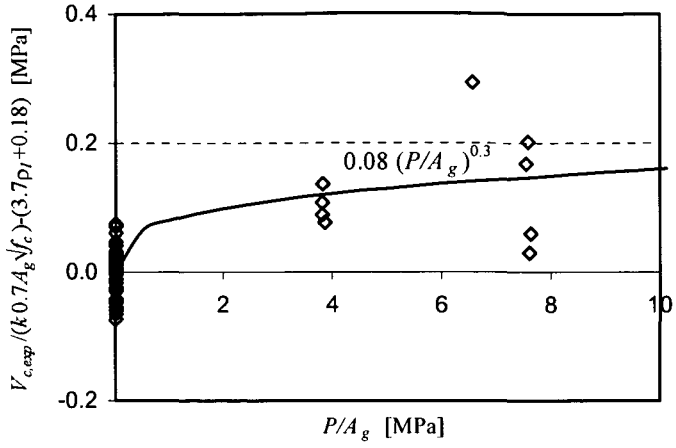


Figure 4.15 Influence of the axial load on normalized shear strength

### 4.3.6 Size Effect

In the brittle type of failure, like diagonal shear failure, with an increasing size (depth) of the member the shear stress at failure considerably decreases. The size effect represents the effect of beam's depth versus maximum aggregate size at a constant aspect ratio, longitudinal reinforcement ratio and concrete compressive strength. As a consequence, high strength concrete members display a more significant size effect in shear than normal strength concrete members. First test evidences of the size effect in shear were presented by Kani (1967). Recently an extensive research on size effect in shear was conducted and many different theories have been proposed, some of them based on fracture mechanics, others based on reduced shear resistance resulting from wider diagonal cracks or some purely empirical models (Bažant and Kim; 1984, Bažant and Sun, 1987; Bažant and Kazemi, 1991; Reineck, 1991; Zararis and Papadakis, 2001; Walraven et al., 1994; Bažant, 1997; Bentz, 2005; Bažant and Yu, 2005a, b). However, all of these researches were carried out on rectangular sections and no size effect tests on diagonal shear failure of circular section members has been published so far in literature.

Considering the tests from the database plotted in Figure 4.16, a slight decrease of shear strength could be observed with increasing the depth. However, data over a broader range of depth are necessary to make any firm conclusion.

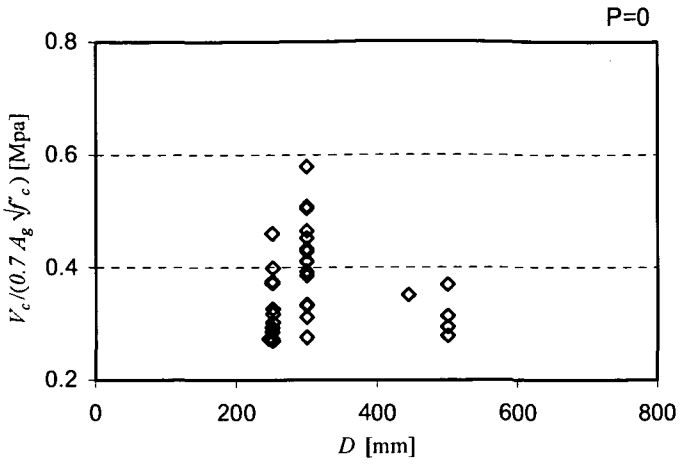


Figure 4.16 Effect of member's depth on normalized shear strength

Because of a lack of test data on circular sections in the proposed model the size effect law introduced by Bažant and Sun (1987) for rectangular sections could be adopted

$$\xi = \frac{1+\sqrt{5.08/d_a}}{\sqrt{1+d/(25d_a)}} \tag{4.22}$$

where $d$ is the section's effective depth and $d_a$ the maximal aggregate size.

### 4.3.7 Comparison of the Proposed Model to Other Models

The shear capacity of reinforced concrete circular section members without shear reinforcement is proposed as follows

$$V_c = \xi\left[3.7\rho_l + 0.18 + 0.08(\frac{P}{A_g})^{0.3}\right]\cdot k\cdot\sqrt{f'_c}\cdot 0.7A_g \tag{4.23}$$

where $\rho_l$ is the longitudinal reinforcement ratio, $P$ the axial load, $A_g$ the section's gross area, $f'_c$ the concrete compressive strength, $k$ is the shear enhancement coefficient and it is defined for different aspect ratios, $a/D$, as

$$k = \begin{cases} 1.00 & \text{for} \quad a/D > 2.5 \\ 1.25 & \text{for} \quad a/D \le 2.5 \end{cases}$$

The size effect coefficient, $\xi$, could be taken as

$$\xi = \frac{1+\sqrt{5.08/d_a}}{\sqrt{1+d/(25d_a)}}$$

The proposed shear capacity model is compared to the existing models of Clarke and Birjandi (1993), as well as of Kowalsky and Priestley (2000), on the basis of 44 test data of specimens without shear reinforcement (Table 3.1).

The statistical comparison of models is provided in Table 4.1. The mean experimental--to-theoretical strength ratio and the standard deviation of the proposed model are 1.01 and 0.13 respectively, which is considerably lower than the mean and standard deviation of models proposed by Clarke et al. and Kowalsky et al. respectively. The higher coefficient of determination of the proposed model indicates that the actual shear strength of the specimens is better captured than by other two models. Furthermore, the lower coefficient of variation of the proposed model indicates its consistency.

The experimental ultimate shear strength versus theoretical ultimate shear strength of specimens of different proposals is plotted in Figure 4.17. The ratio of theoretical to experimental shear strengths across the range of all parameters, such as concrete compressive strength, aspect ratio, axial load ratio and longitudinal reinforcement ratio are plotted in Figures 4.19, 4.20, 4.21 and 4.22. The smaller scatter of data by proposed model indicates that the effect of a particular variable, affecting shear strength, is better captured than by other existing proposals. Thus the proposed model clearly improves the prediction of the shear capacity of circular sections without transverse reinforcement. The experimental shear capacities as well as the theoretical shear capacities calculated by different proposed models are listed in Table 4.2.

Table 4.1 Statistical comparison of models in terms of experimental/theoretical shear strength ratio

| | Clarke and Birjandi (1993) | Kowalsky and Priestley (2000) | Proposed |
|---|---|---|---|
| Mean value | 1.29 | 1.11 | 1.01 |
| Standard deviation | 0.20 | 0.23 | 0.13 |
| Coefficient of variation, $CoV$ [%] | 15 | 21 | 13 |
| Coefficient of determination, $r^2$ | 0.74 | 0.58 | 0.82 |

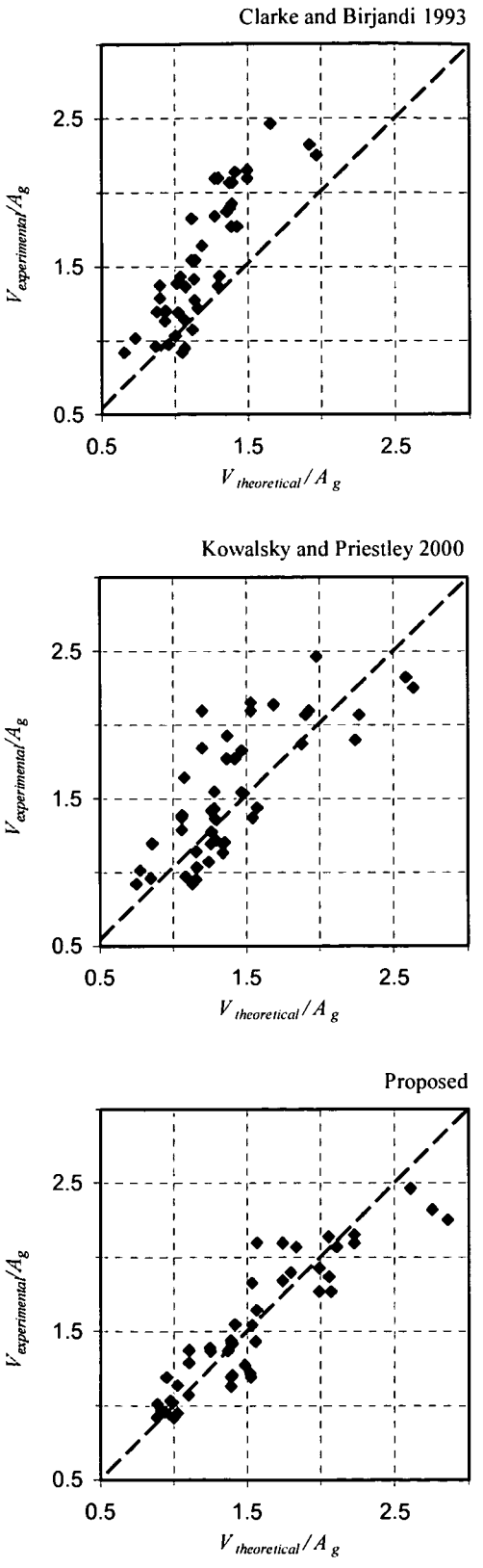


Figure 4.17 Ultimate shear strength of circular section members without shear reinforcement

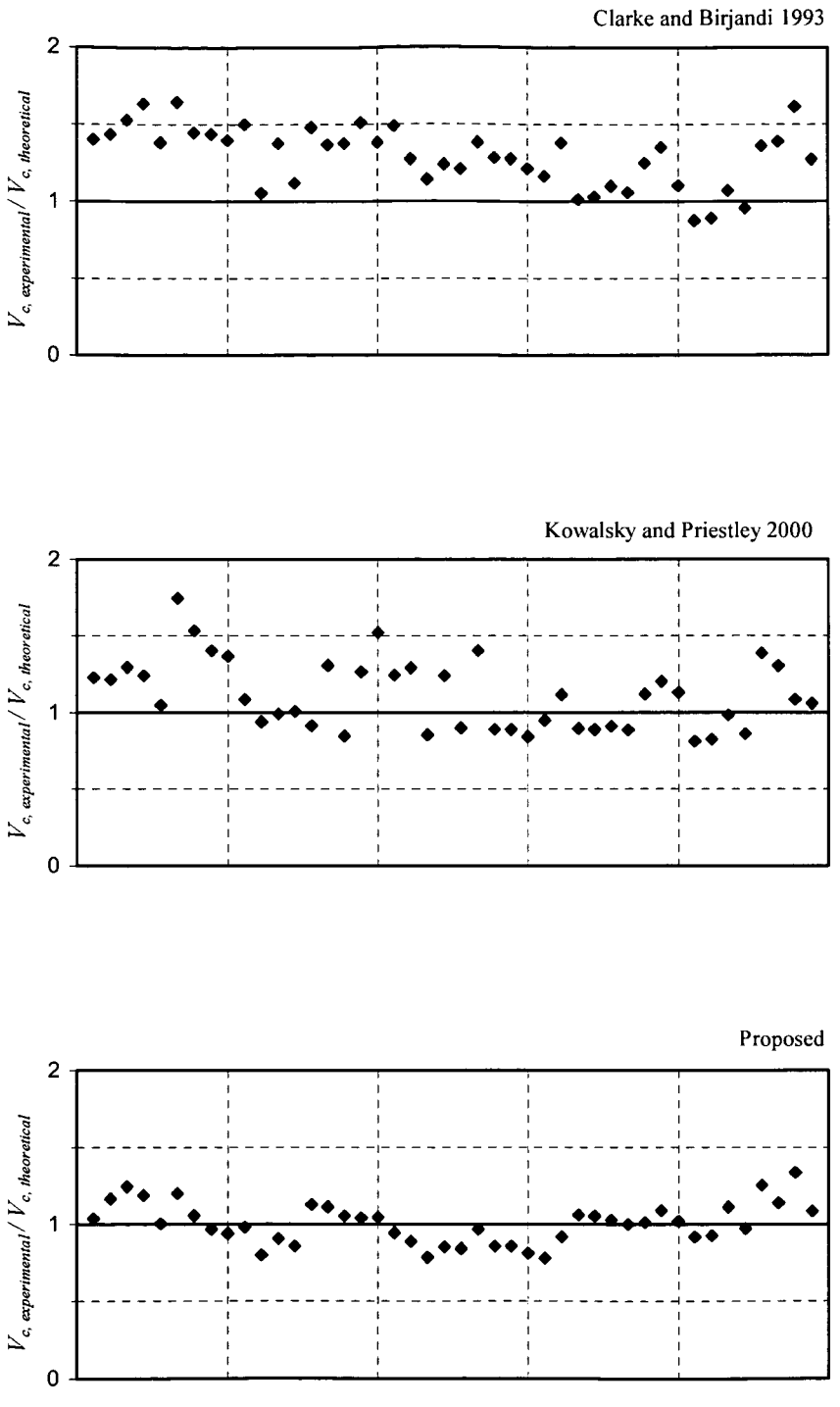


Figure 4.18 Ratio of experimental to theoretical shear strengths of members without shear reinforcement

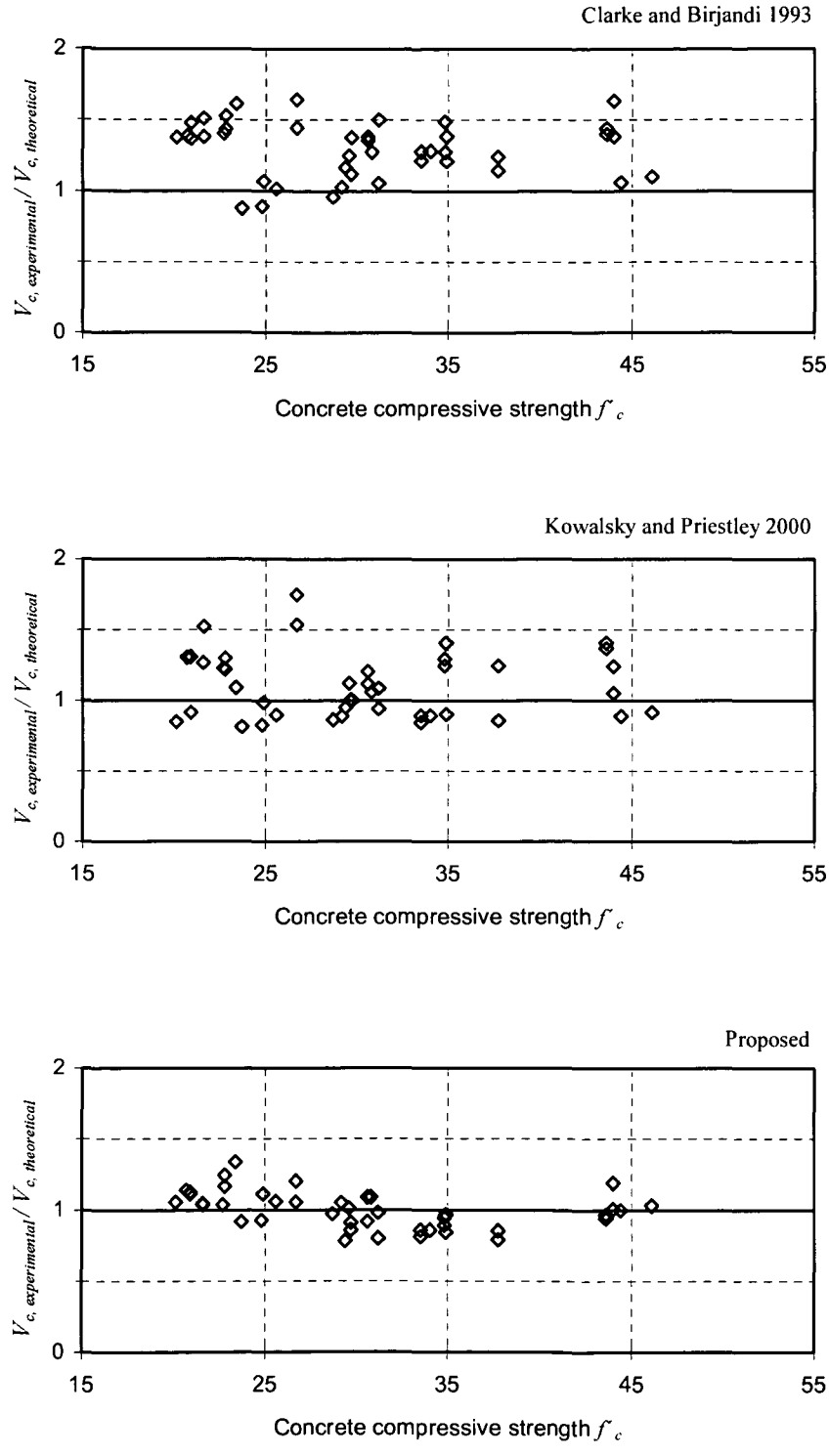


Figure 4.19 Ratio of experimental to theoretical shear strengths versus concrete compressive strength of members without shear reinforcement

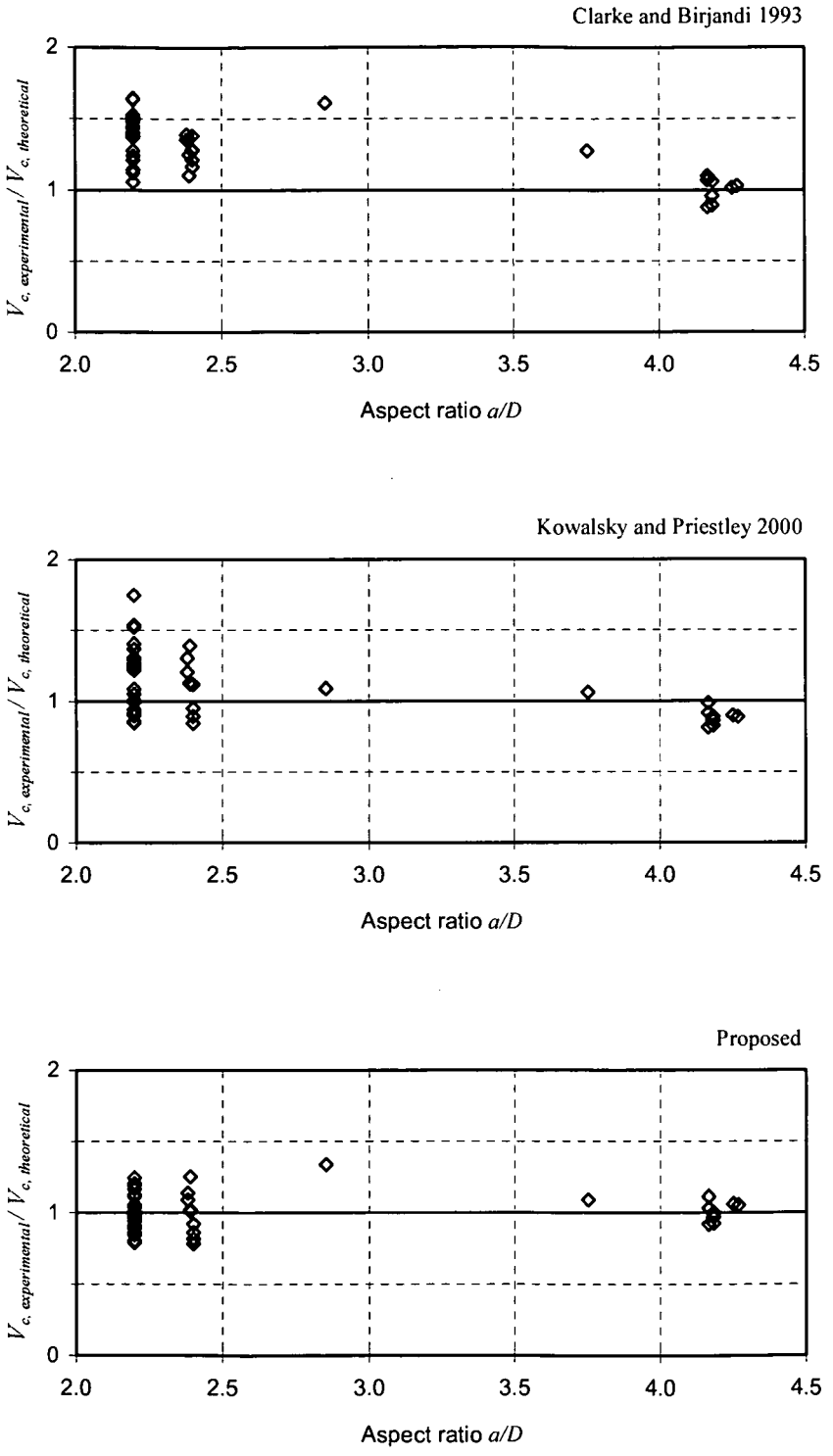


Figure 4.20 Ratio of experimental to theoretical shear strengths versus aspect ratio of members without shear reinforcement

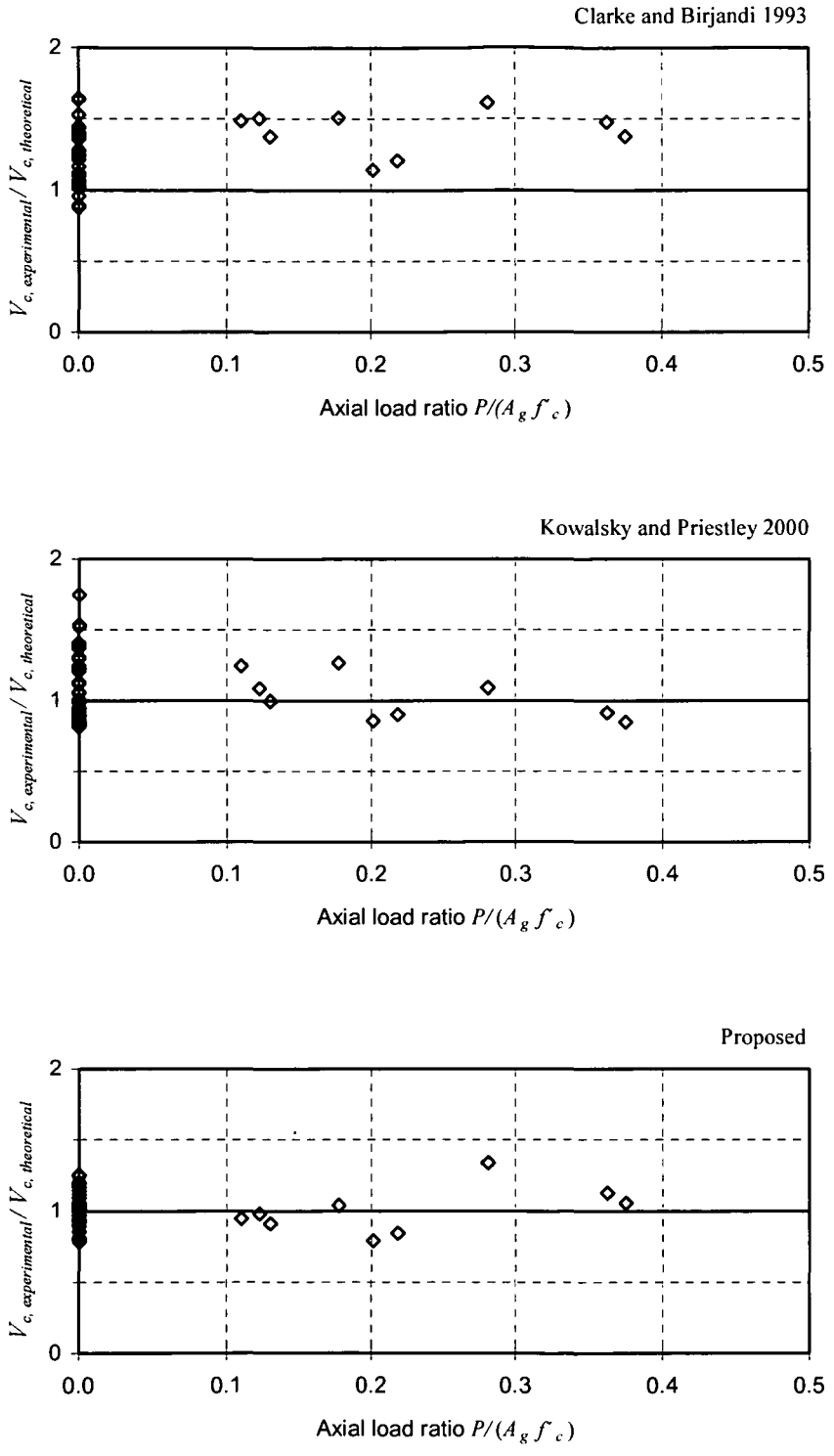


Figure 4.21 Ratio of experimental to theoretical shear strengths versus axial load ratio of members without shear reinforcement

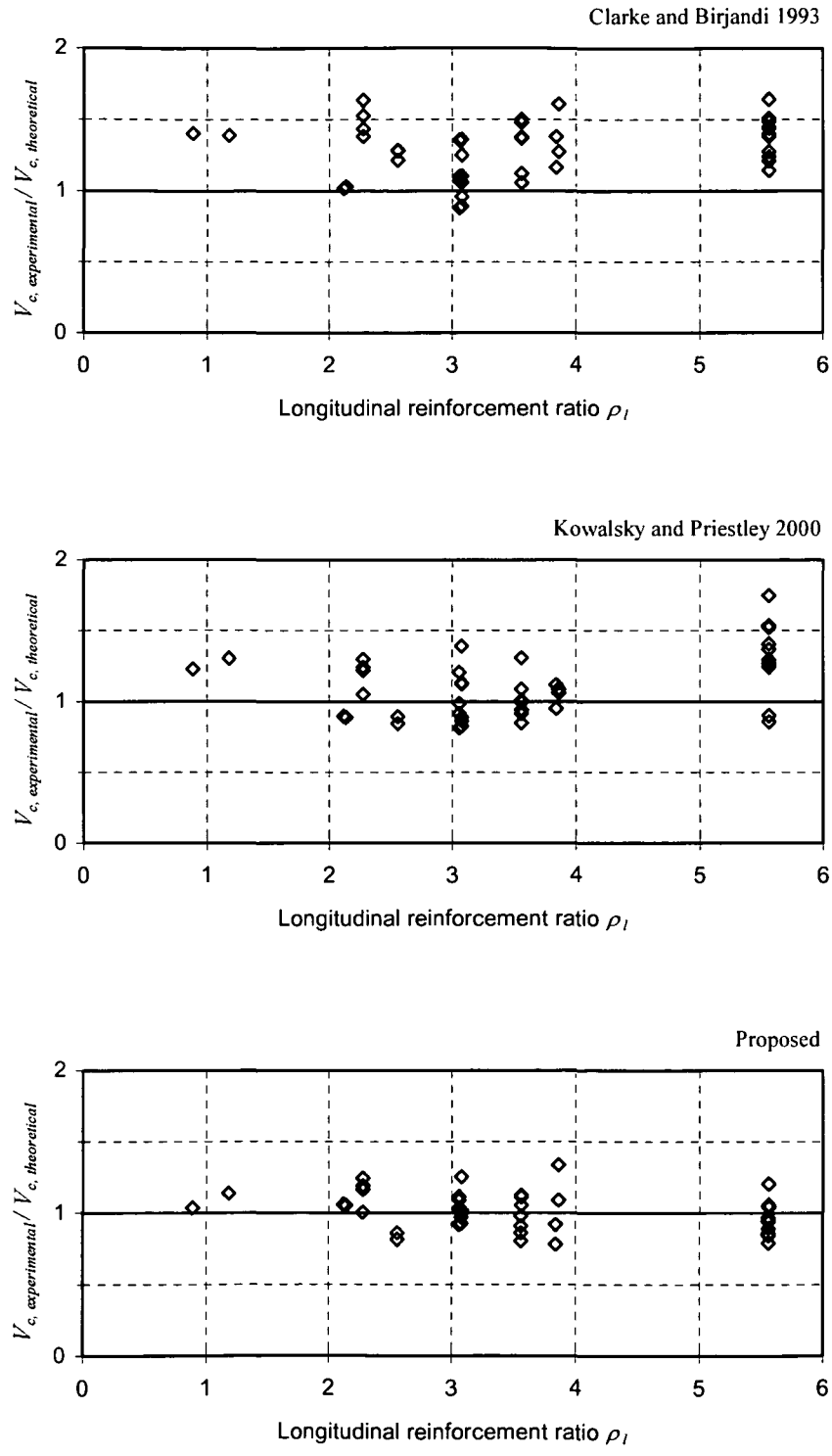


Figure 4.22 Ratio of experimental to theoretical shear strengths versus longitudinal reinforcement ratio of members without shear reinforcement

Table 4.2 Calculated and measured shear capacities of specimens without shear reinforcement

| Specimen | | $V_{experimental}$ [kN] | $V_{theoretical}$ [kN] | | | $V_{experimental}/V_{theoretical}$ | | |
|---|---|---|---|---|---|---|---|---|
| | | | Clarke, Birjandi | Kowalsky, Priestley | Proposed | Clarke, Birjandi | Kowalsky, Priestley | Proposed |
| Clarke, Birjandi (1993) | 01-1 | 65.0 | 46.33 | 52.95 | 62.71 | 1.40 | 1.23 | 1.04 |
| | 03-1 | 91.0 | 63.47 | 74.82 | 78.03 | 1.43 | 1.22 | 1.17 |
| | 03-2 | 97.0 | 63.47 | 74.82 | 78.03 | 1.53 | 1.30 | 1.24 |
| | 04-1 | 129.0 | 78.84 | 103.94 | 108.40 | 1.64 | 1.24 | 1.19 |
| | 04-2 | 109.0 | 78.84 | 103.94 | 108.40 | 1.38 | 1.05 | 1.01 |
| | 05-1 | 148.0 | 89.97 | 84.69 | 123.21 | 1.65 | 1.75 | 1.20 |
| | 05-2 | 130.0 | 89.97 | 84.69 | 123.21 | 1.44 | 1.53 | 1.06 |
| | 06-1 | 152.0 | 105.77 | 108.23 | 157.45 | 1.44 | 1.40 | 0.97 |
| | 06-2 | 148.0 | 105.77 | 108.23 | 157.45 | 1.40 | 1.37 | 0.94 |
| | 29-1 | 146.0 | 97.28 | 134.60 | 148.97 | 1.50 | 1.08 | 0.98 |
| | 29-2 | 86.0 | 81.65 | 91.55 | 107.64 | 1.05 | 0.94 | 0.80 |
| | 30-1 | 132.0 | 95.87 | 132.81 | 145.46 | 1.38 | 0.99 | 0.91 |
| | 30-2 | 90.0 | 80.33 | 89.33 | 105.02 | 1.12 | 1.01 | 0.86 |
| | 31-1 | 146.0 | 98.64 | 160.11 | 129.61 | 1.48 | 0.91 | 1.13 |
| | 31-2 | 98.0 | 71.53 | 74.93 | 88.10 | 1.37 | 1.31 | 1.11 |
| | 32-1 | 134.0 | 97.25 | 158.26 | 127.04 | 1.38 | 0.85 | 1.05 |
| | 33-1 | 151.0 | 99.99 | 119.32 | 145.23 | 1.51 | 1.27 | 1.04 |
| | 33-2 | 116.0 | 83.89 | 76.18 | 110.82 | 1.38 | 1.52 | 1.05 |
| | 34-1 | 174.0 | 117.01 | 139.77 | 184.32 | 1.49 | 1.24 | 0.94 |
| | 34-2 | 125.0 | 98.19 | 96.69 | 140.66 | 1.27 | 1.29 | 0.89 |
| | 35-1 | 159.0 | 139.12 | 186.04 | 202.20 | 1.14 | 0.85 | 0.79 |
| | 35-2 | 125.0 | 100.82 | 100.64 | 146.41 | 1.24 | 1.24 | 0.85 |
| | 36-1 | 164.0 | 135.78 | 182.60 | 194.62 | 1.21 | 0.90 | 0.84 |
| | 36-2 | 136.0 | 98.28 | 96.83 | 140.87 | 1.38 | 1.40 | 0.97 |
| | 41-1 | 77.0 | 183.99 | 265.48 | 275.07 | 1.28 | 0.89 | 0.86 |
| | 42-1 | 50.5 | 183.09 | 263.52 | 273.04 | 1.28 | 0.89 | 0.86 |
| | 42-2 | 70.0 | 183.09 | 263.52 | 273.04 | 1.21 | 0.84 | 0.81 |
| | 45-1 | 47.5 | 200.72 | 246.87 | 299.89 | 1.17 | 0.95 | 0.78 |
| | 46-2 | 59.0 | 203.39 | 251.86 | 305.94 | 1.38 | 1.12 | 0.92 |
| Capon, de Cossio (1965) | 24.6-2-A | 236.0 | 45.80 | 51.94 | 43.84 | 1.02 | 0.90 | 1.06 |
| | 24.6-2-B | 234.0 | 47.64 | 55.27 | 46.57 | 1.03 | 0.89 | 1.05 |
| | 25-3-A | 222.0 | 65.09 | 78.53 | 69.47 | 1.10 | 0.91 | 1.03 |
| | 25-3-B | 234.0 | 63.98 | 76.45 | 67.81 | 1.06 | 0.89 | 1.00 |
| | F-25-3-A | 281.0 | 55.96 | 62.42 | 69.21 | 1.25 | 1.12 | 1.01 |
| | F-25-3-B | 212.0 | 56.85 | 63.98 | 70.75 | 1.35 | 1.20 | 1.09 |
| | F-00 | 71.6 | 43.08 | 42.00 | 46.57 | 1.10 | 1.13 | 1.02 |
| | P-25-3-A | 45.8 | 52.25 | 56.30 | 49.81 | 0.88 | 0.81 | 0.92 |
| | P-25-3-B | 56.8 | 52.79 | 57.14 | 50.68 | 0.89 | 0.82 | 0.93 |
| | P-25-3-C | 67.7 | 53.11 | 57.71 | 51.06 | 1.07 | 0.98 | 1.11 |
| | P-25-3-D | 47.0 | 55.40 | 61.47 | 54.52 | 0.96 | 0.86 | 0.97 |
| | FU-00 | 53.0 | 43.40 | 42.47 | 47.08 | 1.36 | 1.39 | 1.25 |
| | F-A | 46.5 | 36.39 | 38.73 | 44.39 | 1.39 | 1.30 | 1.14 |
| Kim (2000) | YJCCONT | 49.0 | 202.07 | 299.79 | 244.01 | 1.61 | 1.09 | 1.34 |
| Khalifa, Collins (1981) | SC0 | 326.0 | 166.51 | 200.15 | 194.95 | 1.27 | 1.06 | 1.09 |

## 4.4 Evaluation of Shear Reinforcement Capacity

As long as the section is uncracked the shear reinforcement is ineffective in tension. With the appearance of the first diagonal cracks the shear reinforcement is mobilized in resisting shear by tension in it.

Comparing the part of the shear force carried by the shear reinforcement of rectangular and circular sections, the following could be observed. In the case of rectangular sections the stirrup's shear force acting in the direction of the external shear is $2A_{sw}f_{yw}$, where $A_{sw}$ is the cross section of the stirrup and $f_{yw}$ its yield strength, see Figure 4.23. In circular sections, in turn, only the vertical component of the hoop's tension force, $2A_{sw}f_{yw} \cdot cos\,\varphi$, is effective in resisting external shear. It would seem thus that circular sections are weaker in resisting shear than rectangular sections, which, of course, is not a plausible conclusion. There is obviously an additional shear resisting mechanism in curved shear reinforcement of circular sections that has been not identified yet. In the following the shear resisting mechanism of hoops will be discussed in detail.

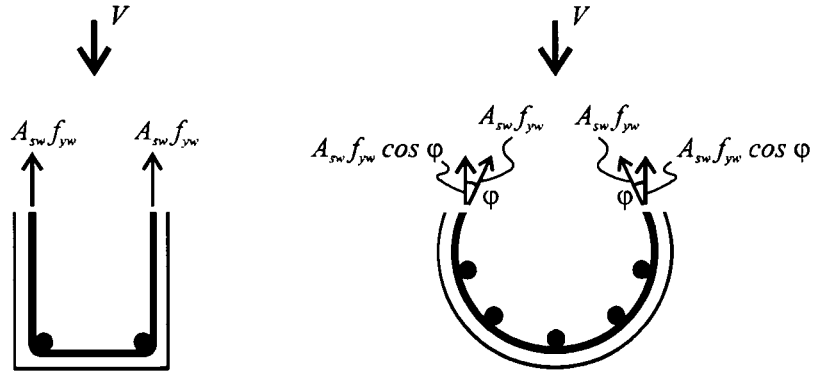


Figure 4.23 Tension force in shear reinforcement in rectangular and in circular sections

### 4.4.1 Shear Resisting Mechanism of Hoops in Circular Sections

As the load on the member further increases, the cracks widen and distribute, see Figure 4.24. At the ultimate state a major diagonal crack forms and the section fails by rupture of the shear reinforcement along the diagonal crack, i.e. diagonal failure plain. At this state the section is already considerably cracked in the vicinity of the major diagonal crack.

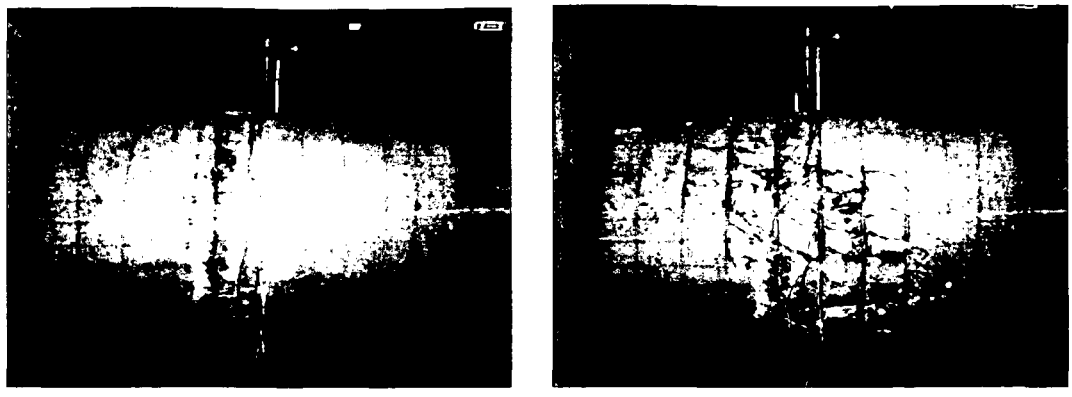

Figure 4.24 Reinforced concrete circular cross-section member under monotonic shear load

In the cracked region the bond between concrete and shear reinforcement is gradually destroyed, hence the shear reinforcement and the concrete could be considered as two partly separated materials. The shear reinforcement is under tension and as a result of the hoops' curved shape the change of its direction induces lateral pressure on the concrete. This pressure is designated as *deviation stresses* and appears only in sections with curved shear reinforcement such as circular hoops or spirals. It is activated as soon as bond is destroyed and the shear reinforcement partly separated from concrete core. Moreover, it is only active in the parts of the hoops within the diagonally cracked zone (Figure 4.25).

As a result of action-reaction, the concrete acts on the hoops with normal pressure equal in magnitude but with opposite direction. It actually represents the reaction of concrete to the tendency of curved hoops to straighten. A similar mechanism develops in post--tensioned concrete elements, where tensioning of tendons in the ducts induces lateral pressure on the concrete section.

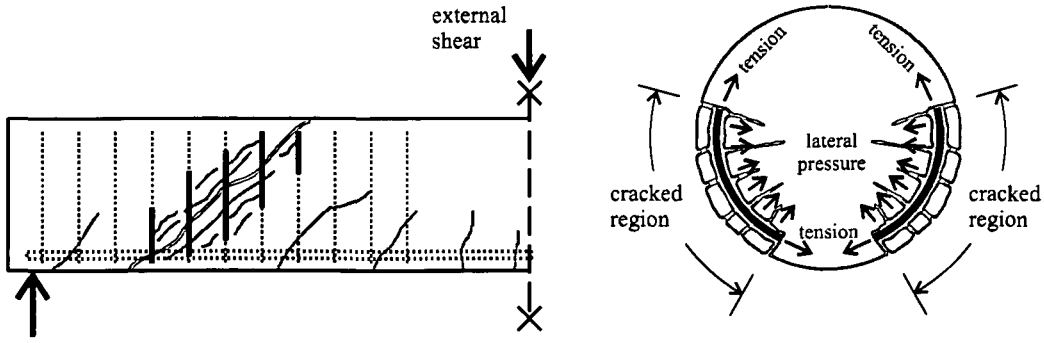


Figure 4.25 Deviation stresses of hoops acting at the section's cracked region

The component of the deviation stresses in the direction of the external shear actually represents an additional shear resisting mechanism of hoops that increases the total shear capacity of the member. The entire shear capacity of shear reinforcement is thus added together from two shear resisting components: the *tension component* – resulting from the tension in shear reinforcement and the *deviation component* – resulting from the shear enhancement of deviation stresses. In the following chapters each of these components will be separately discussed and analytically expressed.

### 4.4.2 Shear Resisting Mechanism by Tension in Hoops – Tension Component

After the section is cracked the shear reinforcement is mobilized in resisting external shear by tension forces in it. This shear-carrying mechanism has been denoted as the tension component. In the limit state it is usually assumed that all transverse reinforcement crossed by a diagonal crack yields and, therefore, each resists a tension force of $A_{sw}f_{yw}$ across the crack, where $A_{sw}$ is the area of the hoop's one leg and $f_{yw}$ is the hoop's yield strength (Figure 4.26). The tension force acts in the hoop's tangential direction and therefore only its component in the direction of the external shear $A_{sw}f_{yw} \cdot cos\varphi_{y,i}$ is active in resisting shear, where $\varphi_{y,i}$ denotes the angle between the direction of the external shear and of the hoop's tension force $A_{sw}f_{yw}$. The total tension force of hoops that resists external shear is then equal to the sum of all hoops' forces crossed by the diagonal crack.

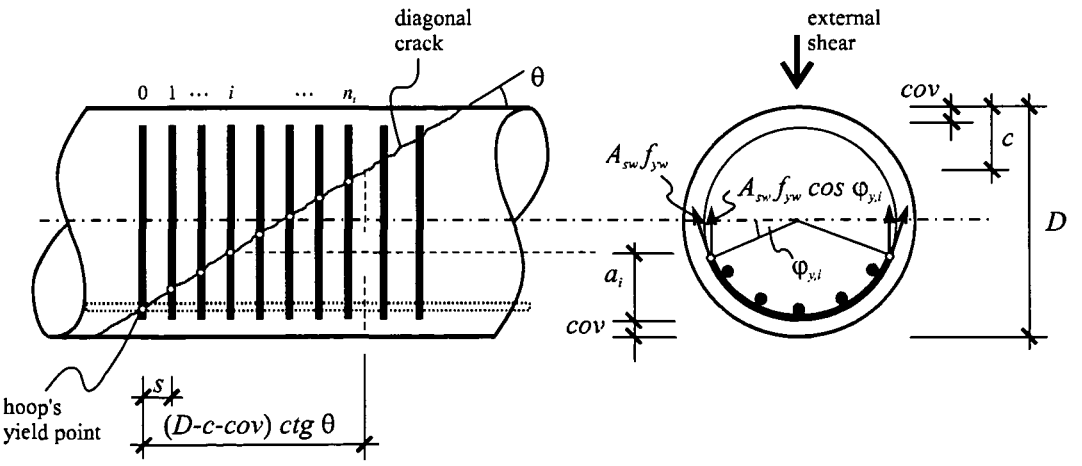


Figure 4.26 Shear carried by tension in hoops crossed by a diagonal crack

In the recently proposed design equation for hoop's capacity (Ang et al., 1989; Kowalsky et al., 2000) and in design equations of stirrups of rectangular sections defined in codes (ACI 318M-02, 2002; Eurocode 2, 1992), a smeared distribution of shear reinforcement has been assumed. Actually, the shear reinforcement consists of a discrete number of bars crossing the diagonal crack. Kim and Mander (2005) made us careful when using these equations since they could be very unconservative in cases of a low number of shear reinforcement crossed by a diagonal crack. To avoid the unconservativeness they proposed applying correction factors to current design formulas for various type of shear reinforcement. Dancygier (2001) showed that the design formula derived by Ang et al. (1989) for circular hoops – which is based on the assumption that the hoop's spacing is sufficiently small compared to section's diameter and thus integral averaging is applied – is valid only when less than four hoops are crossed by the diagonal crack. For all other values the formula is 10% to more than 50% unconservative.

To overcome such deficiencies in this work, instead of integral averaging a strict summation is applied, obtaining a formula valid for an arbitrary range of hoop's spacing/to diameter ratio. The crack pattern is idealized as a series of parallel cracks all occurring at an angle $\theta$ to the member's longitudinal axis (Figure 4.26). In the simple truss analogy the inclination angle of cracks is generally taken to be 45°. However, tests on members under different loading situations showed that the inclination angle is usually lower than 45°. For cyclic load Priestley et al. (1994) proposed taking 30°. The resultant tension force resisting external shear is obtained by summing up all the tension force components traversing the crack plane

$$V_{st} = 2A_{sw}f_{yw}\sum_{i=1}^{n_t} cos\,\varphi_{y,i} \tag{4.24}$$

where $i$ is the index of the hoop that is crossed by a crack, $\varphi_{y,i}$ is the pertaining central angle defined in Figure 4.26 and $n_t$ is the number of hoops active in tension across the crack. Kowalsky and Priestley (2000) noted that shear cannot be transferred across the section's compression zone by tension in hoops – since the cracks are by definition closed in the

compression zone. According to this suggestion, only the hoops outside the compression zone have been considered for resisting shear by tension. Their number is

$$n_t = INT\left[\frac{(D-c-cov)}{s} ctg\theta\right] \tag{4.25}$$

where $D$ is the section's diameter, $c$ the compression zone's depth, $cov$ the concrete cover and $s$ the spacing of the hoops. The crack tip is assumed to pass through the intersection point of the hoop and the longitudinal bottom steel. Note that the number of the hoops is always an integer value and it is zero when their spacing is larger from the reduced section width, i.e. the diagonal crack falls between two hoops. Further, the central angle $\varphi_{y,i}$ is defined as

$$sin\varphi_{y,i} = \frac{D/2-cov-a_i}{D/2-cov} \tag{4.26}$$

where $a_i$ is the ordinate of the particular yield point defined as

$$a_i = i \cdot s \cdot tg\theta \tag{4.27}$$

Expressing $s \cdot tg\theta$ from Equation 4.25 and taking into account a typical value of $c/D = 0.3$ proposed by Kowalsky and Priestley (2000), Equation 4.27 becomes

$$a_i = i \cdot \frac{(0.7D-cov)}{n_t} \tag{4.28}$$

Substituting it into the Equation 4.26, the central angle is expressed as

$$sin\varphi_{y,i} = 1 - \frac{i}{n_t} \cdot \frac{(0.7D-cov)}{(D/2-cov)} \tag{4.29}$$

For typical values of $cov/D$ of 1% to 20% the value of the ratio $(0.7D-cov)/(D/2-cov)$ ranges between 1.41 and 1.67. Taking a middle value of 1.5

$$sin\varphi_{y,i} = 1 - 1.5\frac{i}{n_t} \tag{4.30}$$

and the cosines of the central angle is

$$\cos\varphi_{y,i} = \sqrt{1-\left(1-1.5\frac{i}{n_t}\right)^2} \tag{4.31}$$

Further, the resultant shear resisting force of hoops crossed by a crack is given by

$$V_{st} = 2A_{sw}f_{yw}\sum_{i=1}^{n_t}\sqrt{1-\left(1-1.5\frac{i}{n_t}\right)^2} \tag{4.32}$$

The obtained expression is not suitable for design purpose; hence an inevitable simplification is introduced. The summation term has been defined as the *tension influence coefficient* $k_t$

$$k_t = \sum_{i=1}^{n_t}\sqrt{1-\left(1-1.5\frac{i}{n_t}\right)^2} \tag{4.33}$$

Its graduate course is plotted in Figure 4.27 and it is a result of the realistic discrete distribution of shear reinforcement. It correctly represents the fact that if the crack plane is not traversed by any hoop ($n_t < 1$) the tension influence coefficient is zero and thus the contribution of the hoop's tension component to the members shear capacity is zero. The discrete function could be replaced with sufficient accuracy by the continuous function

$$k_t \cong 0.9n_t \tag{4.34}$$

Thus a simple expression of the shear resisting force in hoops is obtained

$$V_{st} = 1.8A_{sw}f_{yw}\cdot n_t \tag{4.35}$$

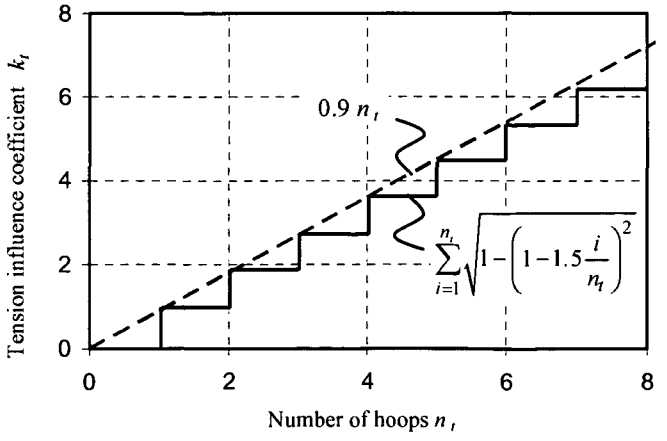


Figure 4.27 Tension influence coefficient as a function of the hoops' number

However, there is another aspect that should be considered. Current design procedure ignores the influence of shear reinforcement on concrete shear capacity, providing for total shear strength a simple superposition of concrete and shear reinforcement capacity. As several studies show, the concrete shear mechanism can interact with hoops in different ways, see Ang, Priestley and Paulay (1989), Wong, Paulay and Priestley (1993), Russo and Puleri (1997); ASCE-ACI Committee 445 (1998, 2000). The shear reinforcement indeed enhances the concrete shear capacity even if the shear reinforcement is not intersected by cracks and thus not activated in tension. This is a result of the following mechanism: the shear reinforcement improves the contribution of the dowel mechanism by supporting the longitudinal bars and it enhances the contribution of the aggregate interlock by forcing the cracks to redistribute in a closer spacing and over a wider area (Park and Paulay, 1975). This additional shear-carrying mechanism will be introduced into the proposed model in a way that the number of hoops $n_t$ will not be rounded down, obtaining in such a way an additional shear capacity portion.

### 4.4.3 Relation between the Hoop's Tension and the Deviation Function

There is a fundamental difference in the shear carrying mechanism of the transverse reinforcement in the case if it is conducted straight-line or curved. Generally, shear reinforcement is active in carrying shear by tension in it. But in the case of curved reinforcement, such as hoops and spirals, the change of direction of the bar's tension force induces additional lateral pressure on the concrete core, the so called deviation stresses, $f_d$ (Figure 4.28). In straight shear reinforcement (stirrups) this mechanism is not present.

Because of action-reaction, the concrete section acts on hoops with normal pressure, $f_n$, of the same intensity as the deviation stresses, $f_d$, but in the opposite direction (see Figure 4.28a and b). Consider the forces acting on an infinitesimal hoop element: the tension force in hoop $T$; the bond force $dB$, defined as the shear stress $\tau_b$ that develops along the lateral surface of the bar of length $ds$, and the concrete normal force $dN$, defined as the normal stresses $f_n$ along $ds$. The equilibrium in radial direction of an infinitesimal hoop element of length $ds$ defined by angle $d\varphi$ is

$$T\sin\frac{d\varphi}{2}+(T+dT)\sin\frac{d\varphi}{2}=dN \tag{4.36}$$

For very small angles $d\varphi$ it could be assumed that $\sin(d\varphi/2)=d\varphi/2$. The third term on the left side of the equation is small of the second order and could be neglected with respect to the others. Thus the relation between the hoop's tension force and the concrete normal force is obtained

$$\boxed{Td\varphi=dN} \tag{4.37}$$

From the equilibrium in tangential direction it follows that

$$(T+dT)\cos\frac{d\varphi}{2}-T\cos\frac{d\varphi}{2}=dB \tag{4.38}$$

For small angles it holds that $\cos(d\varphi/2)=1$, therefore, Equation 4.38 may be written as

$$\boxed{dT=dB} \tag{4.39}$$

Thus the expression of the fundamental stress transfer mechanism between concrete and steel is obtained, according to which the change of bond forces is directly proportional to the change of tension force in hoops.

Consider more closely the physical nature of the bond. The bond is made of three components: chemical adhesion, friction and mechanical interaction between concrete and steel, i.e., mechanical interlock (Goto, 1971; Lutz and Gergely, 1967; Lutz, 1970).

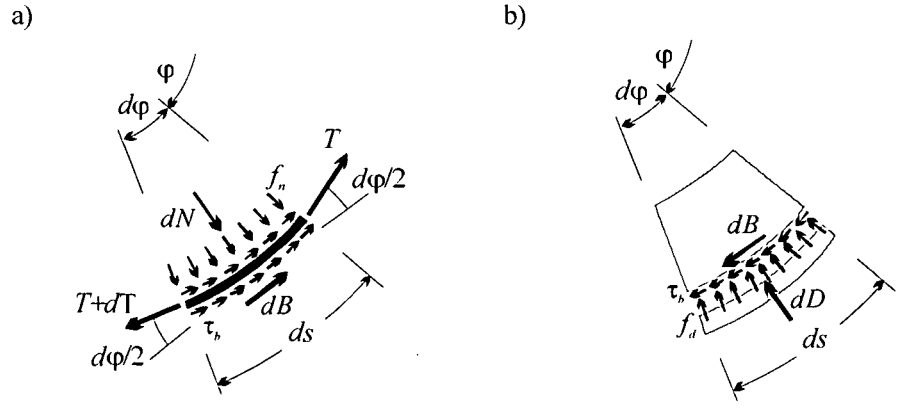


Figure 4.28 Forces acting on a) an infinitesimal hoop element and on b) concrete

Adhesion is lost almost immediately upon loading. As load further increases, a slip between concrete and steel occurs and the contribution of the friction and interlock mechanism to the bond strength is mobilized. Roughly simplifying, it could be assumed that the bond is mainly governed by friction between steel and concrete. On the other hand, bond stresses increase with normal confining pressure exerted by the surrounding concrete on the bar surface (Untrauer and Henry, 1965; *fib* Bulletin, 2003 page 118). The higher the normal pressure, the higher the bond stresses and thus higher tension force is required to separate the concrete and steel surface. This fundamental characteristic of bond is correctly captured by the "frictional concept", where the friction force that develops between two bodies is related to the normal force through the frictional coefficient. Based on the similar physical meaning of the bond and friction forces, the bond force, $dB$, will be related to the normal force, $dN$, through the friction coefficient $\mu$

$$dB = \mu\, dN \tag{4.40}$$

The friction coefficient is proportional to the roughness of the surfaces in contact (concrete and steel). Thus, applying the frictional concept, Equation 4.39 becomes

$$dT = \mu\, dN \tag{4.41}$$

In such a way the hoop's tension force is expressed through the normal force. From the two equilibrium equations (Equation 4.37 and Equation 4.41) by eliminating $dN$, a differential relation of the hoop's tension force as a function of the friction coefficient is obtained

$$\frac{dT}{T} = \mu\, d\varphi \tag{4.42}$$

By integrating both sides, assuming that the friction coefficient is constant, the hoop's tension force function is obtained

$$\int_{T}^{T_{max}} \frac{dT}{T} = \mu \int_{\varphi}^{\varphi_{max}} d\varphi \tag{4.43}$$

$$T = T_{max}\, e^{-\mu(\varphi_{max}-\varphi)} \tag{4.44}$$

The maximal tension force that the hoop can carry is $T_{max} = A_{sw} f_{yw}$, that is when the stresses in the hoop reach the steel yield stress, $f_y$, at a point defined by the angle $\varphi_y$

$$T(\varphi) = A_{sw} f_{yw}\, e^{-\mu(\varphi_y - \varphi)} \tag{4.45}$$

Equation 4.45 represents the hoop's tension function illustrated in Figure 4.29. It is an exponentially increasing function which is zero at the boundary point of the cracked region, i.e., at $\varphi = \varphi_0$, where a perfect bond between the concrete and hoops exists (the friction coefficient is infinite), and it increases with increasing of the angle $\varphi$, reaching its maximum value at the hoop's yield point, where $\varphi = \varphi_y$. We assume a symmetrical branch of the tension function at the other side of the yield point. Here, with a further increase of the angle $\varphi$, the tension function decreases in the same manner, reaching zero at the cracked region's other boundary point.

Substituting, further, Equation 4.45 into the Equation 4.41 – considering that the concrete normal force is equal to the deviation force, $dN = dD$, – the hoop's deviation function is obtained

$$D(\varphi) = \frac{A_{sw} f_{yw}}{\mu} e^{-\mu(\varphi_y - \varphi)} \tag{4.46}$$

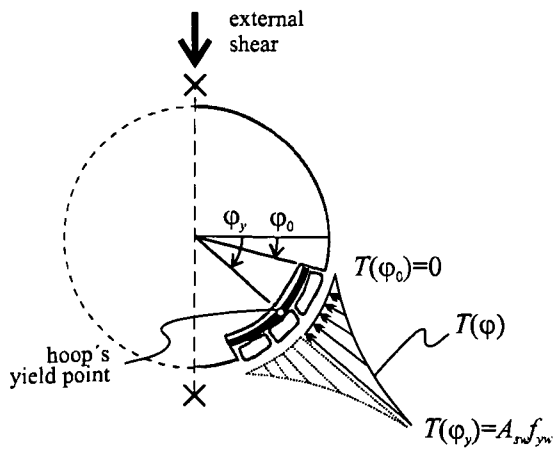


Figure 4.29 Hoop's tension function, T(φ)

It represents the hoop's deviation force at an arbitrary angular distance $\varphi$. The deviation force has its maximum value, $D_{max} = A_{sw} f_{yw} / \mu$, at the yield point, $\varphi = \varphi_y$, and decreases with the distance from the yield point, reaching zero at the boundary point of the cracked region, where $\varphi = \varphi_0$. From the plot of the normalized deviation function in Figure 4.30 two essential characteristics of the function's nature could be observed, i.e.

- The further from the yield point a particular point, the lower the deviation force there. This is a consequence of the fact that the tension force in hoops decreases with increasing the distance from the yield point, and the deviation force is indeed proportional to the tension force.
- A higher friction coefficient results in a lower deviation force. At the points where the bond between concrete and steel is stronger (higher friction coefficient) the concrete is less or not at all cracked, hence it follows that the shear reinforcement is not mobilized in tension. Consequently, no deviation forces act.

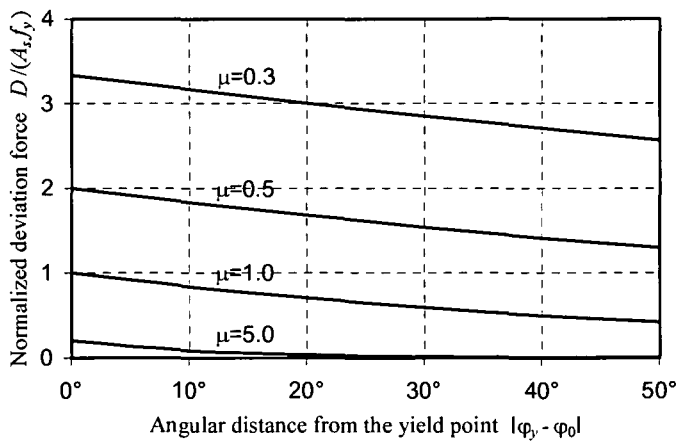


Figure 4.30 Normalized deviation force at an arbitrary angular distance from the yield point

However, in all derivations it was assumed that the friction coefficient is a constant value. In fact, the friction coefficient is not a constant value but varies along the hoop's perimeter depending on the "goodness of the bond" between concrete and steel, which in turn is different at a different angular distance from the yield point. Simplified, it could be assumed that in the vicinity of the yield point the concrete is extensively cracked, the bond is

noticeably destroyed, thus we have a weaker friction force, i.e., the coefficient of friction is lower. If the observed point is farther from the yield point the concrete is less cracked, the bond between concrete and steel is stronger, resulting in a higher friction coefficient. At the points where the concrete section is not cracked a perfect bond between steel and concrete could be assumed with an infinitely high friction coefficient.

For concrete and steel the friction coefficient is around 0.6 (Leonhardt et al., 1973). However, in the case of not entirely separated materials – but "constrained" by a partial bond between them – a higher frictional coefficient should be taken into consideration. Usually it is between 1.0 and 1.5 (*fib* Bulletin, 2003 page 118).

As a result of the change of the friction coefficient along the reinforcing bar, the deviation force decreases actually slightly stronger with the angular distance from the yield point as by assumed constant friction coefficient (Figure 4.31). However, the change of the deviation function is unknown and additional research should be carried out to define its nature. In order to simplify, in this work a constant friction coefficient of 1.5 has been assumed along the whole length of one hoop.

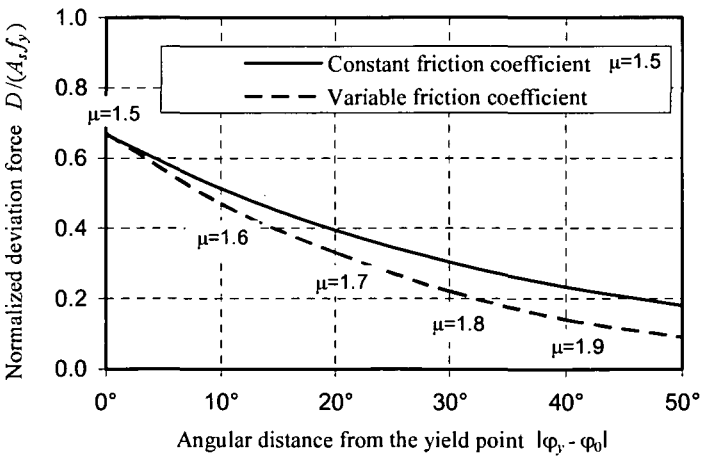


Figure 4.31 Change of the deviation force with respect to the distance from the yield point

### 4.4.4 Shear Resisting Mechanism of Hoops Resulting from Deviation Forces – Deviation Component

With increasing shear load the section is more and more diagonally cracked. At the ultimate load the member fails by rupture of the shear reinforcement along the major diagonal crack. At this stage a considerable region of the section along the failure plane is cracked (Figure 4.32). In the cracked region the bond between the hoops and concrete is heavily destroyed and the hoops act with deviation forces on the concrete section. At the places where the section is uncracked the bond between steel and concrete is perfect and the section acts like a homogenous material, thus no deviation forces act.

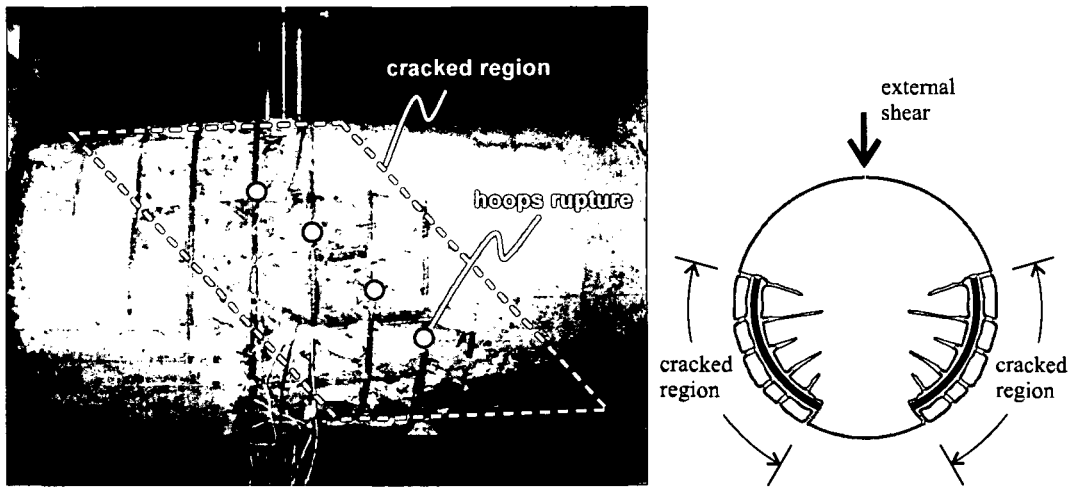


Figure 4.32 Cracked region of a circular cross-section member under shear load

Unlike the shear resisting mechanism by tension in the hoops, the deviatoric component is not solely active at the hoop's yield point, but along the whole arc length of the hoops within the cracked region (Figure 4.32 right). Each hoop in the cracked region acts with a resultant deviation force on concrete of different magnitude, resulting from a different arc length of a particular stirrup. To obtain the total shear capacity of the shear reinforcement, resulting from the deviation forces, the following two steps are required in calculation:

- to obtain the *resultant deviation force of one hoop*, the deviation function along the hoop's arc length, within the cracked region, should be integrated and then

- to obtain the total deviation force, the component of the resultant deviation force of each hoop in the direction of the external shear should be expressed and summed up along the number of all hoops in the cracked region.

### Resultant Deviation Force of One Hoop

As the diagonal crack propagates through the member on the section's lateral surface, two symmetrical cracked regions form. Consequently, each particular hoop acts on the concrete section with two symmetrically located resultant deviation forces, $D_{h,i}$, with regard to the axis of the external shear force (Figure 4.33). Here $i$ denotes the particular hoop within the cracked region. The resultant deviation force, $D_{h,i}$, is obtained by integrating the deviation function (Equation 4.46) along the hoop's arc length within the cracked region. Since the deviation function is symmetrical with regard to the yield point, the resultant deviation force could be simply calculated by integrating the deviation function $D(\varphi)$ from angle $\varphi_{0,i}$ – denoting the cracked region's boundary point – to the angle $\varphi_{y,i}$ and then multiplying it by two to take into account the function's descending and ascending branch

$$D_{h,i} = 2\frac{A_{sw} f_{yw}}{\mu} \int_{\varphi_{0,i}}^{\varphi_{y,i}} e^{-\mu(\varphi_{y,i}-\varphi)} d\varphi \tag{4.47}$$

$$D_{h,i} = 2\frac{A_{sw} f_{yw}}{\mu^2}(1 - e^{-\mu(\varphi_{y,i}-\varphi_{0,i})}) \tag{4.48}$$

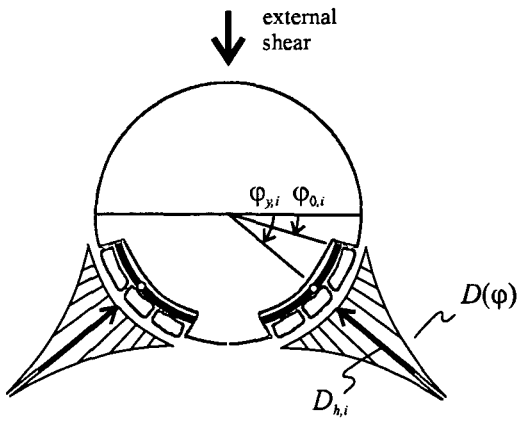


Figure 4.33 Deviation function and the resultant deviation force of a particular hoop

The resultant deviation force of a particular hoop, $D_{h,i}$, acts at the centre of gravity of the area under the function $D(\varphi)$, which is located at the hoop's yield point. The magnitude of the resultant deviation force generally depends on the magnitude of the friction coefficient and of the central angle that defines the cracked region. The influence of these two variables could be summed up in one coefficient as follows

$$\lambda_i = 2 \cdot \frac{1 - e^{-\mu(\varphi_{y,i} - \varphi_{0,i})}}{\mu^2} \tag{4.49}$$

Its course is plotted in Figure 4.34 for different friction coefficients and central angles $\varphi_{y,i} - \varphi_{0,i}$. Some important conclusions could be drawn about the physical nature of the deviatoric shear resisting mechanism. For a constant friction coefficient, the longer the hoop's arc length within the cracked concrete strut, i.e., the larger the angle $\varphi_{y,i} - \varphi_{0,i}$, the larger the hoop's resultant deviation force. Further, the higher the friction coefficient (e.g., a better bond between concrete and steel is assumed), the lower the hoop's resulting deviation force. The resultant deviation function of one hoop is

$$D_{h,i} = A_{sw} f_{yw} \cdot \lambda_i \tag{4.50}$$

Each particular hoop acts on concrete with a resultant deviation force $D_{h,i}$ oriented to the centre of the circle represented by a hoop.

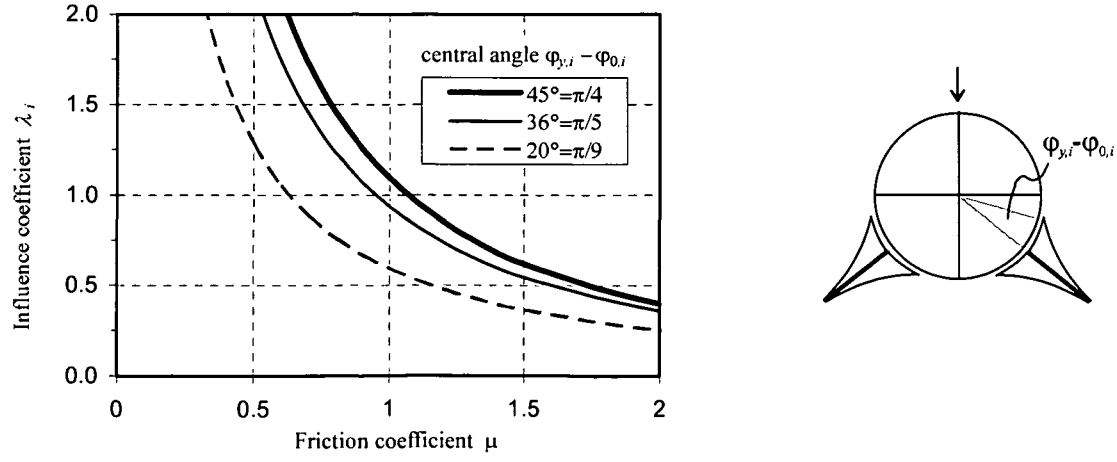


Figure 4.34 Influence coefficient versus friction coefficient for different central angles of one hoop

## Total Deviation Force of Hoops

The hoop's total deviation force is obtained by summing up the components of the resultant deviation force of each particular hoop, $D_{h,i}$, in the direction of the external shear along the cracked region (Figure 4.35). Thus

$$V_{sd} = 2A_{sw}f_{yw}\sum_{i=0}^{n_d}\lambda_i \cdot sin\varphi_{y,i} \tag{4.51}$$

where

$$\lambda_i = 2\cdot\frac{1-e^{-\mu(\varphi_{y,i}-\varphi_{0,i})}}{\mu^2} \tag{4.52}$$

The coefficient 2 in Equation 4.51 denotes that each hoop corresponds with two resultant deviation forces symmetrically. It has been assumed that the diagonal crack starts exactly at the intersection of the hoop with the bottom longitudinal reinforcement. In Equation 4.51, $n_d$ denotes the number of hoops crossed by the diagonal crack. Note that only hoops with a yield point under the axis of symmetry actually enhance the member's shear capacity (shaded area in Figure 4.35), since only their component counteracts to the external shear force. If the yield point is beyond the symmetry axis the component of the deviation force acts in the same direction as the external shear and has no shear enhancing effect. Therefore solely hoops under the symmetry axis have been considered.

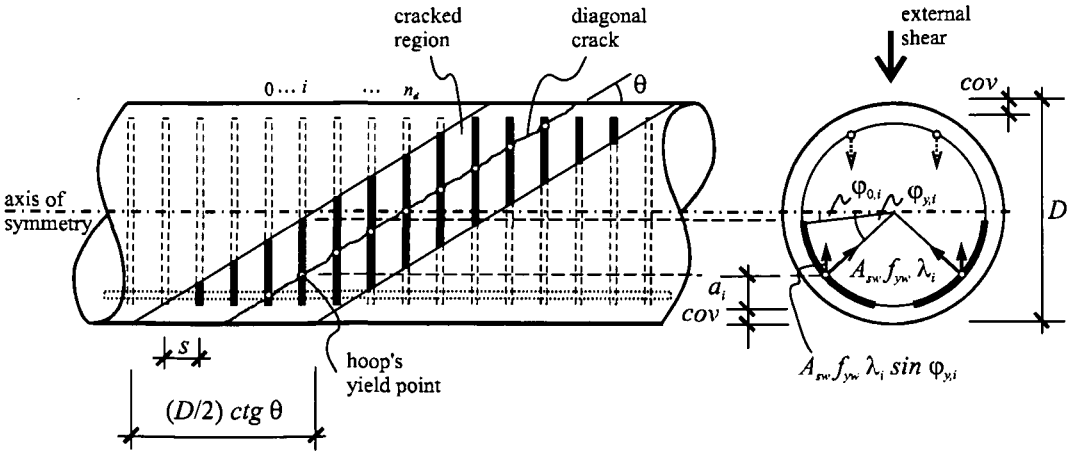


Figure 4.35 Hoop's deviatoric shear carrying capacity along the member's cracked region

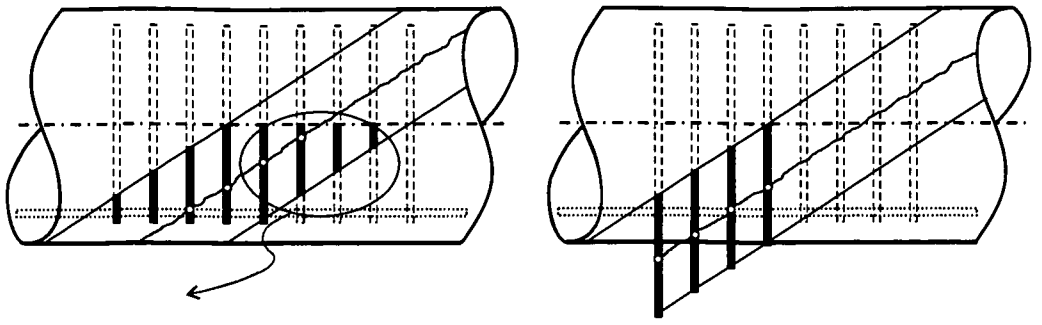

Figure 4.36 Transformation of hoops

The magnitude of the influence coefficient, $\lambda_i$, of a particular hoop depends on the value of the central angle $\varphi_{y,i} - \varphi_{0,i}$. However, all hoops within the inclined cracked region have a different arc length and consequently a different central angle. The following transformation enables us to obtain a simple solution. The parallelogram, formed by hoops below the member's axis of symmetry (Figure 4.36 left), has been vertically divided in two similar triangles; the part marked with an ellipse is moved under the other triangle. In such a way the hoops are coupled and a constant hoop's arc length along the whole cracked region is obtained, each of them with an equal central angle, see Figure 4.36 right. Instead of having each particular hoop of a different central angle we obtain the same number of hoops but with the same central angle, $\varphi_{max}$.

The central angle will be derived from the geometry in Figure 4.37. Consider the hoop with a yield point on the section's symmetry axis, intersecting both outer boundary lines of the cracked region. The diagonally cracked region is assumed to extend to $(D/2)ctg\theta$. The corresponding chord of the circle is $D/2$. From the geometry the central angle follows as

$$sin(\varphi_{max}) = \frac{D/4}{D/2 - cov} \tag{4.53}$$

for a typical value of $cov/D$ of up to 10% the maximal central angle is obtained

$$\varphi_{max} = 34° - 38° \cong \frac{\pi}{5} \tag{4.54}$$

This simplification makes possible carrying out the summation in Equation 4.51 along the same number of hoops but with a constant influence coefficient for each hoop.

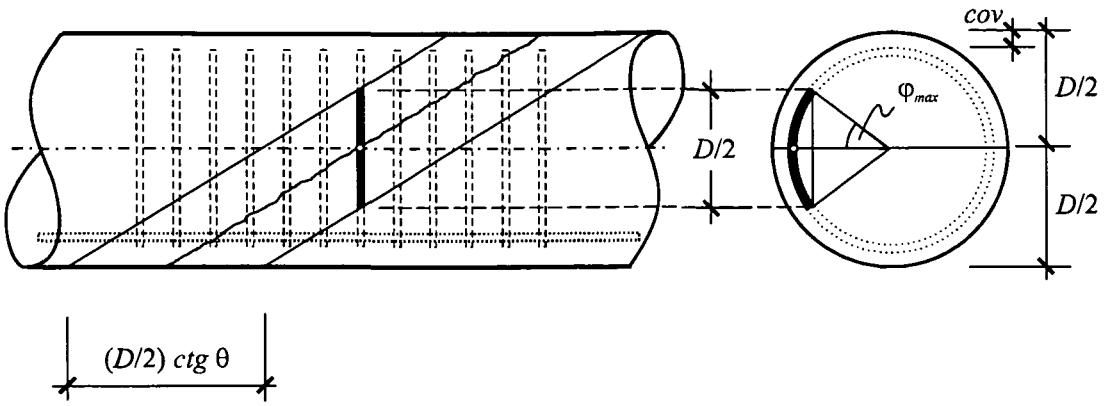


Figure 4.37 Hoop's maximal central angle

From Figure 4.34 the influence coefficient, for an assumed friction coefficient of 1.5 and for $\varphi_{max} = \pi/5$, is obtained

$$\lambda = \lambda_i(\pi/5) = 0.53 \tag{4.55}$$

This allows us to factor the constant influence coefficient, $\lambda$, out of the sum in Equation 4.51 and the hoop's total deviatoric component is thus simplified as

$$V_{sd} = 2A_{sw}f_{yw}\,\lambda \sum_{i=0}^{n_d} sin\varphi_{y,i} \tag{4.56}$$

The number of hoops, $n_d$, under the symmetry axis crossed by the diagonal crack is

$$n_d = INT\left[\frac{(D/2-cov)}{s}ctg\theta\right] \tag{4.57}$$

and the central angle, $\varphi_{y,i}$, is given by

$$sin\varphi_{y,i} = \frac{D/2-cov-a_i}{D/2-cov} \tag{4.58}$$

Following the same procedure as in chapter 4.4.2, it is obtained that

$$a_i = i \cdot \frac{(D/2-cov)}{n_d} \tag{4.59}$$

and the central angle is

$$sin\varphi_{y,i} = 1 - \frac{i}{n_d} \tag{4.60}$$

Thus the total deviatoric shear capacity of the hoops is

$$V_{sd} = 2A_{sw}f_{yw}\,\lambda \sum_{i=0}^{n_d}\left(1-\frac{i}{n_d}\right) \tag{4.61}$$

Because of the simplification, the summation term has been defined as the *deviation influence coefficient* $k_d$

$$k_d = \sum_{i=0}^{n_d}\left(1-\frac{i}{n_d}\right) \tag{4.62}$$

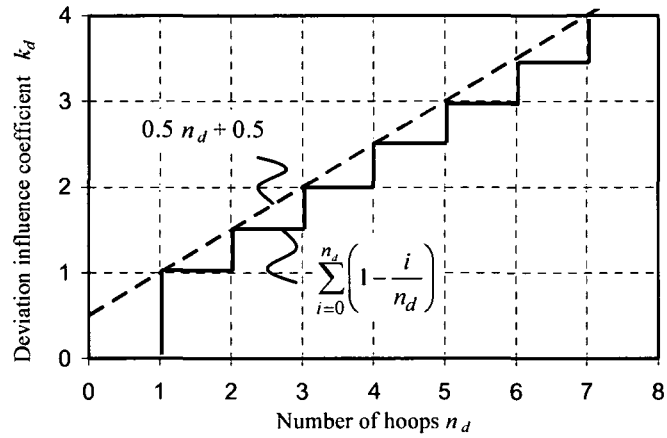


Figure 4.38 Deviation influence coefficient as a function of hoop's number

This discrete function could be replaced by the continues function (Figure 4.38)

$$k_d \cong 0.5n_d + 0.5 \tag{4.63}$$

and a simple expression of the deviatoric shear capacity of hoops is obtained

$$V_{sd} = 2A_{sw}f_{yw}\cdot\lambda\cdot(0.5n_d + 0.5) \tag{4.64}$$

where the number of hoops crossed by the crack is calculated from

$$n_d = INT\left[\frac{(D/2-cov)}{s}ctg\theta\right] \tag{4.65}$$

and the influence coefficient is taken as $\lambda = 0.53$ for an assumed friction coefficient of $\mu = 1.5$.

### 4.4.5 Total Shear Force Carried by Shear Reinforcement

The total shear force carried by the hoops of circular sections is added together from the tension and deviation component

$$V = A_{sw} f_{yw} \left(1.8 \cdot n_t + \lambda \cdot n_d + 1\right) \tag{4.66}$$

where the number of hoops active in tension and in deviation is respectively

$$n_t = \left(D - c - cov\right) ctg\theta / s \tag{4.67}$$

$$n_d = INT\left[\left(D/2 - cov\right) ctg\theta / s\right] \tag{4.68}$$

and $\lambda = 0.53$ for an assumed friction coefficient of $\mu = 1.5$.

In the thesis only circular hoops have been considered. In practice, for the convenience of construction, mostly spiral hoops are used. The shear capacity of spirals is however less than the shear capacity of circular hoops. When the diagonal shear plane cuts a spiral, one of its legs runs broadly parallel to the crack and is thus less beneficial in carrying shear than the other one, see Feltham (2004) for more details. Clarke and Birjandi (1993) proposed reducing the shear capacity of spirals compared to hoops with an efficiency coefficient. The larger the spiral's pitch the flatter the inclination of one leg and the lower its contribution to the shear capacity. The efficiency coefficient has been thus defined as a function of the spiral's pitch which in turn is expressed as a proportion of the effective depth. As a consequence, in the case of spiral reinforcement the proposed equation 4.66 should be additionally multiplied by the reduction coefficient defined in Figure 4.39.

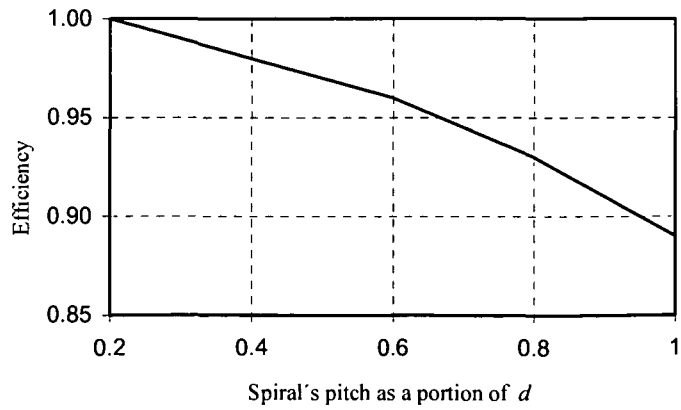


Figure 4.39 Spiral's efficiency as a function of its pitch

# 5 DISCUSSION OF RESULTS AND COMPARISON TO OTHER MODELS

## 5.1 Verification of the Proposed Model for Monotonic Load

The proposed model for the capacity of circular cross section members under shear load is

$$V = \xi\left[3.7\rho_l + 0.18 + 0.08\left(\frac{P}{A_g}\right)^{0.3}\right] \cdot k \cdot \sqrt{f_c'} \cdot 0.7A_g + A_{sw} f_{yw}\left(1.8 \cdot n_t + \lambda \cdot n_d + 1\right)$$

with

$$\xi = \frac{1+\sqrt{5.08/d_a}}{\sqrt{1+d/(25d_a)}}$$

$$k = \begin{cases} 1.00 & \text{for} \quad a/D > 2.5 \\ 1.25 & \text{for} \quad a/D \le 2.5 \end{cases}$$

$$n_t = \frac{(D-c-cov)}{s} ctg\theta$$

$$n_d = INT\left[\frac{(D/2-cov)}{s} ctg\theta\right]$$

$$\lambda = 0.53$$

$\rho_l$ is the longitudinal reinforcement ratio, $P$ the axial load, $A_g$ the sections gross area, $f_c'$ the

concrete compressive strength, $A_{sw}$ the cross section of the stirrup, $f_{yw}$ its yield strength, $a$ the shear-span, $D$ is the section's diameter, $c$ the compression zone's depth, $cov$ the concrete cover, $s$ the spacing of the hoops, $\theta$ the crack's inclination angle, $d$ is the section's effective depth and $d_a$ the maximal aggregate size.

The model has been verified on the database of 62 circular members with shear reinforcement (Table 3.2) by comparing it to the two existing models – Clarke et al. (1993) and Kowalsky et al. (2000). The validity of the models is compared by calculating the statistic values of their mean strength, standard deviation, coefficient of determination $r^2$ and coefficient of variation $CoV$ [%]. The closer the mean strength to 1.0 and the lower the standard deviation, the better the model. The coefficient of determination provides a measure of the strength of the correlation of the data with the model. Its value is between 0 and 1.0 and the closer it is to 1.0, the higher is the correlation between the proposed model and the experimental values. The coefficient of variation is a statistical measure of the dispersion of data points around the mean. Thus for a good prediction it should be as low as possible.

The statistical comparison of experimental/theoretical shear strength calculated by the existing models and by the proposed one is provided in Table 5.1. The coefficient of determination by Clarke et al., Kowalsky et al. and the proposed model are 0.85, 0.66 and 0.88 respectively, meaning that the shear capacities predicted by the proposed model are in stronger correlation with the experimental values. The model proposed by Clarke et al. has a mean strength ratio of 1.23, standard deviation of 0.13 and coefficient of variation 10%, whereas the model of Kowalsky et al. is slightly more conservative, with a mean strength ratio of 1.25, standard deviation of 0.21 and coefficient of variation 16%. The proposed model provides the closest agreement with experimental data, with a mean strength ratio of 1.01, standard deviation of 0.11 and coefficient of variation 10%.

The experimental ultimate shear strength versus theoretical ultimate shear strength of specimens of different proposals is plotted in Figure 5.1. The ratios between theoretical and experimental shear strengths across the range of all parameters, such as concrete compressive strength, aspect ratio, axial load ratio and longitudinal reinforcement ratio are

plotted in Figures 5.2 to 5.6. The smaller scatter of data by the proposed model indicates that the influence of a particular variable affecting shear strength appears to be well represented. Thus the proposed model clearly improves the prediction of the shear capacity of circular sections with transverse reinforcement.

The experimental shear capacities as well as the theoretical shear capacities calculated by different proposed models are listed in Table 5.2.

Table 5.1 Statistical comparison of models in terms of experimental/theoretical shear strength ratio

| | Clarke and Birjandi (1993) | Kowalsky and Priestley (2000) | Proposed |
|---|---|---|---|
| Mean value | 1.23 | 1.25 | 1.01 |
| Standard deviation | 0.13 | 0.21 | 0.11 |
| Coefficient of variation, $CoV$ [%] | 10 | 16 | 10 |
| Coefficient of determination, $r^2$ | 0.85 | 0.66 | 0.88 |

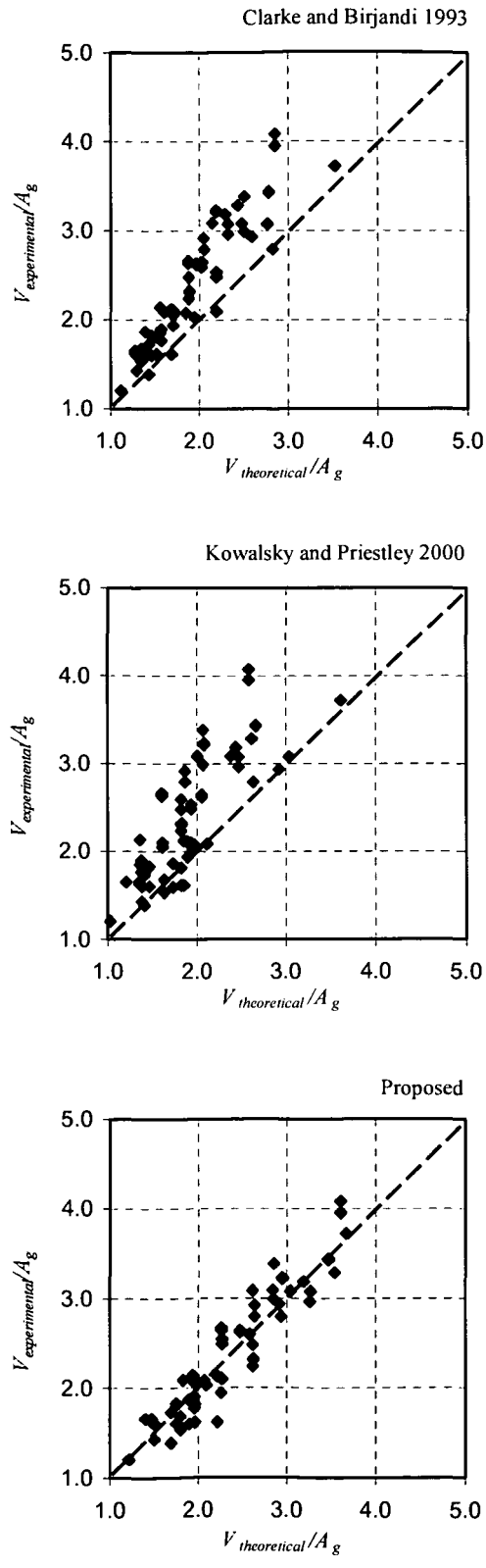


Figure 5.1 Ultimate shear strength of circular section members with shear reinforcement

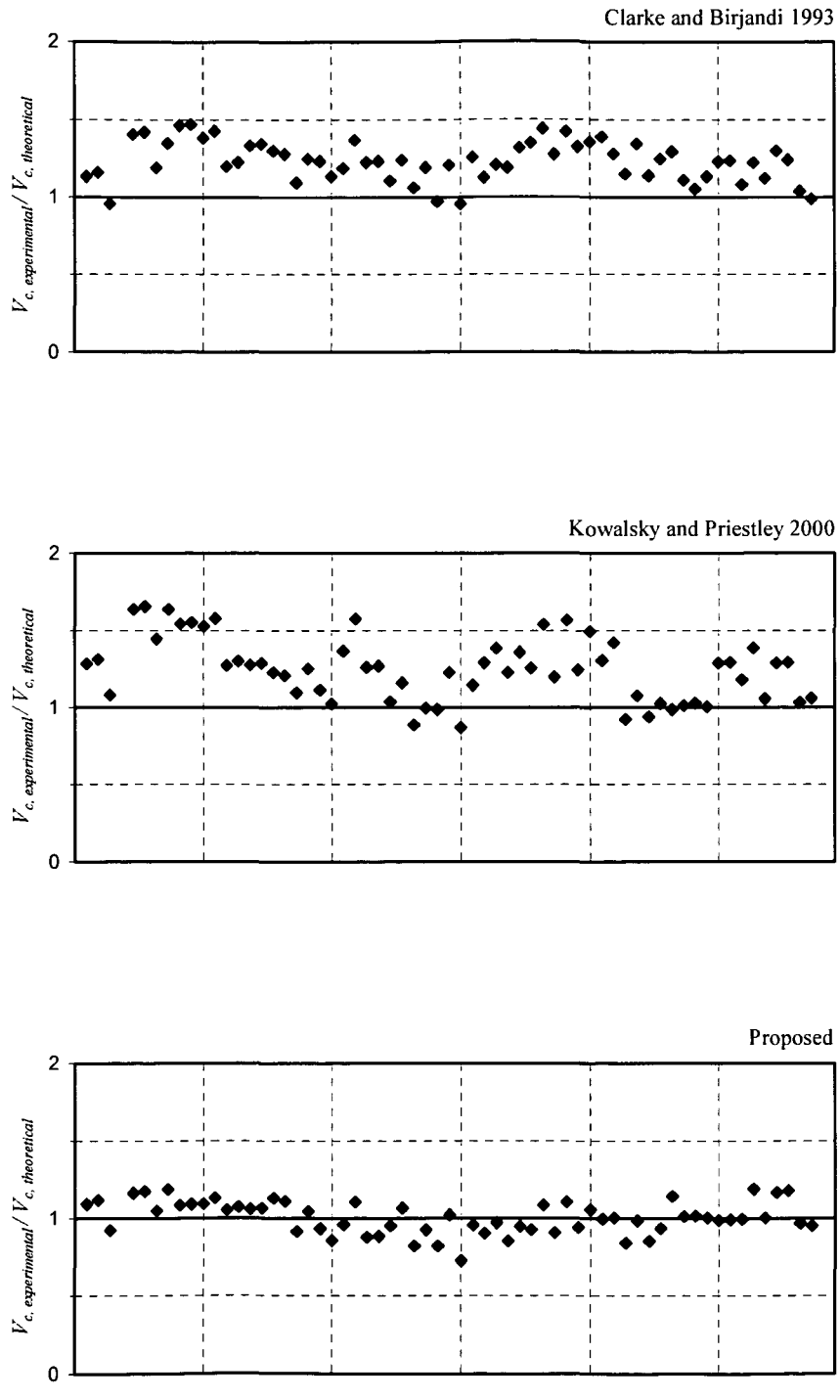


Figure 5.2 Ratio of experimental to theoretical shear strengths of members with shear reinforcement

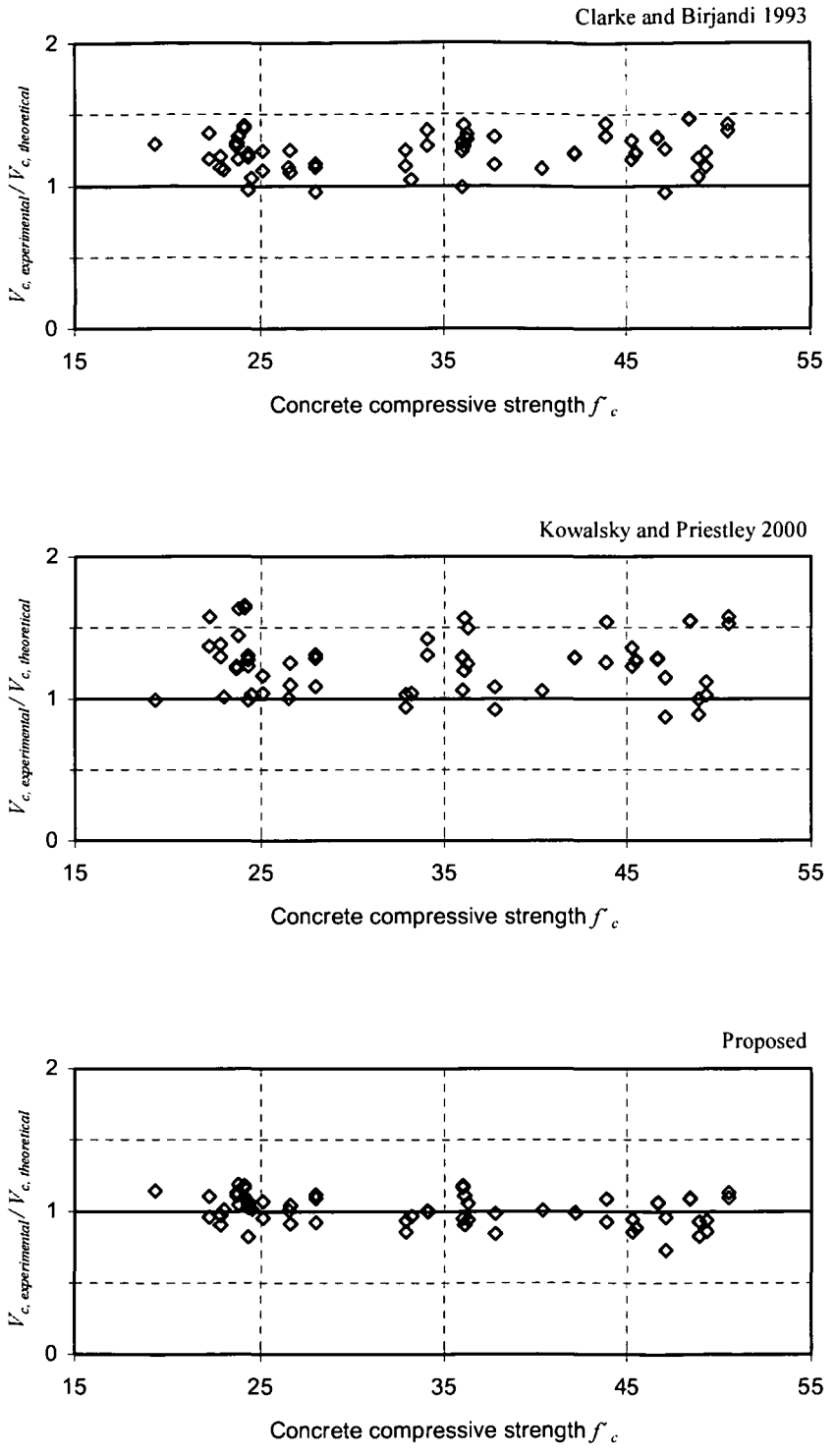


Figure 5.3 Ratio of experimental to theoretical shear strengths versus concrete compressive strength of members with shear reinforcement

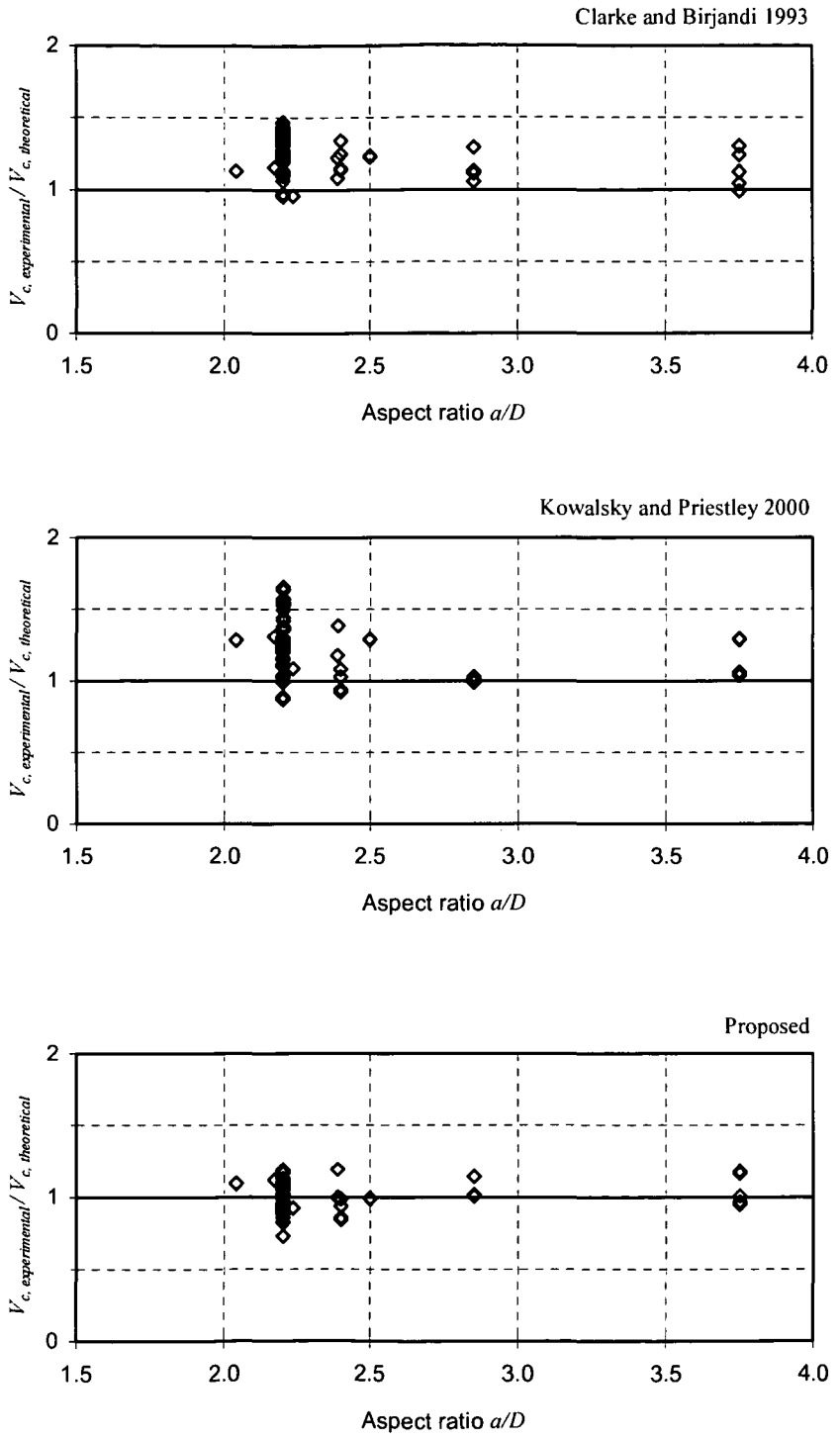


Figure 5.4 Ratio of experimental to theoretical shear strengths versus aspect ratio of members with shear reinforcement

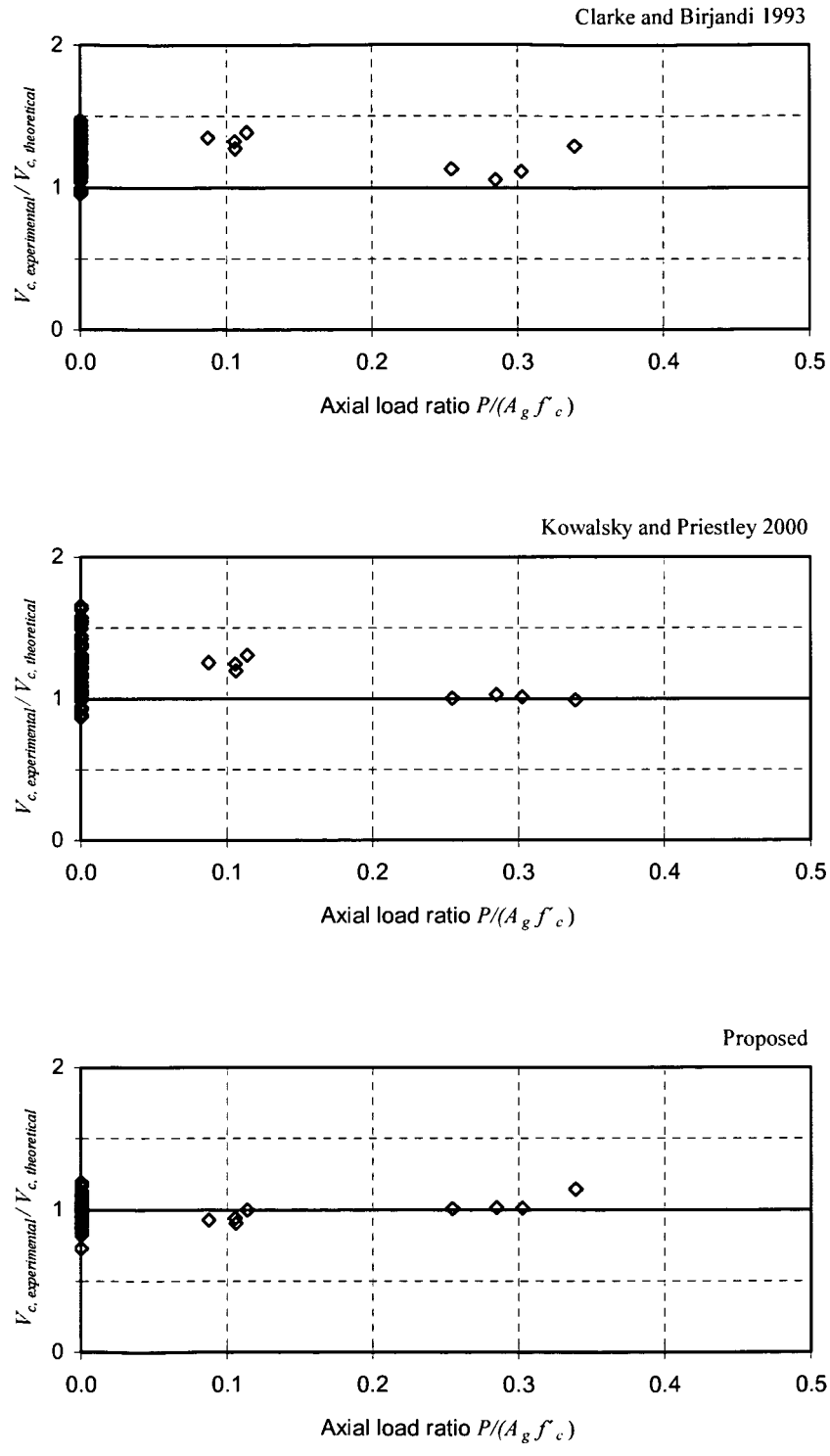


Figure 5.5 Ratio of experimental to theoretical shear strengths versus axial load ratio of members with shear reinforcement

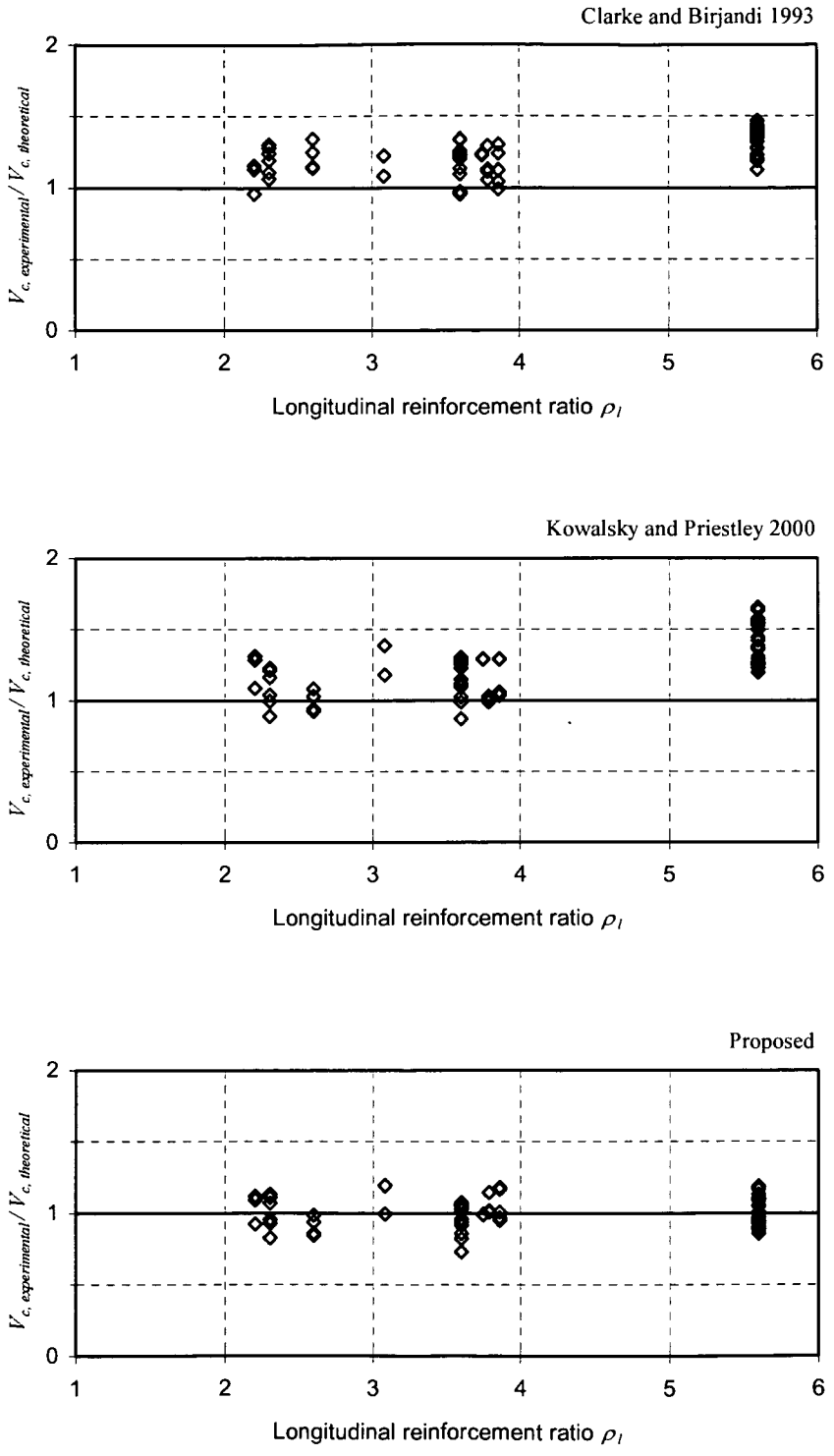


Figure 5.6 Ratio of experimental to theoretical shear strengths versus longitudinal reinforcement ratio of members with shear reinforcement

Table 5.2 Calculated and measured shear capacities of specimens with shear reinforcement

| Specimen | | $V_{experimental}$ [kN] | $V_{theoretical}$ [kN] | | | $V_{experimental}/V_{theoretical}$ | | |
|---|---|---|---|---|---|---|---|---|
| | | | Clarke, Birjandi | Kowalsky, Priestley | Proposed | Clarke, Birjandi | Kowalsky, Priestley | Proposed |
| Clarke, Birjandi (1993) | M1/2 | 45.0 | 39.75 | 35.09 | 41.17 | 1.13 | 1.28 | 1.09 |
| | M1/3 | 46.0 | 39.75 | 35.09 | 41.17 | 1.16 | 1.31 | 1.12 |
| | M1/4 | 38.0 | 39.75 | 35.09 | 41.17 | 0.96 | 1.08 | 0.92 |
| | 11-1 | 186.0 | 132.40 | 113.59 | 159.89 | 1.40 | 1.64 | 1.16 |
| | 11-2 | 188.0 | 132.40 | 113.59 | 159.89 | 1.42 | 1.66 | 1.18 |
| | 12-1 | 211.0 | 177.26 | 146.21 | 201.53 | 1.19 | 1.44 | 1.05 |
| | 12-2 | 239.0 | 177.26 | 146.21 | 201.53 | 1.35 | 1.63 | 1.19 |
| | 13-1 | 227.0 | 154.96 | 147.15 | 208.90 | 1.46 | 1.54 | 1.09 |
| | 13-2 | 228.0 | 154.96 | 147.15 | 208.90 | 1.47 | 1.55 | 1.09 |
| | 14-1 | 279.0 | 201.72 | 182.72 | 254.86 | 1.38 | 1.53 | 1.09 |
| | 14-2 | 288.0 | 201.72 | 182.72 | 254.86 | 1.43 | 1.58 | 1.13 |
| | 15-1 | 145.0 | 120.68 | 113.92 | 137.82 | 1.20 | 1.27 | 1.05 |
| | 15-2 | 148.0 | 120.68 | 113.92 | 137.82 | 1.23 | 1.30 | 1.07 |
| | 16-1 | 185.0 | 138.83 | 145.13 | 174.69 | 1.33 | 1.27 | 1.06 |
| | 16-2 | 186.0 | 138.83 | 145.13 | 174.69 | 1.34 | 1.28 | 1.06 |
| | 17-1 | 117.0 | 89.90 | 95.23 | 103.62 | 1.30 | 1.23 | 1.13 |
| | 17-2 | 115.0 | 89.90 | 95.23 | 103.62 | 1.28 | 1.21 | 1.11 |
| | 19-1 | 113.0 | 103.18 | 103.17 | 123.70 | 1.10 | 1.10 | 0.91 |
| | 19-2 | 129.0 | 103.18 | 103.17 | 123.70 | 1.25 | 1.25 | 1.04 |
| | 20-1 | 149.0 | 120.74 | 133.72 | 159.78 | 1.23 | 1.11 | 0.93 |
| | 20-2 | 137.0 | 120.74 | 133.72 | 159.78 | 1.13 | 1.02 | 0.86 |
| | 21-1 | 131.0 | 110.29 | 95.86 | 136.62 | 1.19 | 1.37 | 0.96 |
| | 21-2 | 151.0 | 110.29 | 95.86 | 136.62 | 1.37 | 1.58 | 1.11 |
| | 22-1 | 163.0 | 132.96 | 129.19 | 185.30 | 1.23 | 1.26 | 0.88 |
| | 22-2 | 164.0 | 132.96 | 129.19 | 185.30 | 1.23 | 1.27 | 0.89 |
| | 23-1 | 101.0 | 91.14 | 97.46 | 105.94 | 1.11 | 1.04 | 0.95 |
| | 23-2 | 113.0 | 91.14 | 97.46 | 105.94 | 1.24 | 1.16 | 1.07 |
| | 24-1 | 114.0 | 107.31 | 128.66 | 138.44 | 1.06 | 0.89 | 0.82 |
| | 24-2 | 128.0 | 107.31 | 128.66 | 138.44 | 1.19 | 0.99 | 0.92 |
| | 25-1 | 98.0 | 100.90 | 99.43 | 119.28 | 0.97 | 0.99 | 0.82 |
| | 25-2 | 122.0 | 100.90 | 99.43 | 119.28 | 1.21 | 1.23 | 1.02 |
| | 26-1 | 114.0 | 119.31 | 131.12 | 156.72 | 0.96 | 0.87 | 0.73 |
| | 26-2 | 150.0 | 119.31 | 131.12 | 156.72 | 1.26 | 1.14 | 0.96 |
| | 27-1 | 125.0 | 111.04 | 96.90 | 138.13 | 1.13 | 1.29 | 0.90 |
| | 27-2 | 134.0 | 111.04 | 96.90 | 138.13 | 1.21 | 1.38 | 0.97 |
| | 28-1 | 158.0 | 132.80 | 128.95 | 184.94 | 1.19 | 1.23 | 0.85 |
| | 28-2 | 175.0 | 132.80 | 128.95 | 184.94 | 1.32 | 1.36 | 0.95 |
| | 37-1 | 232.0 | 171.85 | 184.82 | 250.01 | 1.35 | 1.26 | 0.93 |
| | 37-2 | 218.0 | 151.48 | 141.72 | 200.97 | 1.44 | 1.54 | 1.08 |
| | 38-1 | 209.0 | 163.94 | 174.70 | 230.67 | 1.27 | 1.20 | 0.91 |
| | 38-2 | 206.0 | 144.84 | 131.60 | 186.20 | 1.42 | 1.57 | 1.11 |
| | 39-1 | 217.2 | 164.13 | 174.93 | 231.17 | 1.32 | 1.24 | 0.94 |
| | 39-2 | 197.0 | 145.02 | 131.88 | 186.59 | 1.36 | 1.49 | 1.06 |
| | 40-1 | 225.0 | 161.95 | 172.44 | 225.53 | 1.39 | 1.30 | 1.00 |
| | 40-2 | 183.0 | 142.98 | 128.84 | 182.16 | 1.28 | 1.42 | 1.00 |
| | 43-1 | 313.0 | 272.27 | 339.08 | 371.58 | 1.15 | 0.92 | 0.84 |
| | 43-2 | 366.0 | 272.27 | 339.08 | 371.58 | 1.34 | 1.08 | 0.98 |
| | 44-1 | 301.0 | 263.69 | 320.30 | 352.02 | 1.14 | 0.94 | 0.86 |
| | 44-2 | 329.0 | 263.69 | 320.30 | 352.02 | 1.25 | 1.03 | 0.93 |

Table 5.2 (Continued)

| Specimen | | $V_{experimental}$ [kN] | $V_{theoretical}$ [kN] | | | $V_{experimental}/V_{theoretical}$ | | |
|---|---|---|---|---|---|---|---|---|
| | | | Clarke, Birjandi | Kowalsky, Priestley | Proposed | Clarke, Birjandi | Kowalsky, Priestley | Proposed |
| Khalifa, Collins (1981) | SC1 | 324.0 | 250.59 | 328.86 | 283.66 | 1.29 | 0.99 | 1.14 |
| | SC2 | 478.0 | 430.09 | 472.42 | 473.11 | 1.11 | 1.01 | 1.01 |
| | SC3 | 578.0 | 548.20 | 561.54 | 569.48 | 1.05 | 1.03 | 1.01 |
| | SC4 | 456.0 | 402.43 | 454.93 | 453.83 | 1.13 | 1.00 | 1.00 |
| Merta et al. (2003) | 1 | 430.0 | 349.66 | 334.23 | 435.80 | 1.23 | 1.29 | 0.99 |
| | 2 | 432.0 | 349.66 | 334.23 | 435.80 | 1.24 | 1.29 | 0.99 |
| Capon, de Cossio (1965) | F-25 | 59.5 | 54.98 | 50.55 | 59.79 | 1.08 | 1.18 | 1.00 |
| | F-12.5 | 82.0 | 66.98 | 59.26 | 68.92 | 1.22 | 1.38 | 1.19 |
| Kim (2000) | YJC200R | 323.0 | 287.33 | 306.31 | 321.34 | 1.12 | 1.05 | 1.01 |
| | YJC150R | 411.0 | 315.60 | 319.16 | 352.66 | 1.30 | 1.29 | 1.17 |
| | YJC100R | 479.0 | 385.75 | 370.54 | 406.90 | 1.24 | 1.29 | 1.18 |
| | YJC200W | 315.0 | 302.70 | 304.51 | 325.44 | 1.04 | 1.03 | 0.97 |
| | YJC100W | 434.0 | 439.34 | 409.80 | 456.84 | 0.99 | 1.06 | 0.95 |

## 5.2 Verification of the Proposed Model for Cyclic Load

The usual way of estimation of the member's shear capacity under cyclic load is to multiply its capacity under monotonic load by the so called "degradation coefficient". It takes into account the degradation of the shear capacity under cyclic reversal and is usually defined as a function of the displacement ductility demand, see Figures 2.1 and 2.2. The degradation coefficient has been suggested in a variety of ways, i.e., with its application only to the concrete capacity term (Priestley et al., 1994; Kowalsky and Priestley, 2000) or with its application to both concrete and truss mechanism capacity (Sezen and Moehle, 2004). The former procedure is explained by the degradation of concrete component with increasing ductility due to the widening of cracks, which results in a reduced aggregate interlock capacity. The latter procedure is however based on observations that the concrete degradation leads to reduction in bond capacity of longitudinal and shear reinforcement and as a consequence in degradation of the truss mechanism as well.

The proposed model has been verified on a database of 29 elements tested under cyclic shear. These experiments were partly carried out in the frame of an extensive research started in 1987 at the University of California at San Diego to study the various problems

related to seismic response of bridge piles (Ang et al., 1989; Priestley et al., 1994a,b; Wong et al., 1993; Priestley and Benzoni, 1996). Another extensive research was conducted at the Kawashima Earthquake Engineering Laboratory at the Tokyo Institute of Technology (published on the home page of the University of Washington http://www.ce.washington.edu/~peera1/).

In the proposed model the strength degradation coefficient proposed by Sezen et al., 2004, was applied. It was found that the model better predicts the member's actual shear capacity if the degradation coefficient is applied solely on concrete capacity term (as proposed by Priestley et al., 1994) rather than on both concrete and truss mechanism capacities (as proposed by Sezen et al., 2004).

Figure 5.7 Shear strength degradation with displacement ductility by Sezen and Moehle (2004)

The statistical comparison of experimental/theoretical shear strength calculated by the model of Kowalsky et al. (2000) and by the proposed model is provided in Table 5.3 in terms of mean, standard deviation, coefficient of variation and coefficient of determination. The mean value of the proposed model is closer to 1.0 and the scatter of data is lower than in the model proposed by Kowalsky et al., meaning that the member's shear capacity calculated by the proposed model is closer to their actual shear capacity. The experimental ultimate shear strength versus theoretical ultimate shear strength of specimens is plotted in Figure 5.1.

Table 5.3 Details and test results of specimens with circular cross-section under cyclic load

| Ref. | Specimen | $D$ [mm] | a/$D$ [-] | $f'_c$ [MPa] | $cov$ [mm] | $f_{yl}$ [MPa] | $\rho_l$ [%] | $f_{yw}$ [MPa] | $\rho_w$ [%] | $s$ [mm] | S/H | $P$ [kN] | $P/(f'_c A_g)$ [-] | $V_{test}$ [kN] | $\mu$ [-] |
|---|---|---|---|---|---|---|---|---|---|---|---|---|---|---|---|
| Ang | 1 | 400 | 2.0 | 37.5 | 21 | 436 | 3.2 | 328 | 0.24 | 60 | S | 0 | 0.00 | 320 | 2.5 |
| et al. | 2 | 400 | 2.0 | 37.2 | 21 | 296 | 3.2 | 328 | 0.24 | 60 | S | 0 | 0.00 | 228 | 4.0 |
| (1989) | 3 | 400 | 2.5 | 36.0 | 21 | 436 | 3.2 | 328 | 0.24 | 60 | S | 0 | 0.00 | 298 | 4.0 |
| | 4 | 400 | 2.0 | 30.6 | 21 | 436 | 3.2 | 316 | 0.24 | 165 | S | 0 | 0.00 | 295 | 1.4 |
| | 5 | 400 | 2.0 | 31.1 | 21 | 436 | 3.2 | 328 | 0.35 | 40 | S | 0 | 0.00 | 340 | 2.4 |
| | 6 | 400 | 1.5 | 30.1 | 21 | 436 | 3.2 | 328 | 0.24 | 60 | S | 0 | 0.00 | 390 | 1.3 |
| | 7 | 400 | 2.0 | 29.5 | 21 | 448 | 3.2 | 372 | 0.18 | 80 | S | 0 | 0.00 | 280 | 1.6 |
| | 8 | 400 | 2.0 | 28.7 | 21 | 448 | 3.2 | 372 | 0.47 | 30 | S | 721 | 0.20 | 475 | 4.0 |
| | 10 | 400 | 2.0 | 31.2 | 21 | 448 | 3.2 | 332 | 0.47 | 120 | S | 784 | 0.20 | 450 | 4.0 |
| | 11 | 400 | 2.0 | 29.9 | 21 | 448 | 3.2 | 372 | 0.24 | 60 | S | 751 | 0.20 | 404 | 2.5 |
| | 12 | 400 | 1.5 | 28.6 | 21 | 436 | 3.2 | 328 | 0.47 | 30 | S | 359 | 0.10 | 527 | 3.0 |
| | 13 | 400 | 2.0 | 36.2 | 21 | 436 | 3.2 | 326 | 0.47 | 30 | S | 455 | 0.10 | 443 | 4.0 |
| | 14 | 400 | 2.0 | 33.7 | 21 | 424 | 3.2 | 326 | 0.24 | 60 | S | 0 | 0.00 | 311 | 2.0 |
| | 15 | 400 | 2.0 | 34.8 | 21 | 436 | 1.9 | 326 | 0.24 | 60 | S | 0 | 0.00 | 230 | 4.0 |
| | 16 | 400 | 2.0 | 33.4 | 21 | 436 | 3.2 | 326 | 0.24 | 60 | S | 420 | 0.10 | 379 | 1.5 |
| | 17 | 400 | 2.5 | 34.3 | 21 | 436 | 3.2 | 326 | 0.24 | 60 | S | 431 | 0.10 | 329 | 2.0 |
| | 18 | 400 | 1.5 | 35.0 | 21 | 436 | 3.2 | 326 | 0.24 | 60 | S | 440 | 0.10 | 507 | 1.4 |
| | 19 | 400 | 1.5 | 34.4 | 21 | 436 | 3.2 | 326 | 0.18 | 80 | S | 432 | 0.10 | 436 | 1.3 |
| | 20 | 400 | 1.8 | 36.7 | 21 | 482 | 3.2 | 326 | 0.18 | 80 | S | 807 | 0.17 | 487 | 1.5 |
| | 21 | 400 | 2.0 | 33.2 | 21 | 436 | 3.2 | 326 | 0.18 | 80 | S | 0 | 0.00 | 258 | 1.1 |
| | 22 | 400 | 2.0 | 30.9 | 21 | 436 | 3.2 | 310 | 0.18 | 220 | S | 0 | 0.00 | 280 | 1.5 |
| | 23 | 400 | 2.0 | 32.3 | 21 | 436 | 3.2 | 332 | 0.35 | 160 | S | 0 | 0.00 | 339 | 2.0 |
| | 24 | 400 | 2.0 | 33.1 | 21 | 436 | 3.2 | 310 | 0.36 | 110 | S | 0 | 0.00 | 338 | 4.0 |
| | 25 | 400 | 1.5 | 32.8 | 21 | 296 | 3.2 | 0 | 0.00 | 0 | S | 0 | 0.00 | 233 | 1.2 |
| Priestley | C1A | 610 | 2.0 | 31.0 | 21 | 324 | 2.5 | 359 | 2.54 | 127 | S | 592 | 0.07 | 573 | 2.8 |
| et al. (1994a,b) | C3A | 610 | 2.0 | 34.5 | 21 | 324 | 2.5 | 324 | 2.54 | 127 | S | 1780 | 0.18 | 733 | 3.1 |
| Wong et al. (1993) | 2 | 400 | 2.0 | 37.0 | 21 | 475 | 3.2 | 340 | 0.22 | 65 | S | 1830 | 0.39 | 515 | 2.0 |
| Priestley | 1 | 610 | 1.5 | 30.0 | 20 | 462 | 0.5 | 361 | 0.14 | 76.2 | S | 503 | 0.06 | 400 | 10.0 |
| et al. (1996) | 2 | 610 | 1.5 | 30.0 | 20 | 462 | 1.1 | 361 | 0.08 | 127 | S | 503 | 0.06 | 587 | 4.0 |

Table 5.4 Statistical comparison of models in terms of experimental/theoretical shear strength ratio

| | Kowalsky and Priestley (2000) | Proposed |
|---|---|---|
| Mean value | 1.24 | 1.19 |
| Standard deviation | 0.14 | 0.12 |
| Coefficient of variation, $CoV$ [%] | 12 | 10 |
| Coefficient of determination, $r^2$ | 0.88 | 0.92 |

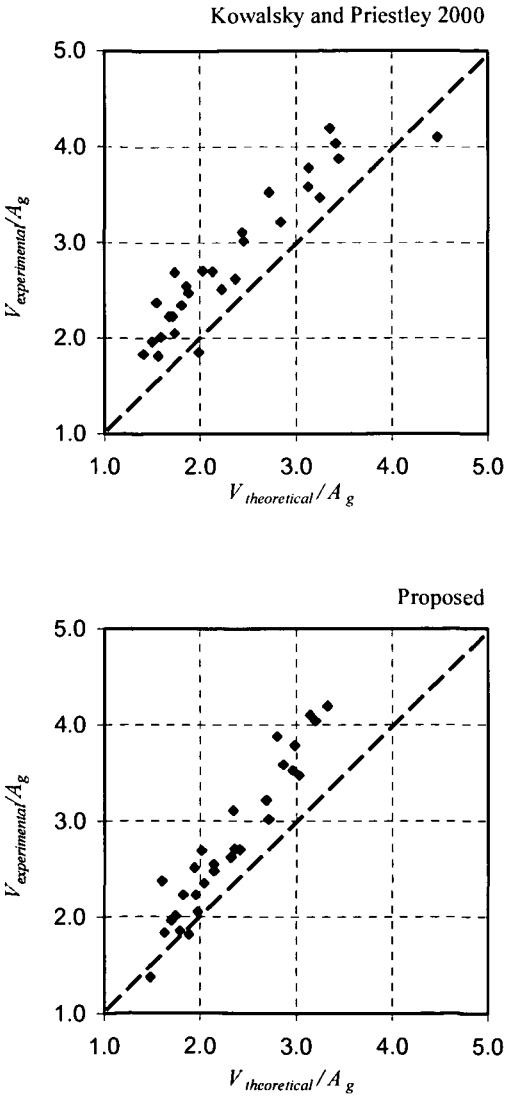


Figure 5.8 Ultimate shear strength of circular section members with shear reinforcement under cyclic load

## 5.3 Adequacy of the Proposed Model for Design

The proposed formula is a predictive and not a design equation, representing therefore the characteristic shear resistance of the member. It follows that higher average values of the strength ratios are inevitable. In the model measured concrete compression strength and reinforcement yield strength was used. In the design situations, however, nominal material strengths would be used. According to the Eurocode, to obtain the design value of the material property partial safety factors for the material properties should be applied. These are $\gamma_c = 1.5$ for concrete and $\gamma_s = 1.15$ for steel. By applying the strength reduction factors a reasonable lower bound of data is obtained, resulting in an adequately conservative design equation suitable for incorporation into design codes, see Figures 5.8 and 5.9.

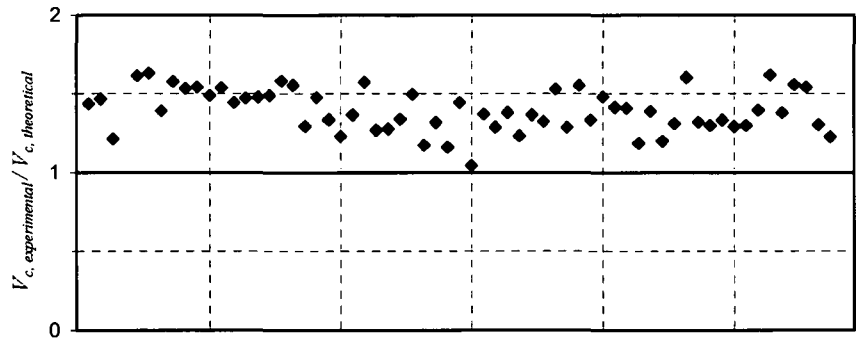


Figure 5.9 Ratio of experimental to design shear strengths of circular section members with shear reinforcement

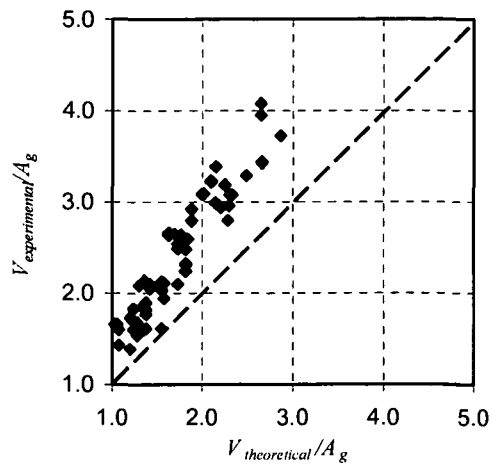


Figure 5.10 Design shear strength of circular section members with shear reinforcement

# 6 CONCLUSION AND FUTURE WORK

In the thesis, an analytical model for the prediction of the shear capacity of reinforced concrete members with circular cross-section transversely reinforced with circular hoops has been developed. The proposed shear capacity model is a semi-empirical equation based on the truss analogy by adding an empirical concrete shear capacity term to the capacity of the shear reinforcement.

The concrete shear capacity, taken as the capacity of the member without shear reinforcement, has been derived by a parameter study of the main variables affecting shear strength such as the concrete compressive strength, the longitudinal reinforcement ratio, the member's shear span-to-depth ratio and the axial load level. Applying a curve fit on the test data of members without shear reinforcement the influence of the individual variable has been derived.

The shear reinforcement capacity is derived analytically, based on the truss analogy, by taking into account the identified additional deviatoric shear resisting mechanism of hoops present only by members with curved transverse reinforcement. Based on the shear database of transversely reinforced circular members, the validity and accuracy of the proposed model have been compared to other recently proposed models.

The statistical comparison of experimental/theoretical shear capacity calculated by the existing models and by the proposed one indicates that the section's shear capacity predicted by the proposed model are in stronger correlation with the experimental values as well as the effect of a particular variable, affecting shear strength, is better captured than by other existing proposals. Thus the proposed model clearly improves the prediction of the shear capacity of reinforced concrete circular cross-section members. By applying the strength reduction factors a sufficiently conservative design equation could be obtained, suitable for design purposes and incorporation in design codes.

The applicability of the proposed model has been verified on a database of members tested under uniaxial cyclic shear. With the application of a strength degradation coefficient, proposed so far in literature, the members shear capacity under cyclic load with increasing ductility has been expressed. The proposed model has been compared to a recently proposed model and it has been found that it predicts reasonably well the shear capacity of circular sections under cyclic load as well.

However, since no circular cross-section specimens with an aspect ratio lower than 2 have been tested so far, it is not possible to make a firm conclusion about the member's shear capacity enhancement within this range. Likewise, no data of circular cross-section specimens tested over a broad range of variable depth are available in literature. Consequently the size effect of circular section specimens could not be investigated and properly estimated. In order to overcome these deficiencies as well as to be able to propose a general design equation a comprehensive experimental research is necessary in the future.

# 7 LIST OF FIGURES AND TABLES

Figure 2.1 (Left) Degradation coefficient k of concrete shear strength with displacement ductility and (Right) axial load contribution to the concrete shear capacity (Priestley et al. 1994) ..... 20

Figure 2.2 (Left) Degradation coefficient $\gamma$ of concrete shear strength with displacement ductility and (Right) Aspect ratio enhancement coefficient $\alpha$ (Kowalsky et al., 2000) ..... 20

Table 3.1 Details and test results of specimens with circular cross-section without shear reinforcement ..... 26

Table 3.2 Details and test results of specimens with circular cross-section with shear reinforcement ..... 27

Table 3.2 (Continued) ..... 28

Figure 4.1 Components of shear strength in a beam without and with shear reinforcement ..... 30

Figure 4.8 Effect of longitudinal reinforcement ratio, $\rho_l$, on normalized shear strength ..... 40

Figure 4.9 Effect of longitudinal reinforcement ratio, $\rho_l$, on normalized shear strength for specimens with different aspect ratio, a/D, and axial load, P ..... 41

Figure 4.10 Normalized shear strength versus longitudinal reinforcement ratio ..... 41

Figure 4.11 Effect of longitudinal reinforcement yield strength on normalized shear strength ..... 42

Figure 4.12 Effect of the members' aspect ratio on normalized shear strength ..... 44

Figure 4.13 Influence of the members' aspect ratio on normalized shear strength ..... 44

Figure 4.14 Effect of compressive axial load ratio on normalized shear strength ..... 45

Figure 4.15 Influence of the axial load on normalized shear strength ..... 46

Figure 4.16 Effect of member's depth on normalized shear strength ..... 47

Table 4.1 Statistical comparison of models in terms of experimental/theoretical shear strength ratio ..... 48

Figure 4.17 Ultimate shear strength of circular section members without shear reinforcement ..... 49

Figure 4.18 Ratio of experimental to theoretical shear strengths of members without shear reinforcement ..... 50

Figure 4.19 Ratio of experimental to theoretical shear strengths versus concrete compressive strength of members without shear reinforcement ..... 51

Figure 4.20 Ratio of experimental to theoretical shear strengths versus aspect ratio of members without shear reinforcement ..... 52

Figure 4.21 Ratio of experimental to theoretical shear strengths versus axial load ratio of members without shear reinforcement ..... 53

Figure 4.22 Ratio of experimental to theoretical shear strengths versus longitudinal reinforcement ratio of members without shear reinforcement ..... 54

Table 4.2 Calculated and measured shear capacities of specimens without shear reinforcement ..... 55

Figure 4.23 Tension force in shear reinforcement in rectangular and in circular sections ..... 56

Figure 4.24 Reinforced concrete circular cross-section member under monotonic shear load ..... 57

Figure 4.25 Deviation stresses of hoops acting at the section's cracked region ..... 57

Figure 4.26 Shear carried by tension in hoops crossed by a diagonal crack ..... 58

Figure 4.27 Tension influence coefficient as a function of the hoops' number ..... 61

Figure 4.28 Forces acting on a) an infinitesimal hoop element and on b) concrete ..... 63

Figure 4.29 Hoop's tension function, $T(\varphi)$ ..... 65

Figure 4.30 Normalized deviation force at an arbitrary angular distance from the yield point ..... 66

Figure 4.31 Change of the deviation force with respect to the distance from the yield point ..... 67

Figure 4.32 Cracked region of a circular cross-section member under shear load ..... 68

Figure 4.33 Deviation function and the resultant deviation force of a particular hoop ..... 69

Figure 4.34 Influence coefficient versus friction coefficient for different central angles of one hoop ..... 70

Figure 4.35 Hoop's deviatoric shear carrying capacity along the member's cracked region ..... 71

Figure 4.36 Transformation of hoops ..... 72

Figure 4.37 Hoop's maximal central angle ..... 73

Figure 4.38 Deviation influence coefficient as a function of hoop's number ..... 74

Figure 4.39 Spiral's efficiency as a function of its pitch ..... 56

Table 5.1 Statistical comparison of models in terms of experimental/theoretical shear strength ratio ..... 78

Figure 5.1 Ultimate shear strength of circular section members with shear reinforcement ..... 79

Figure 5.2 Ratio of experimental to theoretical shear strengths of members with shear reinforcement ..... 80

Figure 5.3 Ratio of experimental to theoretical shear strengths versus concrete compressive strength of members with shear reinforcement ..... 81

Figure 5.4 Ratio of experimental to theoretical shear strengths versus aspect ratio of members with shear reinforcement ..... 82

Figure 5.5 Ratio of experimental to theoretical shear strengths versus axial load ratio of members with shear reinforcement ..... 83

Figure 5.6 Ratio of experimental to theoretical shear strengths versus longitudinal reinforcement ratio of members with shear reinforcement ..... 84

Table 5.2 Calculated and measured shear capacities of specimens with shear reinforcement ..... 85

Table 5.2 (Continued) ..... 86

Figure 5.7 Shear strength degradation with displacement ductility by Sezen and Moehle (2004) ..... 87

Table 5.3 Details and test results of specimens with circular cross-section under cyclic load ..... 88

Table 5.4 Statistical comparison of models in terms of experimental/theoretical shear strength ratio ..... 89

Figure 5.8 Ultimate shear strength of circular section members with shear reinforcement under cyclic load ..... 89

Figure 5.9 Ratio of experimental to design shear strengths of circular section members with shear reinforcement ..... 90

Figure 5.10 Design shear strength of circular section members with shear reinforcement ..... 90

# 8 REFERENCES

ACI 318M-02 and Commentary ACI 318RM-02 (2002), "Building Code Requirements for Structural Concrete", American Concrete Institute (ACI), Farmington Hills, Michigan

ACI-ASCE Committee 426 on Shear and Diagonal Tension (1973), "The Shear Strength of Reinforced Concrete Members", *Journal of the Structural Division*, ASCE, V. 99, No. ST6, June, pp. 1091-1187.

ACI-ASCE Committee 445 on Shear and Torsion (1998), "Recent Approaches to Shear Design of Structural Concrete", *Journal of Structural Engineering*, ASCE, V. 124, No. 12, Dec., pp. 1375-1417.

ACI-ASCE Committee 445 on Shear and Torsion (2000), "Recent Approaches to Shear Design of Structural Concrete", *Report*, ACI, ACI 445R-99, pp. 1-55.

Ahmad, S.H., Khaloo, A.R., Poveda, A. (1986), "Shear Capacity of Reinforced High-Strength Concrete Beams", *ACI Journal*, ACI, V. 83, No. 2, Jan-Feb, pp. 297-305.

Ang, B.G.,Priestley, M.J.N., Paulay, T. (1989), "Seismic Shear Strength of Circular Reinforced Concrete Columns", *ACI Structural Journal*, ACI, V. 86, No. 1, Jan.-Feb., pp. 45-59.

Bažant, Z.P. (1997), "Fracturing Truss Model: Size Effect in Shear Failure of Reinforced Concrete", *Journal of Engineering Mechanics*, ASCE, V. 123, No. 12, Dec., pp. 1276-1288.

Bažant, Z.P., Kazemi, M. T. (1991), "Size Effect on Diagonal Shear Failure of Beams without Stirrups", *ACI Structural Journal*, ACI, V. 88, No. 3, May-June, pp. 268-276.

Discussion to: Bažant, Z.P., Kazemi, M. T. (1992), "Size Effect on Diagonal Shear Failure of Beams without Stirrups", *ACI Structural Journal*, ACI, V. 89, No. 2, March-April, pp. 211-215.

Bažant, Z.P., Kim, J.K. (1984), "Size Effect in Shear Failure of Longitudinally Reinforced Beams", *ACI Journal*, ACI, V. 81, No. 5, Sept.-Oct., pp. 456-468.

Discussion to: Bažant, Z.P., Kim, J.K. (1985), "Size Effect in Shear Failure of Longitudinally Reinforced Beams", *ACI Journal Proceedings*, ACI, V. 82, No. 4, July-Aug., pp. 579-583.

Bažant, Z.P., Sun, H.H. (1987), "Size Effect in Diagonal Shear Failure: Influence of Aggregate Size and Stirrups", *ACI Materials Journal*, ACI, V. 84, No. 4, July-Aug., pp. 259-272.

Bažant, Z.P., Yu, Q. (2005a), "Designing Against Size Effect on Shear Strength of Reinforced Concrete Beams Without Stirrups: I. Formulation", *Journal of Structural Engineering*, ASCE, Vol.131, No. 12, Dec., pp. 1877-1885.

Bažant, Z.P., Yu, Q. (2005b), "Designing Against Size Effect on Shear Strength of Reinforced Concrete Beams Without Stirrups: II. Verification and Calibration", *Journal of Structural Engineering*, ASCE, Vol. 131, No. 12, Dec., pp. 1886-1897.

Bentz, C.E. (2005), "Empirical Modeling of Reinforced Concrete Shear Strength Size Effect for Members without Stirrups", *ACI Structural Journal*, ACI, Vol.102, No. 2, March-April, pp. 232-241.

Bhide, S.B., Collins M.P. (1989), "Influence of Axial Tension on the Shear Capacity of Reinforced Concrete Members", *ACI Structural Journal*, ACI, V. 86, No. 5, Sept.-Oct., pp. 570-581.

Capon, M.J.F., de Cossio, R.D. (1965), "Diagonal Tension in Concrete Members of Circular Section", *Ingenieria*, Mexico, April, pp. 257-280, (Translation by Portland Cement Association, Foreign Literature Study No. 466, 1966).

Clarke, J.L., Birjandi, F.K. (1993), "The Behaviour of Reinforced Concrete Circular Sections in Shear", *The Structural Engineer*, Institution of Structural Engineers, V. 71, No. 5, March, pp. 73-81.

Collins, M.P. (1978), "Toward a Rational Theory for RC Members in Shear", *Journal of the Structural Division*, ASCE, V. 104, No. 4, April, pp. 649-666.

Collins, M.P., Bentz, E.C, Kim, Y.J. (2002), "Shear Strength of Circular Reinforced Columns", *Published in S.M. Uzumeri Symposium: Behavior and Design of Concrete Structures for Seismic Performance, ACI Fall Convention in Toronto, October 16, 2000*, American Concrete Institut, Farmington Hills, Michigan, ISBN 0-87031-072-0, pp. 45-86.

Dancygier, A.N. (2001), "Shear Carried by Transverse Reinforcement in Circular RC Elements", *Journal of Structural Engineering*, ASCE, V. 127, No.1, Jan., pp. 81-83.

Desai, S.B. (2004), "Influence of Constituents of Concrete on Its Tensile Strength and Shear Strength", *ACI Structural Journal*, ACI, Vol. 101, No. 1, Jan.-Feb., pp. 29-38.

Elzanaty, A.H., Nilson, A.H., Slate, F.O. (1986), "Shear Capacity of Reinforced Concrete Beams Using High-Strength Concrete", *ACI Structural Journal*, ACI, V. 83, No. 3, March-April, pp. 290-296.

Eurocode 2 (2004), "Design of Concrete Structures: ENV1992-1-1: Part 1.1: General rules and rules for buildings, CEN"

Féderation Internationale du béton (fib) (2003), "Seismic assessment and Retrofit of Reinforced Concrete Buildings, State-of-the-Art Report", *fib Bulletin nr. 24*, International Federation for Structural Concrete fib, Lausanne, Switzerland, ISSN 1562-3610, ISBN 2-88394-064-9

Feltham, I. (2004), "Shear in Reinforced Concrete Piles and Circular Columns", *The Structural Engineer*, V. 82, No. 11, June, pp. 27-31.

Goto, Y. (1971), "Crackes Formed in Concrete Around Deformed Tension Bars", *ACI Journal*, ACI, Vol.68, No. 4, April, pp. 244-251.

Kani,G.N.J. (1966), "Basic Facts Concerning Shear Failure", *Journal of the American concrete institute*, ACI, V. 63, No. 6, June, pp. 675-692.

Discussion to: Kani,G.N.J. (1966), "Basic Facts Concerning Shear Failure", *Journal of the American concrete institute*, ACI, V. 63, No. 12, Dec., pp. 1511-1528.

Kani, G.N.J. (1967), "How Safe are our Large Concrete Beams?", *ACI Journal*, ACI, Vol. 64, No. 3, March, pp. 128-141.

Khalifa, J.U., Collins, M.P. (1981), "Circular Reinforced Concrete Members Subjected to Shear", *University of Toronto, Department of Civil Engineering*, Publication 81-08, Dec.

Kim, J.H., Mander, J.B. (2005), "Theoretical Shear Strength of Concrete Columns Due to Transverse Steel", *Journal of Structural Engineering*, ASCE, Vol. 131, No. 1, January, pp. 197-199.

Kim, J.K, Park, Y.D. (1996), "Prediction of Shear Strength of Reinforced Concrete Beams without Web Reinforcement", *Materials Journal*, ACI, V. 93, No. 3, May-June, pp. 213-222.

Kowalsky, M.J., Priestley, M.J.N. (2000), "Improved Analytical Model for Shear Strength of Circular Reinforced Concrete Columns in Seismic Regions", *Structural Journal*, ACI, V. 97, No. 3, May-June, pp. 388-396.

Krefeld, W.J., Thurston, C.W. (1966), "Contribution of Longitudinal Steel to Shear Resistance of Reinforced Concrete Beams", *ACI Journal*, ACI, Vol. 63, No. 3, March, pp. 325-343.

Discussion to: Krefeld, W.J., Thurston, C.W. (1966), "Contribution of Longitudinal Steel to Shear Resistance of Reinforced Concrete Beams", *ACI Journal*, ACI, Vol. 63, No. 9, Sept., pp. 1023-1026.

Kuchma, D.A. (2000), http://cee.uiuc.edu/kuchma/sheardatabank.

Leonhardt, F., Mönning, E. (1973), "Vorlesungen über Massivbau I", *2th Edition*, Springer-Verlag, Berlin, ISSN 3-540-06488-5, ISBN 0-387-06488-5.

Lutz, L. A. (1970), "Analysis of Stresses in Concrete Near a Reinforcing Bar Due to Bond and Transverse Cracking", *ACI Journal*, ACI, Vol.67, No. 10, October, pp. 778-787.

Lutz, L. A., Gergely, P. (1967), "Mechanics of Bond and Slip of Deformed Bars in Concrete", *ACI Journal*, ACI, Vol.64, No. 11, November, pp. 711-721.

Marti, P. (1992), "State-of-the-Art of Membrane Shear Behavior - European Work", *Proceedings of the International Workshop on Concrete Shear in Earthquake, University of Houston Texas, USA, 13-16 January 1991*, Elsevier Science Publisher, ISBN 1-85166-729-6, pp. 187-195.

Marti, P. (1999), "How to Treat Shear in Structural Concrete", *ACI Structural Journal*, ACI, V. 96, No. 3, May-June, pp. 408-414.

Mathey, R.G, Watstein, D. (1963), "Shear Strength of Beams Without Web Reinforcement Containing Deformed Bars of Different Yield Strengths", *ACI Journal*, ACI, Vol. 60, No. 2, Feb., pp. 183-206.

McGregor, J.G. (2005), "Reinforced Concrete Mechanics and Design, 4th Edition", , Pearson Prentice Hall, Upper Saddle River, New Jersey, ISBN 0-13-142994-9.

Merta, I. (2004), "Shear Strength of Reinforced Concrete Circular Cross Section Members", *Poster presentation: 5th International Conference on Fracture Mechanics of Concrete and Concrete Structures, Vail, Colorado, USA; 12.-16. April.*

Merta, I. (2004a), "Shear Strength of Reinforced Concrete Circular Cross Section Members", *Proceedings of the Fourth International Conference on Concrete under Severe Conditions; CONSEC'04*, Seoul National University, Korea Concrete Institute, Seoul, Korea, ISBN 89-89499-02-X, pp. 1025 - 1032.

Merta, I., Bedenik, B.S., Sparowitz, L. (2003), "Shear Strength Investigation of Reinforced Concrete Circular Cross Section Members", *Gradbeni Vestnik (Slovenian Civil Engineer Journal)*, 4, pp. 81 - 86.

Merta, I., Kolbitsch, A. (2006), "Analytical Evaluation of the Effective Area of Reinforced Concrete Circular Sections under Shear", *Proceedings of the Tenth East Asia-Pacific Conference on Structural Engineering and Construction, EASEC-10,* Bangkok, Thailand, 3-5 August 2006.

Mitchell, D., Collins, M.P. (1974), "Diagonal Compression Field Theory - A Rational Model for Structural Concrete in Pure Torsion", *ACI Journal*, ACI, V. 71, No. 8, Aug., pp. 396-408.

Mörsch, E. (1902), "Der Betoneisenbau, seine Anwendung und Theorie", Wayss & Freytag A.G.

Mörsch, E. (1912), "Der Eisenbetonbau - seine Theorie und Anwendung", *4th Edition*, Konrad Wittwer, Stuttgart.

Nielsen, M.P. (1999), "Limit Analysis and Concrete Plasticity, 2nd Edition", CRC Press LLC, ISBN 0-8493-9126-1.

Pacific Earthquake Engineering Research Center (PEER) (2006), University of California, Berkeley, http://nisee.berkeley.edu/spd/index.html.

Park, R., Paulay, T. (1975), "Reinforced Concrete Structures", John Wiley & Sons, ISBN 0-471-65917-7.

Pauw, A. (1961), "Static Modulus of Elasticity of Concrete as Affected by Density", *Journal of the American concrete institute*, ACI, V. 68, No. 6, June, pp. 679-687.

Priestley, M.J.N., Seible, F., Xiao, Y., Verma, R. (1994a), "Steel Jacket Retrofitting of Reinforced Concrete Bridge Columns for Enhanced Shear Strength - Part 1: Theoretical Considerations and Test Design", *ACI Structural Journal*, ACI, V. 91, No. 4, July-Aug., pp. 394-405.

Priestley, M.J.N., Seible, F., Xiao, Y., Verma, R. (1994b), "Steel Jacket Retrofitting of Reinforced Concrete Bridge Columns for Enhanced Shear Strength - Part 2: Test Results and Comparison with Theory", *ACI Structural Journal*, ACI, V. 91, No. 5, Sept.-Oct., pp. 537-551.

Priestley, M.J.N., Verma, R., Xiao,Y. (1994), "Seismic Shear Strength of Circular Reinforced Concrete Columns", *Journal of Structural Engineering*, ASCE, V. 120, No. 8, Aug., pp. 2310-2329.

Discussion to: Priestley, M.J.N., Verma, R., Xiao, Y. (1996), "Seismic Shear Strength of Circular Reinforced Concrete Columns", *Journal of Structural Engineering*, ASCE, V. 122, No. 4, April, pp. 461-467.

Priestley,M.J.N., Benzoni, G. (1996), "Seismic Performance of Circular Columns with Low Longitudinal Reinforcement Ratios", *ACI Structural Journal*, ACI, V. 93, No. 4, July-Aug., pp. 474-485.

Rebeiz, K.S. (1999), "Shear Strength Prediction for Concrete Members", *Journal of Structural Engineering*, ASCE, V. 125, No. 3, March, pp. 301-308.

Regan, P.E. (1993), "Research on shear: a benefit to humanity or a waste of time?", *Structural Engineering*, ASCE, V. 71, No. 19, Oct., pp. 337-347.

Reineck, K.H. (1991), "Ultimate Shear Force of Structural Concrete Members without Transverse Reinforcement Derived from a Mechanical Model", *ACI Structural Journal*, ACI, V. 88, No. 5, Sept-Oct, pp. 592-602.

Reineck, K.H., Kuchma, D.A., Kim, K.S., Marx, S. (2003), "Shear Database for Reinforced Concrete Members without Shear Reinforcement", *ACI Structural Journal*, ACI, V. 100, No. 2, March-April, pp. 240-249.

Discussion to: Reineck, K.H., Kuchma, D.A., Kim, K.S., Marx, S. (2004), "Shear Database for Reinforced Concrete Members without Shear Reinforcement", *ACI Structural Journal*, ACI, Vol.101, No. 1, Jan-Feb, pp. 139-144.

Ritter, W. (1899), "Die Bauweise Hennebique (Hennebique's Construction Method)", *Schweizerische Bauzeitung*, Vol. 33, No. 7, Februar, pp. 59-61.

Russo, G., Puleri, G. (1997), "Stirrup Effectiveness in Reinforced Concrete Beams under Flexure and Shear", *ACI Structural Journal*, ACI, Vol. 94, No. 3, May-June, pp. 227-238.

Russo, G., Somma, G., Mitri, D. (2005), "Shear Strength Analysis and Prediction for Reinforced Concrete Beams without Stirrups", *Journal of the Structural Division*, ASCE, V. 131, No. 1, January, pp. 66-74.

Sezen, H., Moehle, J.P. (2004), "Shear Strength Model for Lightly Reinforced Concrete Columns", *Journal of Structural Engineering*, ASCE, V. 130, No. 11, Nov., pp. 1692-1703.

University of Washington (2006), http://www.ce.washington.edu/~peera1/

Untrauer, R. E., Henry, R. L. (1965), "Influence of Normal Pressure on Bond Strength", *Journal of the American concrete institute*, ACI, Vol.62, No. 5, May, pp. 577-585.

Vecchio,F.J., Collins, M.P. (1986), "The Modified Compression-Field Theory for Reinforced Concrete Elements Subjected to Shear", *Journal*, ACI, V. 83, No. 2, March-April, pp. 219-231.

Vecchio, F.J., Collins, M.P., Aspiotis, J. (1994), "High-Strength Concrete Elements Subjected to Shear", *ACI Structural Journal*, ACI, V. 91, No. 4, July-Aug., pp. 423-433.

Walraven, J.C. (1981), "Fundamental Analysis of Aggregate Interlock", *Journal of the Structural Division*, ASCE, V. 107, No. ST11, November, pp. 2245-2270.

Walraven, J.C. Lehwalter, N. (1994), "Size Effect in Short Beams Loaded in Shear", *ACI Structural Journal*, ACI, V.91, No. 5, Sept-Oct, pp. 585-593.

Watanabe, F., Ichinose, T. (1992), "Strength and Ductility Design of RC Members Subjected to Combined Bending and Shear", *Proceeding: International Workshop on Concrete Shear in Earthquakes*, University of Houston Texas, USA, 13-16 January 1991, Elsevier Science Publisher, ISBN 1-85166-729-6, pp. 429-438.

Wong, Y.L., Paulay, T., Priestley, M.J.N. (1993), "Response of Circular Reinforced Concrete Columns to Multi-Directional Seismic Attack", *ACI Structural Journal*, ACI, V. 90, No. 2, March-April, pp. 180-191.

Zararis, P.D., Papadakis, G.Ch. (2001), "Diagonal Shear Failure and Size Effect in RC Beams without Web Reinforcement", *Journal of Structural Engineering*, ASCE, V. 127, No. 7, July, pp. 733-741.

Zsutty, T. (1968), "Beam Shear Strength Prediction by Analysis of Existing Data", *Journal*, ACI, V. 65, No. 11, Nov., pp. 943-951.